

NEW LANDSLIDE RAINFALL THRESHOLDS IN LANDSLIDE RISK
REGIONS OF THAILAND



A Thesis Submitted in Partial Fulfillment of the Requirements for the
Degree of Doctor of Philosophy in Civil, Transportation
and Geo-resources Engineering
Suranaree University of Technology
Academic Year 2022

เกณฑ์น้ำฝนใหม่สำหรับเตือนภัยดินถล่มในพื้นที่เสี่ยงภัยดินถล่ม
ของประเทศไทย



วิทยานิพนธ์นี้เป็นส่วนหนึ่งของการศึกษาตามหลักสูตรปริญญาวิศวกรรมศาสตรดุษฎีบัณฑิต
สาขาวิชาวิศวกรรมโยธา ขนส่ง และทรัพยากรธรณี
มหาวิทยาลัยเทคโนโลยีสุรนารี
ปีการศึกษา 2565

NEW LANDSLIDE RAINFALL THRESHOLDS IN LANDSLIDE RISK REGIONS
OF THAILAND

Suranaree University of Technology has approved this thesis submitted in partial fulfillment of the requirements for the Degree of Doctor of Philosophy.

Thesis Examining Committee




(Assoc. Prof. Dr. Cherdsak Suksiripatanapong)

Chairperson



(Prof. Dr. Avirut Chinkulkijniwat)

Member (Thesis Advisor)



(Asst. Prof. Dr. Pornpot Tanseng)

Member



(Prof. Dr. Suksun Horpibulsuk)

Member



(Dr. Somjai Yubonchit)

Member



(Assoc. Prof. Dr. Chatchai Jothityangkoon)

Vice Rector for Academic Affairs
and Quality Assurance



(Assoc. Prof. Dr. Pornsiri Jongkol)

Dean of Institute of Engineering

รัตนา สาลี : เกณฑ์น้ำฝนใหม่สำหรับเตือนภัยดินถล่มในพื้นที่เสี่ยงภัยดินถล่มของ
ประเทศไทย (NEW LANDSLIDE RAINFALL THRESHOLDS IN LANDSLIDE RISK REGIONS
OF THAILAND) อาจารย์ที่ปรึกษา : ศาสตราจารย์ ดร.อวิรุทธิ์ ชินกุลกิจนิวัฒน์, 148 หน้า.

คำสำคัญ: เกณฑ์เตือนจากภัยน้ำฝน/ตารางการณัจจร/คะแนนทักษะ/ระดับความอ่อนไหวต่อเหตุ
ดินถล่ม/เกณฑ์หยุดฝน

วิทยานิพนธ์นี้นำเสนอเกณฑ์น้ำฝนสำหรับเตือนภัยดินถล่มในประเทศไทย สำหรับภาคเหนือ และภาคใต้ซึ่งเป็นพื้นที่ที่มีอุบัติภัยดินถล่มบ่อยครั้ง เนื้อหาประกอบ ความสำคัญและที่มาของปัญหา ทฤษฎีที่เกี่ยวข้อง และเกณฑ์น้ำฝนสำหรับเตือนภัยดินถล่มสำหรับพื้นที่ภาคเหนือ และภาคใต้ โดยเริ่มจากการนำเสนอเกณฑ์น้ำฝนแบบใช้ฝนเกิดเหตุ สำหรับเตือนภัยดินถล่มในภาคใต้ โดยเลือก พารามิเตอร์น้ำฝน คือ ระยะเวลาเกิดฝน (D) และปริมาณฝนเกิดเหตุ (E) และแยกเกณฑ์ตามความอ่อนไหวต่อเหตุดินถล่ม ผู้วิจัยได้นำข้อมูลน้ำฝนที่เกี่ยวข้องกับเหตุดินถล่มในอดีตที่เคยเกิดขึ้นในพื้นที่ภาคใต้ของประเทศไทยระหว่างปี พ.ศ.2531-2561 จำนวน 92 เหตุการณ์ ข้อมูลปริมาณน้ำฝนได้จาก สถานีวัดน้ำฝนของกรมอุตุนิยมวิทยา ส่วนความอ่อนไหวต่อเหตุดินถล่มได้จากแผนที่เตือนภัยพื้นที่อ่อนไหวต่อการเกิดดินถล่มของกรมทรัพยากรธรณี (DMR) ซึ่งแบ่งพื้นที่ที่มีความอ่อนไหวต่อการเกิดดินถล่มไว้ 5 ระดับ คือ ความอ่อนไหวต่อการเกิดดินถล่มระดับสูงมาก มาก ปานกลาง ต่ำ และต่ำมาก ทั้งนี้ เพื่อให้ง่ายต่อการนำเสนอผู้วิจัยจึงจัดกลุ่มของพื้นที่อ่อนไหวต่อการเกิดดินถล่มออกเป็น 2 กลุ่ม คือ กลุ่มความอ่อนไหวระดับใหญ่ และกลุ่มความอ่อนไหวระดับเล็ก สำหรับกลุ่มแรกจะรวมพื้นที่ที่มีความอ่อนไหวต่อเหตุดินถล่มระดับสูงมาก และระดับมากเข้าด้วยกัน ส่วนกลุ่มที่สองจะเป็นการรวมพื้นที่ที่มีความอ่อนไหวต่อเหตุดินถล่มระดับ ปานกลาง ต่ำ และต่ำมาก จากนั้น ผู้วิจัยได้นำเสนอ เกณฑ์น้ำฝนสำหรับเตือนภัยดินถล่มในพื้นที่ภาคใต้เป็นเกณฑ์ที่สอง โดยใช้ข้อมูลน้ำฝนจากเหตุดินถล่มเดียวกันกับการเสนอเกณฑ์น้ำฝนแรก แต่นำเสนอเกณฑ์โดยบูรณาการทั้งพารามิเตอร์จากฝนเกิดเหตุ และฝนสะสม เป็นเกณฑ์น้ำฝนแบบ 3 มิติ โดยใช้สองพารามิเตอร์จากฝนเกิดเหตุ ได้แก่ ระยะเวลาเกิดฝน(D) และปริมาณน้ำฝน (E) และอีกหนึ่งพารามิเตอร์จากฝนสะสม คือปริมาณฝนสะสม 20 วันก่อนเกิดเหตุดินถล่ม (CR20) สำหรับเกณฑ์เตือนภัยดินถล่มที่สามที่นำเสนอเกณฑ์น้ำฝนในพื้นที่ภาคเหนือ ผู้วิจัยได้นำข้อมูลน้ำฝนที่เกี่ยวข้องจากเหตุการณ์ฝน 48 เหตุการณ์ แล้วทำให้เกิดเหตุดินถล่มจำนวน 59 เหตุการณ์ในพื้นที่ภาคเหนือมาทำการวิเคราะห์ และนำเสนอเกณฑ์น้ำฝนโดยใช้พารามิเตอร์น้ำฝนสามพารามิเตอร์คือ ระยะเวลาเกิดฝน(D) ปริมาณน้ำฝน (E) และปริมาณฝนสะสม 25 วันก่อนเกิดเหตุดินถล่ม (CR25) โดยนำระยะเวลาเกิดฝนของฝนเกิดเหตุมาพิจารณาร่วมด้วย เพื่อแบ่งเกณฑ์ออกเป็น 2 ส่วน คือเกณฑ์สำหรับฝนที่มีระยะเวลาไม่นาน (short duration

rainfall) และเกณฑ์สำหรับฝนที่มีระยะเกิดฝนเป็นเวลานาน (long duration rainfall) โดยใช้ระยะเวลา 3 วัน เป็นจุดแบ่งสำหรับฝนที่มีระยะเกิดฝนไม่นาน และฝนที่มีระยะเกิดฝนเป็นเวลานาน

ประสิทธิภาพการทำนายเหตุดินถล่มของเกณฑ์น้ำฝนที่นำเสนอในวิทยานิพนธ์นี้ จะใช้ตารางการถ่วงจรรยา (contingency table) คะแนนทักษะ (skill scores) กราฟ ROC (Receiver operating characteristic) และพื้นที่ใต้กราฟ ROC ในการประเมิน แล้วพบว่า เกณฑ์ที่นำเสนอมีความแม่นยำในการทำนายเหตุดินถล่มสูง และยังช่วยลดความผิดพลาดในการเตือนภัยผิดพลาดเมื่อเทียบกับเกณฑ์ปกติ



สาขาวิชา วิศวกรรมโยธา

ปีการศึกษา 2565

ลายมือชื่อนักศึกษา วิมล สาลี

ลายมือชื่ออาจารย์ที่ปรึกษา อดิ

RATTANA SALEE : NEW LANDSLIDE RAINFALL THRESHOLDS IN LANDSLIDE RISK REGIONS OF THAILAND. THESIS ADVISOR : PROF. AVIRUT CHINKULKIJNIWAT, Ph.D., 148 PP.

Keyword: RAINFALL THRESHOLD/CONTINGENCY MATRIX/SKILL SCORES/LANDSLIDE SUSCEPTIBILITY LEVEL/INTER-EVENT CRITERIA

This thesis introduces a new set of rainfall thresholds for landslide warning in the northern and the southern parts of Thailand. This thesis comprises five chapters began with introduction. Relevant theories are presented in Chapter 2. The other three chapters presents the landslide rainfall thresholds developed in this study. These thresholds began with a three-dimensional rainfall threshold, namely cumulative rainfall with event rainfall depth-duration (CED) threshold, which introduced for the landslide in the southern part of Thailand. Thereafter, the CED threshold was further elaborated to improve the performance of the CED threshold. The Elaboration was done by integration of relevant spatial variables to the CED threshold. The relevant spatial variables were extracted from susceptibility level indicated in the landslide susceptibility map. The last chapter focused on the landslide rainfall threshold in the northern part of Thailand. Based on the duration of the event rainfall, the CED threshold was categorized for short and long duration rainfalls.



The thresholds in southern part of Thailand were established from the precipitation data corresponding to 92 landslide events in the southern part of Thailand that took place during 1988–2018. To identify a particular event rainfall, a suitable inter-event criterion (IEC) had to be defined that separated two consecutive rainfalls. It was found from this study that, a rainfall intensity no greater than 2 mm/day lasting at least 1 day (IEC_{2,1}) was the criterion established to separate two consecutive rainfalls in the study area. Using quantile regression, an event rainfall depth-duration (ED) threshold was drawn at a probability levels of 5% -95%. A 20-day cumulative event rainfall depth (CR₂₀) was found being the most suitable duration of cumulative rainfall depth. A CR₂₀ of 100 mm was the third rainfall variable to establish a three dimensional threshold that integrated cumulative rainfall with event rainfall depth-duration variable, namely cumulative rainfall with event rainfall depth-duration (CED)

threshold. Thereafter, the landslide susceptibility levels from the susceptibility maps published by the Department of Mineral Resources (DMR) were introduced into a rainfall event-duration (ED) thresholds and became the ED_m and ED_h thresholds. Each for the locations classified for different susceptibility level. In this study, there are two susceptibility levels: the modest and the huge susceptibility levels. The modest susceptibility is a combination of very low, low, and moderate landslide susceptibility levels indicated in DMR maps. The huge susceptibility is a combination of high and very high landslide susceptibility levels indicated in DMR maps.

The northern Thailand is also known one of landslide hotspots. Rainfall-triggered landslides in this region have caused much suffering and many fatalities. In this work, a landslide-triggering rainfall threshold for northern Thailand is proposed based on rainfall data relating to 48 triggering rainfall events that caused 59 landslides in the study area. To account for different mechanism of landslide formation, the threshold was portioned into two parts for different duration of rainfall events. A split point of 3 days was chosen as a separator for portioning the threshold to be 1) a threshold for rainfall events of duration no longer than 3 days and 2) a threshold for rainfall events of duration longer than 3 days. The threshold also required a suitable variable for antecedent rainfalls which was found to be cumulative rainfall over 25-day period (CR₂₅) of 140 mm. Therefore, the thresholds combining cumulative rainfall with rainfall event – duration (CED) were established by incorporating the CR₂₅ of 140 mm into the traditional ED threshold.

Assessment of the introduced thresholds was conducted through a contingency matrix and a set of skill scores. Furthermore, the threshold receiver operating characteristic (ROC) curve, and the area under the ROC curve (AUC) were also employed for the assessment. The introduced threshold shows positive sign of the prediction, particularly in term of false alarm rate, false alarm ratio, and critical success index. The introduced threshold will be useful for landslide warning system in the study area.

School of Civil Engineering
Academic Year 2022

Student's Signature 
Advisor's Signature 

ACKNOWLEDGEMENTS

This work has been done with a great contribution from many people and their assistance must be extremely appreciated. It is a pleasure to convey my gratitude to them all.

In the first place I would like to express my deep gratitude to my Advisor, Prof. Dr. Avirut Chinkulkijniwat, for his supervision, advice, helps with valuable instructions, guidance and suggestions, for his effort to edit and to complete this dissertation, and his moral support during the study periods. Without his constructive devotion and support, this dissertation would not be finished successfully.

In addition, I am grateful for the teachers of civil engineering: Assoc. Prof. Dr. Cherdsak Suksiripatanapong, Assist. Prof. Dr. Pornpot Tanseng, Prof. Dr. Suksun Horpibulsuk, Dr. Somjai Yubonchit, and others person for suggestions and all their help.

I would like to thankful to Miss. Chadanit Wangfaoklang, Miss.Sukanya Thiemrach, Miss.Sirirat Soisompong, Mr. Tanisorn Chingdoun, Mr. Panuwat Ladngern, Mr. Watchapon Kanyamee, for helping me with the planning and working of this assignment. All of them were ever ready to clear my doubts and help me with all the necessary information and equipment.It was each and every individual's contribution that made this assignment a success.

Finally, I most gratefully acknowledge my parents and my friends for all their support throughout the period of this research.

Rattana Salee

TABLE OF CONTENTS

	Page
ABSTRACT (THAI).....	I
ABSTRACT (ENGLISH).....	III
ACKNOWLEDGEMENTS.....	V
TABLE OF CONTENTS.....	VI
LIST OF TABLES.....	IX
LIST OF FIGURES.....	XI
SYMBOLS AND ABBREVIATIONS.....	XVI
CHAPTER	
I INTRODUCTION.....	1
1.1 Background of the study.....	1
1.2 Research objective.....	5
1.3 Scope and limitation of research.....	5
1.4 References.....	5
II THEORETICAL BACKGROUNDS.....	8
2.1 Definition of landslide.....	8
2.2 Types of landslides.....	10
2.3 Landslide Hazard in Thailand.....	13
2.4 Verification procedure for the Weather Forecasting Demonstration Project severe weather forecasts.....	17
2.4.1 Defining the event.....	18
2.4.2 Preparing the contingency table.....	19
2.4.3 Calculating scores using the contingency table.....	24
2.5 Reference.....	29

TABLE OF CONTENTS (Continued)

	Page
III RAINFALL THRESHOLD FOR LANDSLIDE WARNING IN SOUTHERN THAILAND – AN INTEGRATED LANDSLIDE SUSCEPTIBILITY MAP WITH RAINFALL EVENT – DURATION THRESHOLD	31
3.1 Introduction	31
3.2 Data collection and rainfall characteristics in the study area	33
3.3 Landslide triggering rainfall thresholds and the assessment	36
3.4 Assessment of the thresholds	39
3.5 Results and discussions	41
3.6 Conclusions	45
3.7 Reference	46
IV NEW THRESHOLD FOR LANDSLIDE WARNING IN THE SOUTHERN PART OF THAILAND INTERGRATES CUMULATIVE RAINFALL WITH EVENT RAINFALL DEPTH-DURATION	49
4.1 Introduction	49
4.2 Event rainfall depth – duration (<i>ED</i>) threshold	58
4.3 <i>CED</i> Threshold: an integrated cumulative rainfall with event rainfall depth – duration threshold	63
4.4 Conclusions	67
4.5 Reference	69
V LANDSLIDE RAINFALL THRESHOLD FOR LANDSLIDE WARNING IN NORTHERN THAILAND	75
5.1 Introduction	75
5.2 Background of the study area	76
5.3 Data collection and rainfall characterization	78
5.4 Measures of evaluation	84
5.5 The event rainfall – duration thresholds	85
5.6 The cumulative rainfall with rainfall event – duration threshold	89

TABLE OF CONTENTS (Continued)

	Page
5.7 Conclusions.....	94
5.8 Reference	94
APPENDIX A. Publications.....	101
BIOGRAPHY	148



LIST OF TABLES

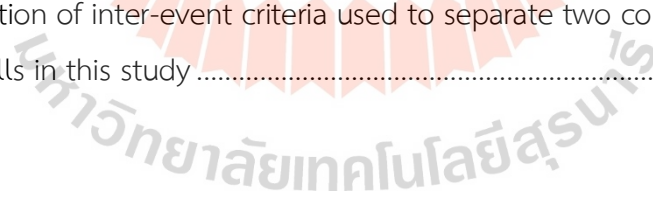
Table		Page
2.1	Major types of landslides according to Varnes (1978) (USGS, 2004)	13
3.1	Duration of rainfalls that caused eighty landslides during 1988–2018 categorized by landslide susceptibility leve	33
3.2	Threshold parameters a and b for the ED, EDm, and EDh thresholds at exceedance probabilities from 5 to 90%.....	38
3.3	Summary of the four contingencies (TP, FP, FN, TN) and the four skill scores (HR, FAR, HK, δ) obtained from the ED, EDm, and EDh thresholds for nine Probabilistic levels	43
3.4	Number of landslides with respect to time that landslide occurred at the very low to moderate susceptibility places.....	44
4.1	A set of inter-event criteria used to characterize rainfall data in the study area.....	55
4.2	Basics statistics of rainfall depth corresponding to various inter-event criteria.....	57
4.3	Basic statistics of interevent duration corresponding to various inter-event Criteria.....	58
4.4	Two-dimensional Kolmogorov–Smirnov test results determined the variation in the distributions of the scatter plots (in double logarithmic rainfall event depth–duration plane) for event rainfalls corresponding to landslides on the west and east sides of the study area.....	60
5.1	Basic statistics of inter-event duration corresponding to various inter-event criteria.....	81
5.2	Frequency distribution of rainfall duration.....	81
5.3	Frequency distribution of rainfall event in mm	82

LIST OF TABLES (Continued)

Table		Page
5.4	Threshold parameters a and b (see Eq. 1) for exceedance probabilities from 5 to 90%. The threshold was portioned to two parts; EDS (for short duration rainfall events) and EDL (for long duration rainfall events) thresholds. The threshold was portioned using a split point at 3 day	88
5.5	Summarizes the four contingencies (TP, FP, FN, TN) and the six skill scores (HR, FAR, FA, CSI, HK, δ) obtained from the ED threshold for ten probabilistic ..levels.....	89
5.6	Summarizes the four contingencies (TP, FP, FN, TN) and the six skill scores (HR, FAR, FA, CSI, HK, δ) obtained from the CED threshold for ten probabilistic levels	91

LIST OF FIGURES

Figure	Page
1.1 Annual rainfall in Thailand 2008-2017 (Source: Thai Meteorological Department).....	1
1.2 Rainfall criteria for different levels in the AP Model.	4
2.1 Principal components of (a) general landslide and (b) typical debris flow (European Soil Portal, 2013).....	9
2.2 Major types of landslides according to Varnes (1978) (AGS, 2007b)	12
2.3 Landslide hazard map of Thailand. Department of Mineral resources, Thailand. First published in 2022.....	6
2.4 Schematic showing the matching of forecast severe weather threat areas with point precipitation observations.....	21
2.5 The contingency table for dichotomous (yes-no) events.....	23
3.1 Locations of landslides and TMD rain gauge stations in the study area.....	32
3.2 Definition of inter-event criteria used to separate two consecutive rainfalls in this study	35



LIST OF FIGURES (Continued)

Figure	Page
3.3	Landslide susceptibility map for Krung Ching subdistrict, Nopphitam district, Nakhon SiThammarat and locations of landslide took place in this area (https://gis.dmr.go.th/DMR-GIS/gis).....36
3.4	Relationship between rainfall event (E) and its duration (D) form triggering rainfalls and non-triggering rainfalls in the Southern Thailand. Gray circles represent the triggering rainfalls that caused landslides and open circles represent the non-triggering rainfall events. The ED threshold drawn from quantile regression at various probability levels of triggering rainfall events.....38
3.5	a) Relationship between rainfall event (E) and its duration (D) form triggering rainfalls and non-triggering rainfalls in the Southern Thailand. Red circles represent the triggering rainfalls that caused landslides at the huge susceptibility places and green circles represent that at the modest susceptibility places. In turn, open green circles and open red circles are for the non-triggering rainfalls in the modest and huge susceptibility places, respectively. b) The ED^m and ED^h thresholds drawn from quantile regression at various probability levels of triggering rainfalls at the modest and the huge susceptibility places, respectively39
3.6	Distribution of triggering and non-triggering rainfalls and the threshold to define the meaning of true positive (TP), true negative (TN), false positive (FP), and false negative (FN)41

LIST OF FIGURES (Continued)

Figure	Page
3.7	Receiver operating characteristic (ROC) and corresponding area under the ROC curve (AUC) of the ED , ED^m and ED^h thresholds44
4.1	Location of the landslide as depicted by the black triangle, and location of the Rain station shown by the black circle. The area in thick black line represents catchment area locations. The thin black line area is a representation of sub catchment area locations. The gradient black and white area will show the elevation value of the area. (Figure created using ESRI ArcGIS 10.5 software, https://www.esri.com/en-us/arcgis/about-arcgis/overview).....53
4.2	Number of landslide events (the proportion is presented in parenthesis) associated with different monsoon periods; including southwest, northeast, and pre-monsoons, on the west side (Figure. 2a) and on the east side (Figure. 2b) of the study area54
4.3	Definition of inter-event criteria used to separate two consecutive rainfalls in this study55
4.4	Scatter plot, in double logarithmic rainfall event depth–duration plane, of 92 triggering events established using (a) $IEC_{2,1}$ and (b) $IEC_{5,1}$. Rainfall thresholds at probability level of 5% based on triggering events defined by inter-event criteria (a) $IEC_{2,1}$ and (b) $IEC_{5,1}$60
4.5	(a) Definition of true positive (TP), true negative (TN), false positive (FP), and false negative (FN) in the contingency matrix. Results from quantile regression at various probability levels and scatter plot, in double logarithmic rainfall event depth–duration plane, of triggering events and non-triggering events in established using (b) $IEC_{2,1}$ and (c) $IEC_{5,1}$62
4.6	Receiver operating characteristic (ROC) curves for ED thresholds established based on inter-event criteria $IEC_{2,1}$ and $IEC_{5,1}$63

LIST OF FIGURES (Continued)

Figure	Page
4.7	Rainfall depth on a failure day is plotted with respect to cumulative rainfall depth (3, 10, 15, 20, 30 days) before the failure day (a). <i>CR3</i> (b), <i>CR10</i> (c), <i>CR15</i> (d), <i>CR20</i> (e), and <i>CR30</i> (f) show relationships between rainfall depth on a failure day and 3-, 10-, 15-, 20-, and 30-day cumulative rainfall depth before the failure day.....
	65
4.8	<i>CED</i> threshold plotted in three -dimensional space.....
	66
4.9	Receiver operating characteristic (ROC) curves for ED and CED thresholds.....
	67
5.1	Location of the landslide as depicted by the red cross on black circle, and location of the Rain station shown by the white triangle. The area in dot-dash line represents boundary of catchment area. The thin dot line represents boundary of sub catchment area. The gradient color shows the elevation value of the area
	75
5.2	The chart shows how consecutive rainfall events were determined to have satisfied both conditions of the inter-event criterion used to define a single rainfall event in this study
	80
5.3	Average monthly rainfall in mm derived from gauge data for 30-year period from 1981 to 2010 (gray column) and for the recent year 2021 (green column)
	88
5.4	(a) From the data of non-triggering and triggering rainfalls, double logarithmic scatter plots were built from data points of rainfall event versus rainfall duration. The rainfall event – duration (<i>ED</i>) threshold was determined at various probability levels using quantile regression. (b) The <i>ED</i> threshold was divided to two categories; short duration rainfall threshold and log duration rainfall threshold, using a split point at 2 days, (c) The <i>ED</i> threshold using a split point at 3 days, (d) The <i>ED</i> threshold using a split point at 4 days.....
	86

LIST OF FIGURES (Continued)

Figure		Page
5.5	Receiver operating characteristic (<i>ROC</i>) curve and the corresponding area under the <i>ROC</i> curve (<i>AUC</i>) generated from the <i>ED</i> thresholds and the <i>CED</i> threshold	87
5.6	Rainfall on a failure day in mm was plotted with respect to cumulative rainfall over 3-, 10-, 15-, 20-, and 25- day period prior to the failure day (a). Rainfall on a failure day in mm was plotted with respect to cumulative rainfall over 25- day period before the failure day (b)	90
5.7	The <i>CED</i> threshold plotted in three -dimensional space. The threshold was portioned at 3-day becoming the <i>CED</i> threshold for rainfall events of their duration no longer than 3 days and the <i>CED</i> threshold for rainfall events of their duration longer than 3 days.....	91
5.8	Flowchart of landslide rainfall assessment using the introduced threshold	93

LIST OF ABBREVIATIONS

AUC	=	area under receiver operating characteristic curve
CED	=	threshold cumulative rainfall with rainfall event – duration threshold.
CR ₂₅	=	cumulative rainfall over 25-day period before a failure day.
CSI	=	critical success index
CV	=	coefficient of variation
E	=	rainfall event in mm
ED	=	threshold rainfall event – duration threshold
ED _L	=	threshold rainfall event – duration threshold for long duration rainfalls
ED _S	=	threshold rainfall event – duration threshold for short duration rainfalls
ED ^m	=	threshold rainfall event – duration threshold for the places classified as the modest susceptibility levels
ED ^h	=	threshold rainfall event – duration threshold for the places classified as the huge susceptibility levels
D	=	duration of rainfall event in day
DR _f	=	Rainfall event in mm on a failure day
FA	=	false alarm ratio
FAR	=	false alarm rate
FN	=	false negative
FP	=	false positive
HK	=	Hanssen and Kuipers score
HR	=	hit rate
IEC	=	Inter – event time criterion
ROC	=	receiver operating characteristic
TP	=	true positive
TN	=	true negative
δ	=	Euclidean distance from the ideal co-ordinate 0,1.

CHAPTER I

INTRODUCTION

1.1 Background of the study

Landslide is known as a natural disaster caused by the gravitational movement of soil or rock mass at the slope hillside. It is widely recognized that rainfall is an important factor to trigger landslides.

The rainwater decreases the shear strength of the sloping soil. Under a certain circumstance, a hill slope that experiences enough rainfall can lose its shear strength and result in slope failure. Figure 1.1 presents cumulative annual rainfall in Thailand during 1981-2017 (Meteorological Department). Since 2010, there were two of seven years (2010 to 2017) that cumulative annual rainfall was significantly greater than the average rainfall (orange dash line). Global climate change might be a major cause of this extreme condition. Accordingly, it is expected that we are going to experience with many years to encounter with torrential rainfalls.

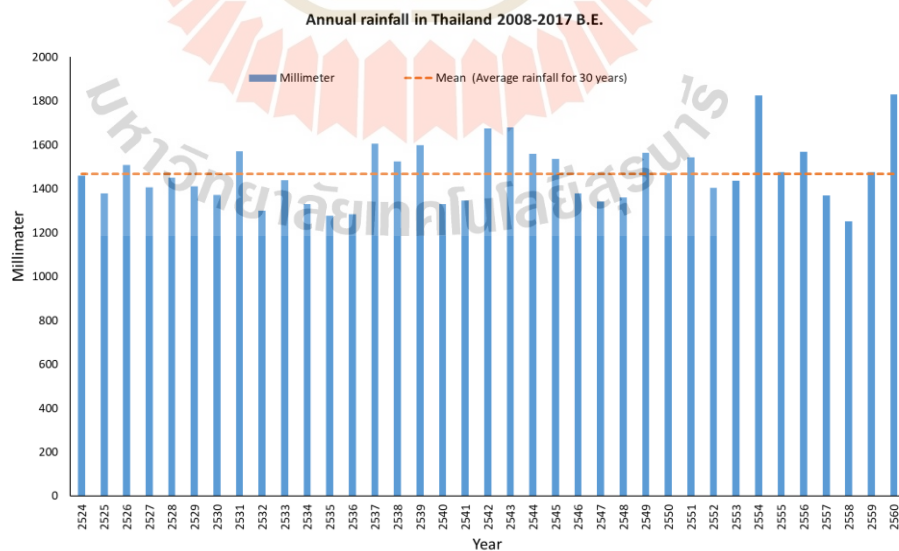


Figure 1.1 Annual rainfall in Thailand 2008-2017

(Source: Thai Meteorological Department)

Note: Estimated rainfall by Inverse Distance Weighting (IDW) using data from the Meteorological Department's weather station

The Southern and the Northern parts of Thailand are two regions most suffering from many landslide disasters (Department of Mineral Resources, 2019). The south is settled on a narrow peninsula between the gulf of Thailand (east side) and Andaman Sea (west side). As reported by Arai et al. (2019), the mean annual rainfall in the south during 1981-2017 was more than 2,000 mm whereas the north was about 1,500 mm. In the South, there are two rain periods from April to November. In the west side of this region, rainfall takes place mostly in September and October. For the east side, rainfall mostly takes place from October to December. The peak of rainfall happens in November and lasts until the early New Year. The Northern Thailand is dominated by mountain ranges in the western and northeastern parts of the region. Broadly defined based on geological composition, there are two mountainous subsystems in the study area. In the western part of the region, mountains run southwards from the Daen Lao Range with the two parallel chains of the Thanon Thong Chai Range, which includes the highest mountain in Thailand, Doi Inthanon (2,565m above mean sea level). In the northeastern part of the region, parallel ranges extending into northern Laos include the Khun Tan Range, the Phi Pan Nam Range, the Phlueng Range, and the western part of the Luang Prabang Range. There also exists a set of strike-slip faults in this region. However, landslides triggered by seismic events are rare in Thailand, and the most recent earthquakes in 2006 and 2014 did not lead to significant landslides (Schmidt-Thomé et al. 2018). The annual average minimum and maximum temperatures are 4 and 40 °C, respectively. The annual rainfall is spread over 122 days on average. Rainfall in this area is under the influence of the southwest monsoon, which starts in May and ends in October. Streams of warm moist air from the Indian Ocean bring abundant rain to the region, especially to the windward side of mountain ranges. However, the southwest monsoon is not the only source of precipitation during this period. The influence of the Inter Tropical Convergence Zone and tropical cyclones can also deposit large amounts of rain. Based on the available records, all major landslides in this area have been triggered by heavy rainfall caused by tropical cyclones. Landslides in Phare and Phetchabun provinces in 2001 were triggered by

continuous heavy rain that fell during Typhoon Usagi. Several landslides in Uttaradit, Sukhothai, Phrae, Lampang and Nan provinces in 2006 were caused by continuous heavy rainfall in the wake of Typhoon Xangsane. More recently, in 2018, landslides at Huay Khab village in Nan province followed ten days of continuous rainfall caused by Typhoon Son-Tinh.

The incident of landslide or earthflow cannot be controlled or hard to control but it can be investigated and warned. It is widely recognized that being proactive is suggested for any measures to encounter with natural disasters. Warning system is one of the most common proactive elements. Basically, there are two approaches; physical and empirical approaches, for developing a landslide warning system which will be activated if the rainfall amount reaches the threshold. The physical approach provides more precise measures but requires detailed geotechnical properties of the sloping ground such groundwater conditions, shear strength, soil water characteristics, geological soil profile, etc. Furthermore, these properties are spatial properties, hence it is more expensive and applicable over a small area (Guzzetti et al., 2007). The empirical approach is established based on precipitation records of landslide incidents. Caine (1980) published the first global rainfall threshold, namely rainfall intensity (I) and rainfall duration (D) or ID threshold, indicating the minimum rainfall conditions that will trigger landslides. Since then, numerous reports on landslide rainfall threshold have been published (Dahal and Hasegawa 2008, Rosi et al. 2012, Sengupta et al. 2010; Vennari et al. 2014, Chang et al. 2008, Segoni et al., 2018). Diversity of suitable rainfall parameters used in the introduced thresholds are mentioned in Peruccacci et al. (2012). In summary, there are three categories of the landslide rainfall threshold; 1) the thresholds measured by incident precipitation, 2) the thresholds measured by antecedent precipitations, and 3) other thresholds involving hydrological conditions. (Guzzetti et al. 2007). Among three threshold types, the thresholds based on an incident precipitation are most widely used since they require less input data and are easy to use (Rosi et al., 2021). However, one key difficulty of this threshold type is to identify the start point of rainfall (Guzzetti et al., 2008). Rosi et al. (2012) stated the need for appropriate criteria to determine the suitable starting point of the rainfall. At present, the answer for identifying the start point of rainfall measurement is not

unique. To avoid this difficulty, some studies focused on the relationship between daily and accumulated rainfalls (Kim et al., 1991, Glade et al., 2000, Giannechchini et al., 2012) This approach is supported by reports that indicate the mutual influence of antecedent and incident precipitations (Rahardjo et al., 2011; Rahimi et al., 2011). However, one shortcoming of this approach is that it might lead to misinformation in some dimension of the incident rainfall.

Presently, in Thailand, there is a national landslide warning system developed by the Department of Water Resources. Rainfall data in the risk areas are continuously recorded and analyzed. If the rainfall parameters reach the threshold, people living in the affected locations will be informed. Furthermore, these data will be sent to the central surveillance laboratory for landslides. The landslide rainfall threshold used in this system was named AP model which was developed by Kasetsart University (Figure 1.2). This threshold uses two rainfall parameters; a cumulative rainfall in three days and incident rainfall over 24 hours, to determine the warning alarm level. When the both rainfall variables reach the threshold, the alarm will be activated.

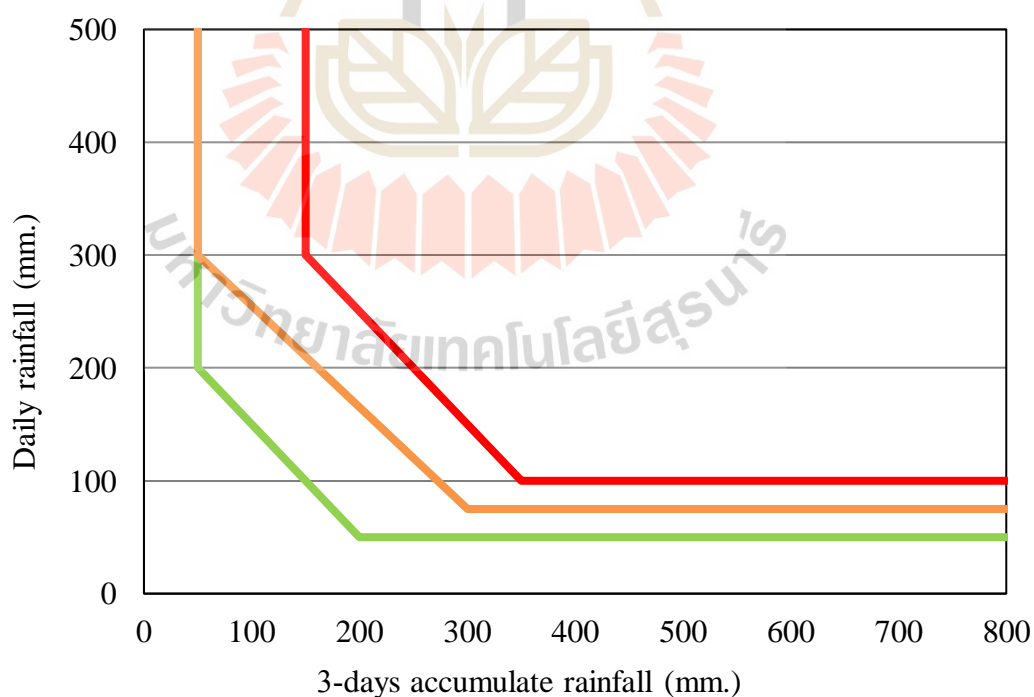


Figure 1.2 Rainfall criteria for different levels in the AP Model.

However, the threshold presently used was developed in (2009). Updated landslides and the relevant rainfall data are necessary for sustainable improvement. Since, topography and climate conditions in Thailand are different from region to region, a threshold that separately developed for each region of Thailand might provide more effective landslide assessment than a threshold that developed for a whole region does. As such, this study gathered landslide events and relevant rainfall data from two selected regions to develop new regional landslide rainfall thresholds; each for each region of the study. Assessment of the thresholds was conducted by contingency matrix and skill scores. Results from this study might be part of enhancing accuracy of the warning and hence life quality of people living in landslide risk locations.

1.2 Research objective

1.2.1 To introduce a set of new landslide rainfall thresholds that integrates temporal and spatial variables to the introduced threshold.

1.2.2 To introduce a set of new landslide rainfall thresholds that explicitly integrates rainfall variables from incident and antecedent rainfalls.

1.3 Scope and limitation of research

1.3.1 A set of relevant rainfall data corresponding to a single point of landslide event was gathered from rainfall stations located in a same catchment area with the location of a considered landslide.

1.3.2 These rainfall stations belong to the Department of Mineral Resources and the Department of Water Resources.

1.3.3 Period of gathered rainfall data was 30 days prior to the event day.

1.4 References

Arai S, Urayama K, Tebakari T, Archvarahuprok B (2019) **Characteristics of gridded rainfall data for Thailand from 1981–2017**. Eng J 23(6):461–468. <https://doi.org/10.4186/ej.2019.23.6.461>

- Caine N (1980) **The Rainfall intensity: duration control of shallow landslides and debris flows.** Geogr Ann Series A Phys Geogr 62(1/2):23. [https:// doi. org/ 10. 2307/ 520449](https://doi.org/10.2307/520449)
- Chang KT, Chiang SH, Lei F (2008) **Analysing the relationship between typhoon-triggered landslides and critical rainfall conditions.** Earth Surf Proc Land 33:1261–1271. [https:// doi.org/10.1002/esp.1611](https://doi.org/10.1002/esp.1611)
- Dahal RK, Hasegawa S (2008) **Representative rainfall thresholds for landslides in the Nepal Himalaya.** Geomorphology 100(3):429–443.[https://doi.org/ 10.1016/ j.geomorph.2008.01.014](https://doi.org/10.1016/j.geomorph.2008.01.014)
- Department of Mineral Resources 2019. **Department of Mineral Resources, 75/10 Rama 6 Road, Thung Phayathai Sub-district, Ratchathewi District, Bangkok 10400, Thailand.** [webmaster@dmr. mail.go.th](mailto:webmaster@dmr.mail.go.th)
- Giannecchini R, Galanti Y, D’Amato Avanzi G (2012) **Critical rainfall thresholds for triggering shallow landslides in the Serchio river valley (Tuscany, Italy).** Nat Hazard 12(3):829–842. [https:// doi. org/ 10.5194/ nhess- 12- 829- 2012](https://doi.org/10.5194/nhess-12-829-2012)
- Glade T (2000) **Applying probability determination to refine landslide-triggering rainfall thresholds using an empirical “antecedent daily rainfall model.”** Pure Appl Geophys 157(6–8):1059–1079. [https:// doi.org/ 10. 1007/ s0002 40050 017](https://doi.org/10.1007/s000240050017)
- Guzzetti F, Peruccacci S, Rossi M, Stark CP (2007) **Rainfall thresholds for the initiation of landslides in central and southern Europe.** Meteorog Atmos Phys 98:239–267. [https:// doi.org/10.1007/s00703-007-0262-7](https://doi.org/10.1007/s00703-007-0262-7)
- Guzzetti F, Peruccacci S, Rossi M, Stark CP (2008) **The rainfall intensity–duration control of shallow landslides and debris flows: an update.** Landslides 5(1):3– 17. [https:// doi.org/10.1007/s10346-007-0112-1](https://doi.org/10.1007/s10346-007-0112-1)
- Kim SK, Hong WP, Kim YM (1991) **Prediction of rainfall-triggered landslides in Korea.** In: Bell DH (ed) landslides, 2nd edn. A.A Balkema Rotterdam, pp 989–994.

- Peruccacci S, Brunetti MT, Luciani S, Vennari C, Guzzetti F (2012) **Lithological and seasonal control of rainfall thresholds for the possible initiation of landslides in central Italy**. *Geomorphology* 139-140:79–90. <https://doi.org/10.1016/j.geomorph.2011.10.000>
- Rahardjo H, Melinda F, Leong EC, Rezaur RB (2011) **Stiffness of a compacted residual soil**. *Eng Geol* 120(1–4):60–67. <https://doi.org/10.1016/j.enggeo.2011.04.006>
- Rahimi A, Rahardjo H, Leong EC (2011) **Effect of Antecedent Rainfall Patterns on Rainfall-Induced Slope Failure**. *J Geotech Geoenviron Eng* 137(5):483–491. [https://doi.org/10.1061/\(asce\)gt.1943-5606.0000451](https://doi.org/10.1061/(asce)gt.1943-5606.0000451)
- Rosi A, Segoni S, Catani F, Casagli N (2012) **Statistical and environmental analyses for the definition of a regional rainfall threshold system for landslide triggering in Tuscany (Italy)**. *J Geogr Sci* 22(4):617–629. <https://doi.org/10.1007/s11442-012-0951-0>
- Rosi, A., Segoni, S., Canavesi, V., Monni, A., Gallucci, A., & Casagli, N. (2021). **Definition of 3D rainfall thresholds to increase operative landslide early warning system performances**. *Landslides*, 18(3), 1045-1057.
- Segoni, S., Piciullo, L., & Gariano, S. L. (2018). **A review of the recent literature on rainfall thresholds for landslide occurrence**. *Landslides*, 15(8), 1483-1501.
- Sengupta A, Gupta S, Anbarasu K (2010) **Rainfall thresholds for the initiation of landslide at Lanta Khola in north Sikkim, India**. *Nat Hazards* 52:31–42. <https://doi.org/10.1007/s11069-009-9352-9>
- Vennari C, Gariano SL, Antronico L, Brunetti MT, Iovine G, Peruccacci S, Terranova O, Guzzetti F (2014) **Rainfall thresholds for shallow landslide occurrence in Calabria, southern Italy**. *Nat Hazards Earth Syst Sci* 14:317–330. <https://doi.org/10.5194/nhess14-317-2014>

CHAPTER II

THEORETICAL BACKGROUNDS

2.1 Definition of landslide

Landslide is conventionally defined as a mass movement of soil (in forms of earth or debris) or rock downward along surface slope under gravitational influence (Varnes, 1984; Cruden, 1991). At present, it has become vital hazard in most mountainous and hilly areas around the world especially those in the tropics and earthquake-influenced zones, as well as areas along the considerably steep river bank or coastline. Landslide impacts depend fundamentally on their size and speed (or momentum), elements at risk within their paths and vulnerability condition of those elements. Every year, landslide incidences have generated large number of deaths and injuries to the at-risk people and substantial damages to the infrastructures (e.g., road, railway, pipeline) and properties (e.g., building, agricultural land) (European Soil Portal, 2013).

Landslide phenomenon is conceptually a direct product of slope instability due to the gravitation as when the gravitational stresses exceed the strength of rock or soil that holds the surface soil layer together, slope failure shall often occur as a consequence. Most landslides are initiated by some triggering factors that shall increase stress and weaken strength of slope materials which include: (1) heavy rainfall, rapid snowmelt, or irrigation that load slopes with water, (2) shaking by earthquake, (3) natural erosion or human activities that increase slope angles or undercut the toes of surface slopes, e.g. road construction, (4) removal of the vegetation cover on land surface by, e.g. wildfire, logging, agriculture, or overgrazing, and (5) loading of slopes with huge piles of rock, ore, or mining waste. Among these factors, the most predominant ones around the world are two natural processes; heavy rainfall and strong earthquake (Corominas and Moya, 2008).

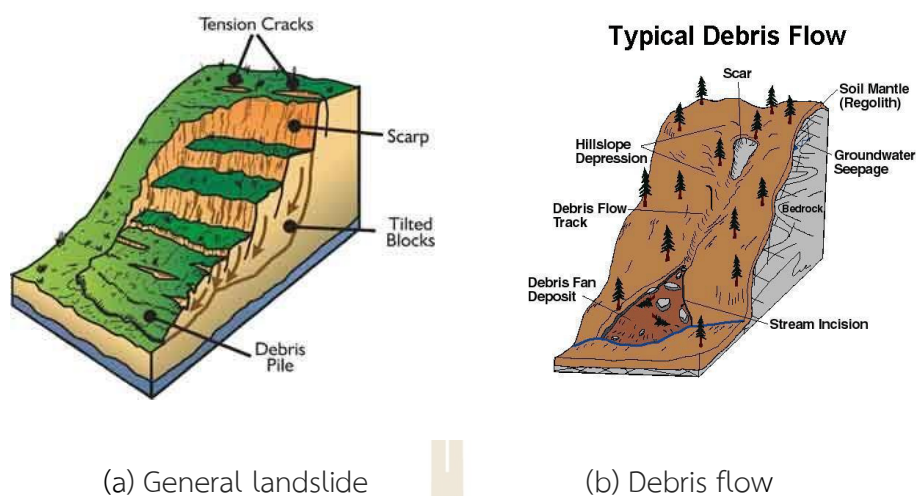


Figure 2.1 Principal components of (a) general landslide and (b) typical debris flow (European Soil Portal, 2013)

Figure 2.1(a) illustrates principal components of the general landslide structure which include tension cracks that appear when land is gradually pulling apart from the hillside. With time, the ground surface on one side of these cracks may slide downhill forming a scarp and if the ground moves far enough, it shall leave an apparent mark called a scar. Typically, a fresh scar often has lighter color without vegetation cover if compared to the surrounding slopes. Landslide volume can vary greatly from less than a cubic kilometer (km^3) for the small and medium-size landslides to more than tens of cubic kilometers for the gigantic ones while speed might vary from a few centimeters per year for the slow-moving slides to several tens of kilometers per hour for the fast and destructive ones (Highland and Bobrowsky, 2008; European Soil Portal, 2013). Typically, the most destructive landslide incidences are often in form of the debris or mud flows as seen in Figure 2.1(b). These flows usually have rather rapid movement with combination volume of loose soil, rock, organic matter, air, and water mixed in the intense surface-water flow due to heavy precipitation or snow-melt.

2.2 Types of landslides

Landslides can be broadly classified into two fundamental categories: shallow type and deep-seated type. Shallow landslides normally involve sudden fail of top soil layer and upper regolith zone while deep-seated ones additionally include bedrock at higher depth and gradually develop over a relatively longer time period. Most natural shallow landslides are triggered by prolonged heavy rainfall that critically increase soil water pressure or accelerated ground due to earthquakes at tectonic fault nearby. Most deep-seated landslides tend to fail incrementally, rather than in the catastrophic manner of the shallow landslide. Their major causes are accumulated rainfall over a long period (e.g., weeks to years) and also massive ground acceleration experienced during large magnitude earthquakes. The latter is commonly found in the seismically active regions around the world.

Standard classification scheme of the existing landslide types has been developed based principally on work of Varnes (1978). In this system, landslides are categorized based on basis of their predominant composed material type (i.e., rock, debris, earth, or mud) in the first term and their movement type (i.e., fall, topple, avalanche, slide, flow, or spread) in the second term. Thus, the landslides can be identified using these terms that refer respectively to their major material and movement mode, e.g., rock fall, debris flow, earth slide, and so forth. In general, the material in landslide mass is either rock or soil (or both); the latter is described as “earth” if mainly composed of the sand-sized or finer particles (with $\geq 80\%$ of the particles are < 2 mm) and “debris” if composed of coarser fragments (with 20% to 80% of known particles are > 2 mm and the remainder are < 2 mm). Figure 2.2 and Table 2.1 provide information on dominant landslide types according to Varnes (1978) mentioned earlier

From Figure 2.2, slides consist of blocks of material moving on well-defined shear planes and there is a distinct zone of weakness that separates slide material from more stable underlying material. These are divided into the rotational slides that move along concave surface and translational slides that often move parallel to the referred ground surface. Falls are the sudden release of rocks or soils dropping freely through the air with little contact with other surfaces until impact. Topples are

similar to falls except that initial movement involves forward rotation of the associated mass. Lateral spreads occur when liquefaction in underlying materials causes surface rocks or soils to move down gentle slopes. Flows move entirely by shearing within the transported mass and act like viscous fluids. They consist of five kinds:

(1) Debris flow-a fast moving landslide in form of liquefied material of mixed and unconsolidated water and debris [as illustrated in Figure 2.1(b).

(2) Debris avalanche-a variety of very rapid to extremely rapid debris flow.

(3) Earth flow-movement of slope material that liquefies and runs out forming a bowl or depression at the head and have a characteristic of “hourglass” shape.

(4) Mudflow-an earth flow consisting of the material wet enough to flow rapidly and contains at least 50% sand, silt, and clay-sized particles. In some cases, mudflows and debris flows are commonly referred to as “mudslides”.

(5) Creep-a slow, steady downward movement of slope-forming soil or rock.

The movement is called complex landslide if it involves combination of two or more types of the integrated movement. Debris flow and mudflow are among the most dangerous landslide-related incidences to life and property of the affected community, especially those in the tropical countries, due to the high speeds and sheer destructive force of their flow (USGS, 2004; AGS, 2007b).

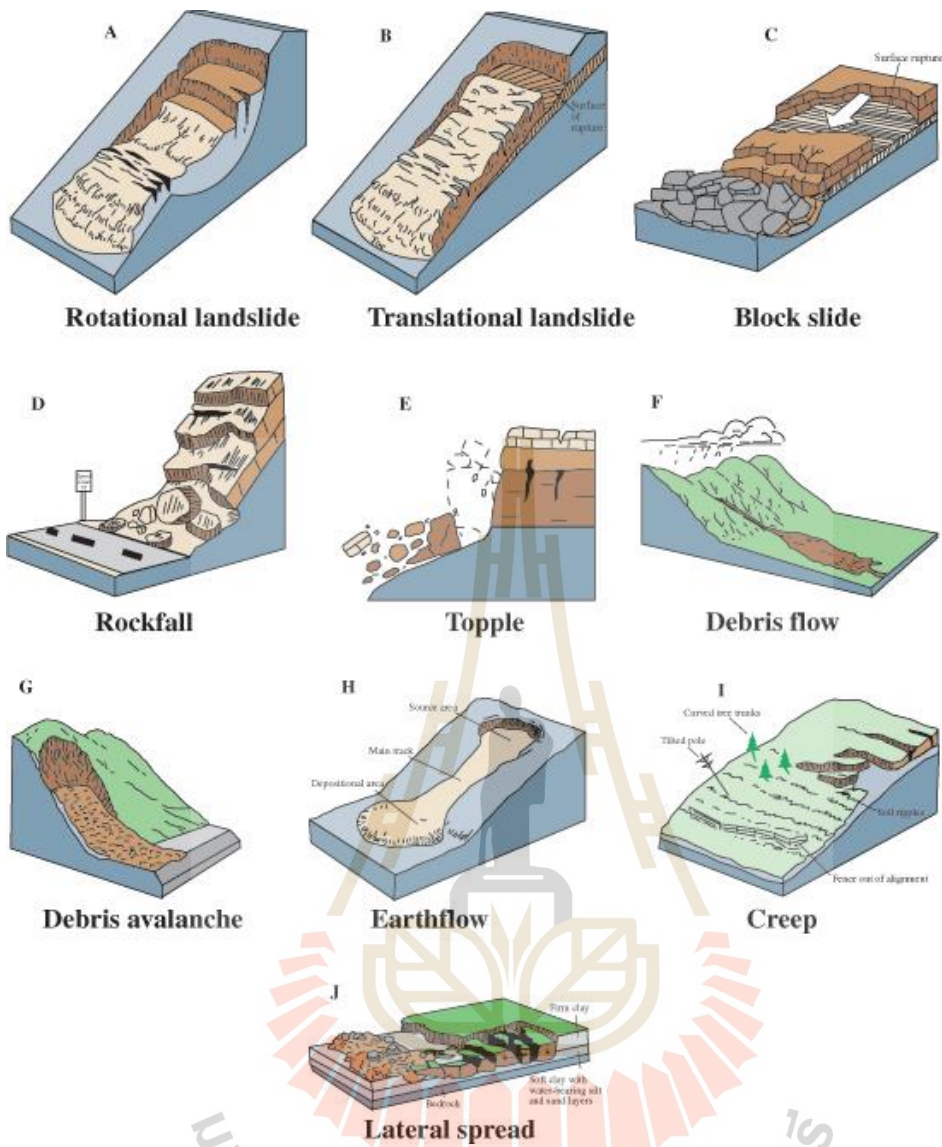


Figure 2.2 Major types of landslides according to Varnes (1978)

Table 2.1 Major types of landslides according to Varnes (1978)

Type of Movement		Type of Material		
		Bedrock	Engineering Soil	
			Predominantly Coarse	Predominantly Fine
Fall		Rock Fall	Debris Fall	Earth Fall
Topples		Rock Topple	Debris Topple	Earth Topple
Slide	Rotational	Rock Slide	Debris Slide	Earth Slide
	Translational			
Lateral Spreads		Rock Spread	Debris Spread	Earth Spread
Flows		Rock Flows	Debris Flows	Earth Flows
		(Deep Creep)	Soil Creep	
Complex		Combination of Two or more Principal Types of Movement		

2.3 Landslide Hazard in Thailand

Rural mountain areas in Thailand have a high hazard potential for landslides. Settlements in hazardous areas are expanding and hill slopes are being deforested. Many former forest areas have been converted into agricultural lands, thereby decreasing slope stability. Since the beginning of the 21st-century disasters caused by landslides have increased in Thailand. The landslides that lead to disasters in villages are in fact debris flows caused by heavy rains and landslides upstream. Landslides resulting from seismic activities are uncommon in Thailand. The landslide hazard risk in Thailand is defined by the hazard (the debris flow, i.e., landslide-prone areas) and the vulnerability (people living in landslide hazard areas). The landslide-prone area mapping is based on the geology and the morphology, and the vulnerability upon settlements. The resulting landslide risk map was used to identify all risk areas and consequently the establishment of a community-based landslide observation

network has been able to reduce the land-slide-related risks. This network focuses on training local people to understand the risks related to landslides and provides villagers with simple tools to detect early signs of threatening landslides and evacuate villagers to safe places. These networks have proven to be very successful because it was possible to sensitize and train villagers on the hazard and the risk with the result to effectively protect human lives during several landslide events.

The types of mass movement that lead to disasters are mainly debris flow and rockfalls. The areas with the highest debris flow hazard in Thailand are in areas with Precambrian and Paleozoic granites, gneisses, and schists that are found mainly in the northwest of the country and at some outcrops in central and southern Thailand (see Fig. 2.1). These rocks are deeply weathered, partly up to 60 m in depth. Some debris flows also occur in areas of folded tertiary rocks in northern and central Thailand. Rockfalls are common in Upper Paleozoic carbonate areas that are mainly bound to the Peninsula, reaching from Surat Thani to the Satun Province. The debris flows are caused by heavy rainfalls that trigger landslides among steeper slopes. These landslides carry slope material and plant residues into streams. Due to the rainfall, these streams swell and transport the landslide material downstream at a very high speed, leading to debris flows. Rockfalls occur due to weathering of tropical karst, mainly among steep, nearly vertical slopes. Since the term debris flow and rockfall are not commonly used among laymen the overall term landslide is preferred.

The landslide hazard in Thailand was mapped and assessed by the department for Mineral Resources (DMR) utilizing a landslide prediction model that runs under a Geographic Information System (GIS). The factors the model calculates are geology, elevation, slope, flow accumulation, flow direction, vegetation, soil type, and saturation (Pantanahiran, 1994). The results of the model were plotted in the form of a landslide hazard zone map on a scale of 1:250,000 for the provincial level and on a scale of 1:2,500,000 for the whole country. Based on this assessment, there are 6563 villages, in 1084 communities (Tambon), located in landslide hazard zones in 54 provinces, mainly in Northern and southern Thailand (Environmental Geology Division, 2003). The landslide-prone area zones are categorized based on empirical

studies. In 2004 the decades-long observations and field studies in the aftermath of landslides have led to the decision in the DMR to categorize slopes steeper than 30 degrees as landslide-prone. The hazard zoning is applied by a combination of slope steepness, soil type, and precipitation.

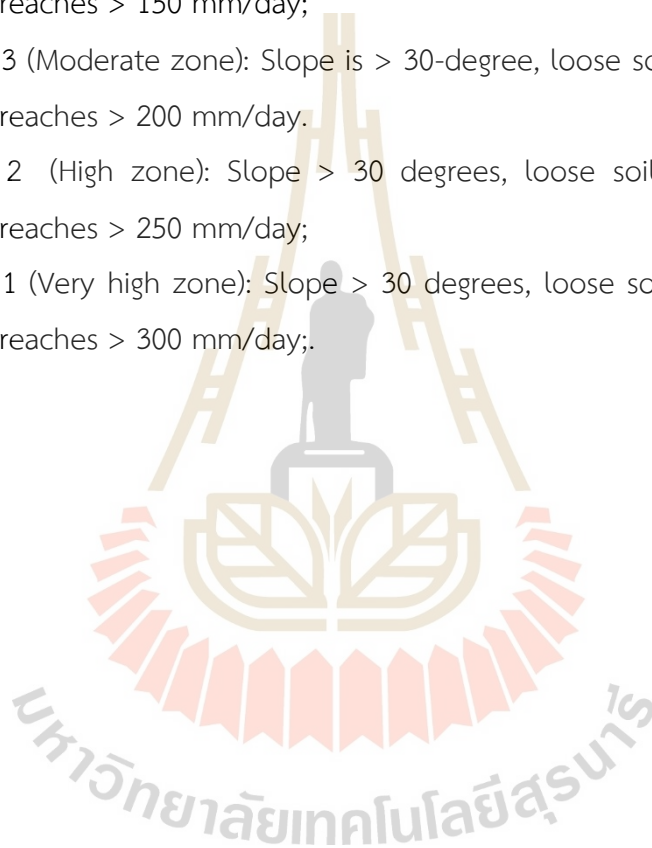
Zone 5 (Very low zone): Slope > 30 degrees, loose soil, landslide hazard if precipitation reaches > 100 mm/day;

Zone 4 (Low zone): Slope > 30-degree, loose soil, landslide hazard if precipitation reaches > 150 mm/day;

Zone 3 (Moderate zone): Slope is > 30-degree, loose soil, landslide hazard if precipitation reaches > 200 mm/day.

Zone 2 (High zone): Slope > 30 degrees, loose soil, landslide hazard if precipitation reaches > 250 mm/day;

Zone 1 (Very high zone): Slope > 30 degrees, loose soil, landslide hazard if precipitation reaches > 300 mm/day;.



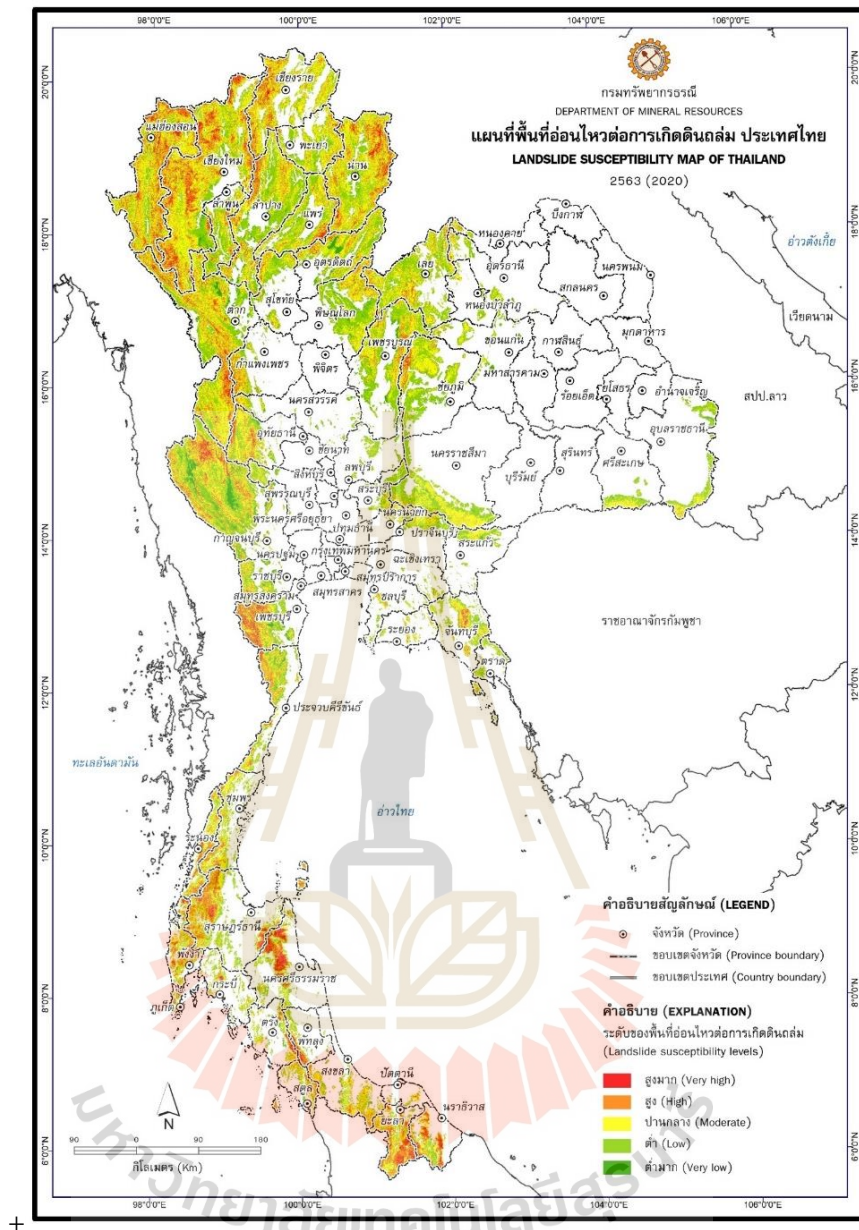


Figure 2.3 Landslide hazard map of Thailand. Department of Mineral resources, Thailand. First published in 2022

Landslides are recurrent and devastated incidences commonly found in Thailand especially in the mountainous regions and their vicinity. The predominant type of landslides discovered is the rainfall-triggered shallow landslide caused by the intense and continuous rainfalls where most vulnerable geologic formation is the granite terrain which can be easily weathered into thin layers of the landslide prone

residual soils (Soralump, 2007). Shallow failures occur due to saturation of top soil layer along the terrain slope which shifts slope property from marginally stable to unstable state. This could result in the rapid movement of soil cover downhill to the surrounded low area (Liu and Wu, 2008). During this period, the landslide may transform into a debris avalanche, with increasing velocity and volume. If the landslide material flows into a gully at the base of the slope, then the run-out of the material can reach long distance (up to several kilometers) (Revellino et al., 2004).

To reduce risk from the current widespread landslide activity, the landslide susceptibility assessment is crucially needed in all areas that are potentially prone to landsliding. However, reports on this issue for Thailand are still infrequent and they typically focused only on small areas where the catastrophic landslides have occurred before (e.g. Naramngam and Tangtham, 1997; Yumuang, 2006; Akkrawintrawong et al., 2008; Oh et al., 2008) but the investigation on basin or regional scales are still rarely found in literature (e.g. LDD, 2001; DMR, 2005). In most cases, only few causative factors were considered and the verification process was largely ignored. To assist the effective susceptibility analysis in broader scale, in this research, the formulation of landslide susceptibility map at basin scale for local Thailand based on three different methods namely; analytical hierarchy process (AHP), frequency ratio (*FR*) model and integrated AHP and FR model in lower Mae Chaem watershed, northern Thailand.

2.4 Verification procedure for the Weather Forecasting Demonstration Project severe weather forecasts

The best procedure to follow for verification depends not only on the purpose of the verification and the users, but also on the nature of the variable being verified. For the African the World Meteorological Organization Severe Weather Forecasting Demonstration Project (SWFDP) s, the main forecast variables are extreme precipitation and strong winds, with extreme defined by thresholds of 30 or 50 mm in 6 hours, 30, 50 or 100 mm in 24 hours. These are therefore categorical variables, and verification measures designed for categorical variables should be applied. In

each case, there are two categories, referring to occurrence or non-occurrence of weather conditions exceeding each specific threshold.

The following subsections describe the suggested procedures for building contingency tables and calculating scores.

2.4.1 Defining the event

Categorical and probabilistic forecasts always refer to the occurrence or non-occurrence of a specific meteorological event. The exact nature of the event being predicted must be clearly stated, so that the user can clearly understand what is being predicted and can choose whether to take action based on the forecast. The event must also be clearly defined for verification purposes, specifically as follows:

- The location or area of the predicted event must be stated.
- The time range over which the forecast is valid must be stated.
- The exact definition of the event must be clearly stated.

Sometimes these aspects will be defined at the beginning of a season or the beginning of the provision of the service and will remain constant, for example, the establishment of fixed forecast areas covering the country. As long as this information is communicated to the forecast user community, then it would not be necessary to redefine the area to which a forecast applies unless the intent is to subdivide the standard area for a specific forecast.

The time range of forecast validity has been established as part of the project definition, for example, 6-h and 24-h total precipitation, and wind maxima over 24 hours. The 24-h period also needs to be stated. The definition which corresponds to the observation validity period needs to be used for verification.

For the Severe Weather Forecasting Demonstration Project, it would be best if the larger countries were to be divided geographically into fixed (constant) areas of roughly the same size, areas which are climatologically homogeneous. Each region should have at least one reporting station. The smaller the area size, the more the forecast is potentially useful. However, the predictability is lower for smaller areas, giving rise to a lower hit rate and higher numbers of false alarms and missed events, that is more difficult to make a good prediction. The sparseness of observational data also imposes constraints on the subdivision of areas. A forecast

cannot be verified without relevant observations. On the other hand, larger areas make the forecasts potentially less useful, for example, to disaster management groups or other users who need detailed enough location information associated with the predicted severe weather to effectively deploy their emergency resources, or to implement effective protective or emergency actions.

To summarize, in choosing the size and location of fixed domains for severe weather warnings, several criteria should be taken into account:

(a) The location and readiness of disaster relief agencies: The domains should be small enough that disaster relief agencies can respond effectively to warnings within the lead time that is normally provided.

(b) The availability of observation data: Each domain should have at least one representative and reliable observation site for forecast verification purposes.

(c) Climatology/terrain type: It is most useful to define regions so that they are as climatologically homogeneous as possible. If there are parts of the domain that are much more likely to experience severe weather than others, these could be kept in separate regions.

(d) Severe weather impacts: The domain locations and sizes should take into account factors affecting potential impacts such as population density and disaster-prone areas.

Within these guidelines, it is also useful if the warning areas are roughly equal in size, as that will help ensure consistent verification statistics. Also, within each country, the warning criteria should be constant for all domains. Finally, for the purposes of the African the Severe Weather Forecasting Demonstration Project, and for possible comparisons with the results of verification of the global model forecasts over multiple countries, it would be useful if the subdomains in all countries would be roughly similar in size.

2.4.2 Preparing the contingency table

The first step in almost all verification activity is to collect a matched set of forecasts and observations. The process of matching the forecast with the corresponding observation is not always simple, but a few general guidelines can be

stated. If the forecast event and the forecast are clearly stated, then it is much easier to match with observations. For the Severe Weather Forecasting Demonstration Project, the forecast event is the expected occurrence of severe weather conditions somewhere in the forecast area, sometime during the valid time period of the forecast. Then:

- A “hit” is defined by the occurrence of at least one observation of severe weather conditions, as defined by the thresholds anywhere in the forecast area, any time during the forecast valid time. Note that by this definition, more than one report of severe weather within the forecast valid area and time period does not add another event; only one hit is recorded.

- A “false alarm” is recorded when severe weather is forecast, but there is no severe weather observed anywhere in the for which the forecast is valid during the valid period.

- A “missed event” is recorded when severe weather is reported outside the area and/or the time period for which the warning is valid, or whenever severe weather is reported and no warning is issued. Only one missed event is recorded on each day, for each region where severe weather has occurred that is not covered by a warning.

- A “correct negative” or “correct non-event” is recorded for each day and each fixed forecast region for which no warning is issued and no severe weather is reported.

If observational data are sparse, it may be difficult to determine whether severe weather occurred, as there is much space between stations for smaller scale convective storms which characterize much of the severe weather occurrences. It is permissible to use proxy data such as reports of flooding to infer the occurrence of severe weather in the absence of observations, but full justification of these subjective decisions must be included with verification reports.

It is possible to incur missed events, false alarms and hits all at once. Consider the following example, represented schematically in Figure 2.3.

In Figure 2.3, the yellow regions represent forecast severe weather areas and the stars represent observations of severe weather; represents

observations of non-severe weather. This case contains one hit (because there are observations of severe weather within the forecast severe weather area), one miss (because there are one or more observations of severe weather that do not lie in a forecast severe weather area) and one false alarm (because there is no severe weather reported in a severe weather forecast area). Note that a false alarm is recorded only because there is a separate forecast area with no report of severe weather. The fact that not all the stations in the larger area reported severe weather does not matter; only one severe weather report is needed to score a hit. If there are no reporting stations in a forecast severe weather area, then forecasts for that area cannot be verified.

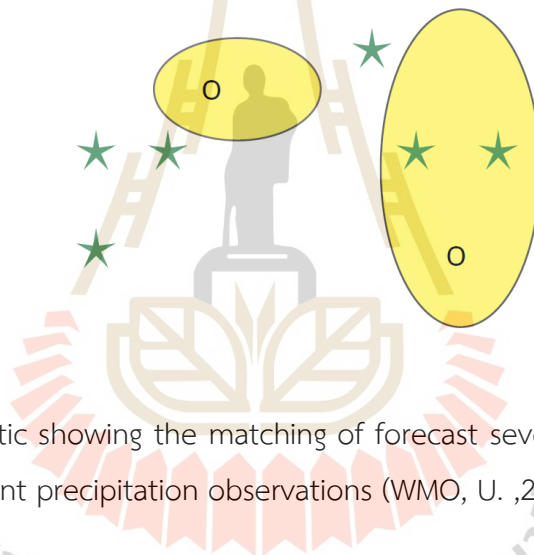


Figure 2.4 Schematic showing the matching of forecast severe weather threat areas with point precipitation observations (WMO, U. ,2014)

In this system, the number of hits cannot be increased by increasing the size of the forecast area. However, increasing the size of the forecast area might reduce the chance of a missed event. This should be kept in mind. If the size of the forecast severe weather area is increased merely to reduce the chance of a missed event, the forecast also becomes less useful, because disaster mitigation authorities may not know where to deploy their resources to assist the needy. Each National Meteorological and Hydrological Service must seek to achieve its own balance between scale (size) of forecast areas and risk of false alarms and missed events.

A contingency table illustrated in Figure 2.2 is then produced by totaling up the number of hits, misses, false alarms and correct negatives for a sufficiently large number of daily cases. Since the nominal verification period is one day, it makes sense to record a single case for each day and each fixed geographical region of each country. If more than one result is recorded for a particular day's forecast, for example, both a hit and a false alarm, then the result for that day should be divided by the number of different outcomes, 2 or 3. The result is the addition of 1 case to the totals of a, b, c and/or d for each day, though the 1 case may be partitioned over 2 or 3 boxes of the table. The sum total of the table in the bottom right corner will then equal the number of days times the number of separate geographical parts of the country for which observation data were available.

It might be most convenient to make two columns of ones and zeros, one each for the forecast and the observation. Then the logic functions of Excel, for example, can be used to automatically produce the totals of a, b, c and d over a sample of cases. A table which is built this way could include several columns for forecasts from different sources, for example, the Regional Specialized Meteorological Centres guidance, and the model output from each of the global centres. Each forecast, when combined with the observations, would lead to a different table. The different tables could be scored to give comparative results. Some examples of Excel spreadsheets are available with the electronic version of this publication:

Event forecast	Event observed		Marginal total
	Yes	No	
Yes	Hit	False alarm	Fc Yes
No	Miss	Correct non-event	Fc No
Marginal total	Obs Yes	Obs No	Sum total

↕

Event forecast	Event observed		Marginal total
	Yes	No	
Yes	a	b	a + b
No	c	d	c + d
Marginal total	a + c	b + d	a + b + c + d = n

Figure 2.5. The contingency table for dichotomous (yes–no) events (WMO, U. ,2014)

(a) European Centre for Medium Range Weather Forecasts calculator – deterministic model forecasts for eastern African locations, matched to observations from eastern African countries that were available on the Global Telecommunication Network (GTS) from September 2010 to May 2011.

(b) National Centers for Environmental Prediction calculator – deterministic model forecasts for eastern African locations, matched to observations from eastern African countries that were available on the Global Telecommunication Network from September 2010 to May 2011.

(c) Calculator, containing a sample of National Meteorological and Hydrological Service severe weather forecasts and observations from Botswana.

A description of how to use these Excel files to carry out verification of forecasts for specific locations and forecast projection times may also be found with the electronic version of this publication.

2.4.3 Calculating scores using the contingency table

Scores that can be computed from the contingency table entries are listed in this section, along with their characteristics, strengths and weaknesses. This is not an exhaustive list of scores that can be computed from the contingency table, but those listed here are considered to be the most useful for verification of severe weather forecasts. These scores are all functions of the entries of the contingency table as shown in Figure 2.3 and are easily computed. The formulae shown below are incorporated into the sample Excel spreadsheet available with the electronic version of this publication.

Computation of these scores should be considered part of analysis and diagnosis functions that are routinely performed by forecasters. These scores all have specific interpretations, discussed below, which help the forecaster perform these diagnosis tasks. The scores provide the most meaningful information if they are computed from large enough samples of cases, say 100 or so. However, severe weather occurrences are rare events, thus the number of forecasts and observations of severe weather may be small (fortunately), which makes the task of verification not only more important but also more challenging.

2.4.3.1 Probability of detection hit rate (*HR*) or prefigureance

The hit rate (*HR*) written in equation (2.1) has a range of 0 to 1 with 1 representing a perfect forecast. As it uses only the observed events *a* and *c* in the contingency table, it is sensitive only to missed events and not false alarms. Therefore, the *HR* can generally be improved by systematically over forecasting the occurrence of the event. The *HR* is incomplete by itself and should be used in conjunction with either the false alarm ratio or the false alarm rate both explained below.

$$HR = \frac{a}{a+b} \quad (2.1)$$

2.4.3.2 False alarm ratio (*FAR*)

The false alarm ratio (*FAR*) written in equation (2.2) is the ratio of the total false alarms (*b*) to the total events forecast (*a + b*). Its range is 0 to 1 and

a perfect score is 0. It does not include c and therefore is not sensitive to missed events. The FAR can be improved by systematically under forecasting rare events. It also is an incomplete score and should be used in connection with the HR .

$$FAR = \frac{b}{a+b} \quad (2.2)$$

2.4.3.3 Frequency bias (B)

The frequency bias (B) written in equation (2.3) hereinafter referred to as bias, uses only the marginal sums of the contingency table, and so is not a true verification measure, as it does not imply matching individual forecasts and observations. Rather, it compares the forecast and observed frequencies of occurrence of the event in the sample. The forecast is said to be unbiased if the event is forecast with exactly the same frequency with which it is observed, so that the frequency bias of 1 represents the best score. Values higher than one indicate over forecasting (too frequently) and values less than 1 indicate under forecasting (not frequent enough). When used in connection with the HR or the FAR , the bias can be used to explain the forecasting strategy with respect to the frequencies of false alarms or misses. Note that the bias also can be computed for the non-events, as $(c + d) / (b + d)$. If the frequency bias is computed for all the categories of the variable, then it gives an indication of the differences between the forecast and observed distributions of the variable.

$$Frequency = \frac{a+b}{a+c} \quad (2.3)$$

2.4.3.4 critical success index, CSI

The critical success index (CSI) written in equation (2.4), is frequently used as a standard verification measure, for example in the United States of America. It has a range of 0 to 1 with a value of indicating a perfect score. The CSI is more complete than the HR and FAR because it is sensitive to both missed events and false alarms. Thus, it is harder to adopt a systematic forecasting strategy that is

guaranteed to improve the score. It does, however, share one drawback with many other scores: it tends to go to 0 as the event becomes rarer. This score is affected by the climatological frequency of the event; if forecasts need to be compared (for example, same forecasts from different sources) using this score, but based on different verification samples, it might be wiser to use the equitable threat score (*ETS*) written in equation (2.5), which adjusts for the effects of differences in the climatological frequencies of the event between samples. For evaluation of a forecast or for comparison of the accuracy of forecasts based on the same dataset, the *CSI* is a good general score. The *ETS* is given by:

$$CSI = \frac{a}{a+b+c} \quad (2.4)$$

$$ETS = \frac{a - a_r}{a+b+c - a_r} \quad (2.5)$$

$$a_r = \frac{(a+b)(a+c)}{T} \quad (2.6)$$

where T is the sample size. The quantity a_r , written in equation (2.6), is the number of forecasts expected to be correct by chance, by just guessing the category to forecast.

2.4.3.5 The Heidke skill score (*HSS*)

In verification, the term skill has a very specific meaning: Skill is the accuracy of a forecast compared with the accuracy of a standard forecast. The standard forecast is usually chosen to be a forecast which is simple to produce, and may already be available to users. The idea of a skill score is to demonstrate whether the forecast offers an improvement over the choice of an unskilled standard forecast.

The Heidke skill score (*HSS*) written in equation (2.8), uses the number correct for both categories to measure accuracy, and the standard forecast is

a simple random guess which of the two categories will occur. The score is in the format:

$$ETS = \frac{(a-b) - \frac{(a+b)(a+c) + (c+d)(b+d)}{T}}{T - \frac{(a+b)(a+c) + (c+d)(b+d)}{T}} \quad (2.7)$$

$$HSS = \frac{Number_{correct} - Number_{chance}}{Total - Number_{chance}} \quad (2.8)$$

where the number correct by chance is the total number of forecasts, both severe and non-severe, that would be expected to be right just by random guessing. When forecasting severe weather, a guess could be made of which of the two categories would occur, like tossing a coin. Anyone can do this; there is no need to be a good forecaster. Yet, some of these guesses would by chance be correct. The idea of the Heidke skill score is to adjust for the number of forecasts that would be correct just by guessing.

The number correct by chance is defined in the same way as for the *ETS*, but both categories are used. The number of forecasts correct is simply the sum of the diagonal elements of the contingency table, (a + d).

The *HSS* ranges from negative values to +1. Negative values indicate that the standard forecast is more accurate than the forecast; skill is negative and a better score would have been obtained by just guessing what the forecast should be. The *HSS* represents the fraction by which the forecast improves on the standard forecast. A perfect forecast gives an *HSS* of 1, no matter how good the standard forecast is.

The *HSS* defined this way is the easiest to apply and use. All the information needed is contained in the contingency table. It turns out that pure chance offers a pretty low standard of accuracy. It is quite easy to improve on a chance forecast. Other standards of comparison are persistence (“no change from the observed weather at the time the forecast was issued” or “what you see is what you get”) or climatology, which for a categorical forecast is defined as the most likely of the two

categories. That is, a climatological forecast is a forecast of no severe weather all the time. This would not be a very useful forecast, but it would score well on most scores since (fortunately) no severe weather occurs much more often than severe weather. In the contingency table, d is much larger than a , b or c . A climatological forecast of no severe weather may therefore be difficult to beat. In practice, though, persistence and climatology are not often used in the *HSS*, because a separate contingency table for the reference forecast must be compiled.

2.4.3.6 The false alarm rate (*FA*)

The false alarm rate (*FA*) written in equation (2.9), is unfortunately often confused with the false alarm ratio. The false alarm rate is simply the fraction of observed non-events that are false alarms. By contrast, the false alarm ratio is referenced to the total number of forecasts; it is the fraction of forecasts that were false alarms. The best score for the *FA* is 0, that is, the wish is to have as few false alarms as possible. The *FA* is not often used by itself but rather is used in connection with the *HR* in a comparative sense. The *HR* is also referenced to the observations, specifically, the total number of observed events.

$$FA = \frac{b}{(b+d)} \quad (2.9)$$

2.4.3.7 The Hanssen–Kuipers score (*KSS*) (Pierce score) (true skill statistic (*TSS*))

The Hanssen–Kuipers score (*KSS*) written in equation (2.10), also known as the true skill statistic (*TSS*), is easiest to remember as the difference between the hit rate and the false alarm rate, as defined in 2.4.3.1 and 2.4.3.6, respectively. This score measures the ability of the forecast to distinguish between occurrences and non-occurrences of the event. The best possible score value is 1, which is obtained when the *HR* is 1 and the *FA* is 0. If $HR = FA$, then the score goes to 0, which is the worst value possible.

This score is used to indicate whether the forecast is able to discriminate situations that lead to the occurrence of the event from those that do not. If, for example, the forecaster attempts to improve the hits by forecasting the

event more often, this score will indicate whether too many false alarms are incurred by doing so. The idea is to increase the *HR* without increasing the *FA* too much.

One disadvantage of this score for rare events is that it tends to converge to the *HR* because the value of *d* becomes very large.

$$KSS = TSS = (HR - FA) = \frac{(ad - bc)}{(a + c)(b + d)} \quad (2.10)$$

2.5 Reference

- AGS (2007) **Guideline for landslide susceptibility, hazard, and risk zoning for land use planning**. Aust Geomech 42(1):13–36
- Corominas, J., & Moya, J. (2008). **A review of assessing landslide frequency for hazard zoning purposes**. Engineering geology, 102(3-4), 193-213. <https://doi.org/10.1016/j.enggeo.2008.03.018>
- Cruden, D. M. (1991). **A suggested method for a landslide summary**. Bulletin of the International Association of Engineering Geology-Bulletin de l'Association Internationale de Géologie de l'Ingénieur, 43(1), 101-110.
- Department of Mineral Resources 2019. **Department of Mineral Resources**, 75/10 Rama 6 Road, Thung Phayathai Sub-district, Ratchathewi District, Bangkok 10400, Thailand. webmaster@dmr.mail.go.th
- Department of Mineral Resources 2022. **Landslide susceptibility map** (last assess September 15th, 2022). <https://gis.dmr.go.th/DMR-GIS/gis>
- Highland, L., & Bobrowsky, P. T. (2008). **The landslide handbook: a guide to understanding landslides** (p. 129). Reston: US Geological Survey.
- Liu, C. N., & Wu, C. C. (2008). **Mapping susceptibility of rainfall-triggered shallow landslides using a probabilistic approach**. Environmental Geology, 55(4), 907-915.
- Naramngam, S., & Tangtham, N. (1997). **Application of GIS and factor of safety in determining landslide hazardous area in Tapi watershed, Changwat Nakhon Si Thammarat**. Warasan Wanasat.

- Pantanahiran, W. (1994). **The use of Landsat imagery and digital terrain models to assess and predict landslide activity in tropical areas** (Ph. D. Thesis).
- Revellino, P., Guadagno, F. M., & Hungr, O. (2008). **Morphological methods and dynamic modelling in landslide hazard assessment of the Campania Apennine carbonate slope**. *Landslides*, 5(1), 59-70.
- Soralump, S. 2007. **Corporation of Geotechnical Engineering data for landslide hazard map in Thailand**. EIT-JSCE Joint seminar on Rock Engineering, Bangkok, Thailand
- Varnes DJ (1978) **Slope movement types and processes**. In: Schuster RL, Krizek RJ (eds) *Landslides, analysis and control*, special report 176: Transportation research board, National Academy of Sciences, Washington, DC., pp. 11–33
- Varnes, D. J. (1984). **Landslide hazard zonation: a review of principles and practice (No. 3)**.
- WMO, U. (2014). **Forecast verification for the African severe weather forecasting demonstration projects**. World meteorological organization Geneva Switzerland, 38.
- Yumuang, S. (2006). **2001 debris flow and debris flood in Nam Ko area, Phetchabun province, central Thailand**. *Environmental Geology*, 51(4), 545-564

CHAPTER III

RAINFALL THRESHOLD FOR LANDSLIDE WARNING IN SOUTHERN THAILAND – AN INTEGRATED LANDSLIDE SUSCEPTIBILITY MAP WITH RAINFALL EVENT – DURATION THRESHOLD

3.1 Introduction

Since the year 2000, the number of landslides per year has been increasing in Thailand (Schmidt-Thomé et al., 2017). Southern Thailand lies on the narrow part of the Malay Peninsula the landforms comprise two parallel mountain chains running north–south: the Phuket and Nakhon Srithammarat ranges; situated to the west and east, respectively. According to the report from the Department of Mineral Resources in 2019, this region is one of Thailand’s hotspots for landslides. The landslides in 1988, which was known among of the worst natural disasters in the Thailand’s history, also occurred in the Southern Thailand. Works on landslide risk assessment constitute one of vital contributions in landslide mitigation measures. Since rainfall is commonly recognized as main temporal factor causing landslides, landslide rainfall threshold is commonly used as one of the vital components of landslide early warning system (Aleotti, 2004; Salee et al., 2022; Chinkulkijniwat et al., 2022). The most common parameters used to define the rainfall threshold are those based on characteristic of triggering landslide rainfall event (Caine, 1980; Aleotti, 2004; Guzzetti et al., 2008; Vennari et al., 2014; Vessia et al., 2014; He et al., 2020; Gariano et al., 2019; Peruccacci et al., 2017). Other than rainfall characteristics, a landslide can be influenced by many spatial factors, such as slope aspect, gradient, relative relief, lithology, degree of weathering, depth, permeability, porosity, etc. Incorporating these spatial factors to the rainfall threshold might enhance the efficiency of the landslide prediction. A landslide susceptibility map carries the relevant information; relating to geomorphology, geological, meteorological soil, land use, land cover and hydrologic conditions, of the terrain and classifies the terrain into zones with differing

likelihoods that landslides may occur. Integration of the landslide rainfall threshold and the landslide susceptibility map would benefit the landslide prediction. In fact, number of recent works reported the succession of the joint use of the landslide rainfall thresholds and the landslide susceptibility maps (Segoni et al., 2015; Jemec Auflic et al., 2016; Segoni et al., 2018). Recently, the Department of Mineral Resources updated Thailand landslide susceptibility maps for the provincial level (<https://gis.dmr.go.th/DMR-GIS/gis>). These maps present five landslide susceptibility levels; including very high, high, moderate, low, and very low landslide susceptibility levels. This study used these susceptibility maps as a proxy to include the spatial factors carried by the landslide susceptibility map to the landslide rainfall threshold in the Southern Thailand. A contingency table and a set of skill scores were used to assess the performance of the threshold.

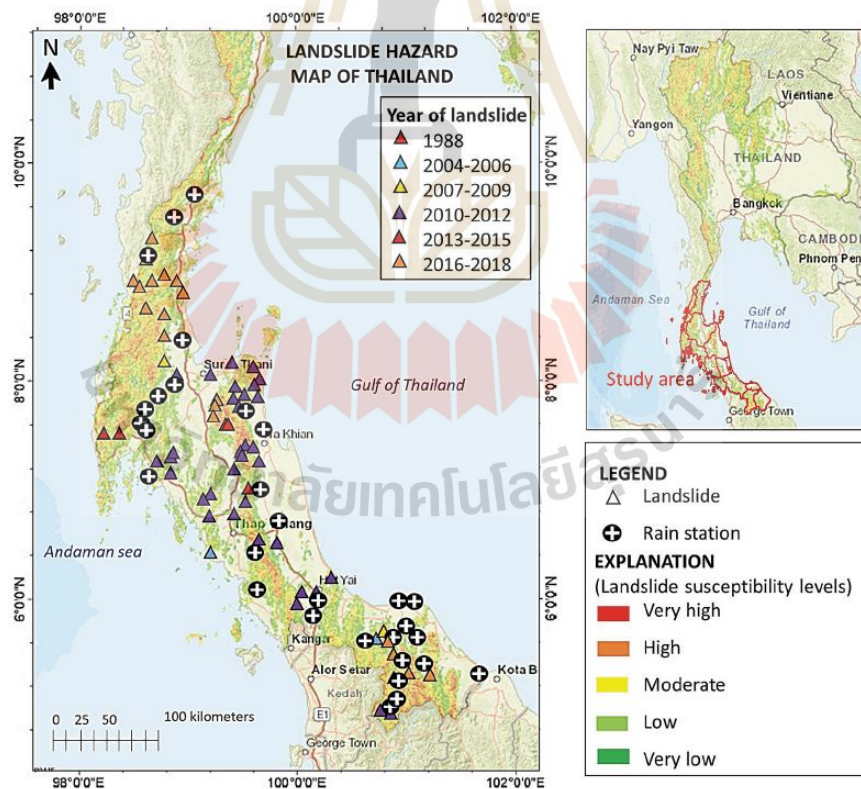


Figure 3.1 Locations of landslides and TMD rain gauge stations in the study area

Table 3.1 Duration of rainfalls that caused eighty landslides during 1988–2018 categorized by landslide susceptibility level

Duration (day)	Landslide susceptibility levels				
	Very high	High	Moderate	Low	Very low
1	7	1	0	0	0
2	1	2	0	0	0
3	2	10	0	0	0
4	0	5	7	0	0
5	1	5	0	0	0
6	0	3	0	0	0
7	0	5	6	0	0
8	0	2	0	0	0
9	0	3	0	0	0
10	0	0	1	3	0
11	0	0	4	7	0
12	0	0	1	1	0
13	0	0	0	3	0
Total	11	36	19	14	0

3.2 Data collection and rainfall characteristics in the study area

The authors gathered ninety-two landslide events that took place during 1988 to 2018 in the south of Thailand reported by the Department of Mineral Resources, Ministry of Natural Resources and Environment. Among ninety-two landslides, some landslides took place at the same time and their locations are close to each other. Under this condition, the largest landslide was chosen to represent the others. After this process, ninety-two landslides were reduced to eighty landslides. The Relevant rainfall data from the years when these eighty landslide events occurred were gathered from Thai Meteorological Department (*TMD*) rain gauge stations located in the catchment area (Figure 3.1) where the considered landslide is located. Inverse

distance weighting (*IDW*) was employed to map the amount of rainfalls at the landslide locations.

To identify a rainfall event, a criterion that separates two consecutive rainfalls must be defined. The criterion is defined by a combination of the rainfall intensity threshold *A* and rainfall duration *B* and termed as inter-event criterion ($IEC_{A,B}$). The condition that distinguished two consecutive rainfall events had to satisfy the combined criterion. On the basis of an assumption that inter-event times have an exponential distribution for which the mean equals the standard deviation (Bonta and Rao 1988), the suitable *IEC* was identified on the basis of a variation coefficient (*CV*) of inter-event times equal to 1.0. Salee et al. (2022) reported that the inter-event criterion of $IEC_{2,1}$ can be used to distinguish two consecutive rainfalls in Southern Thailand. Accordingly, a criterion $IEC_{2,1}$ was used as the inter-event criterion to distinguish two consecutive rainfalls collected in this study. Distinction of two consecutive rainfall events is a condition that satisfied the combined criterion. As depicted in Figure 3.2, if rainfall intensity is no greater than 2 mm/day for at least 1 day, two consecutive rainfall events are considered to have occurred.

Regarding to the landslide susceptibility maps published by the Department of Mineral Resources, there are five susceptibility levels of landslide; very low susceptibility (green color), low susceptibility (light green color), moderate susceptibility (yellow color), high susceptibility (orange color), and very high susceptibility (red color). Eighty landslide locations were mapped to the corresponding susceptible maps for the provincial level to identify the landslide susceptibility level at those locations. Figure 3.3 presents three landslides took place in Krung Ching subdistrict, Nopphitam district, Nakhon Si Thammarat (the other landslides had been mapped to the corresponding susceptibility maps in a similar manner). Table 3.1 summaries, from eighty landslides, the number of landslide events took place for each landslide susceptibility level in the Southern Thailand. A greater number of landslides was found for the higher landslide susceptibility level. However, the number of landslides for very high susceptibility was small. It was because the places classified as very high susceptibility level were generally far from communities; hence, many landslides were neglected and not

reported. Table 3.1 also presents, from the triggering rainfall events, distribution of duration for the rainfalls that triggered the landslides at the places of different susceptibility levels. There is no doubt that many of the landslides at the very high susceptibility places were caused by rainfall events that lasts for only one-day. In turn, no landslide at very low to moderate susceptibility places occurred with rainfall duration less than 4 days.

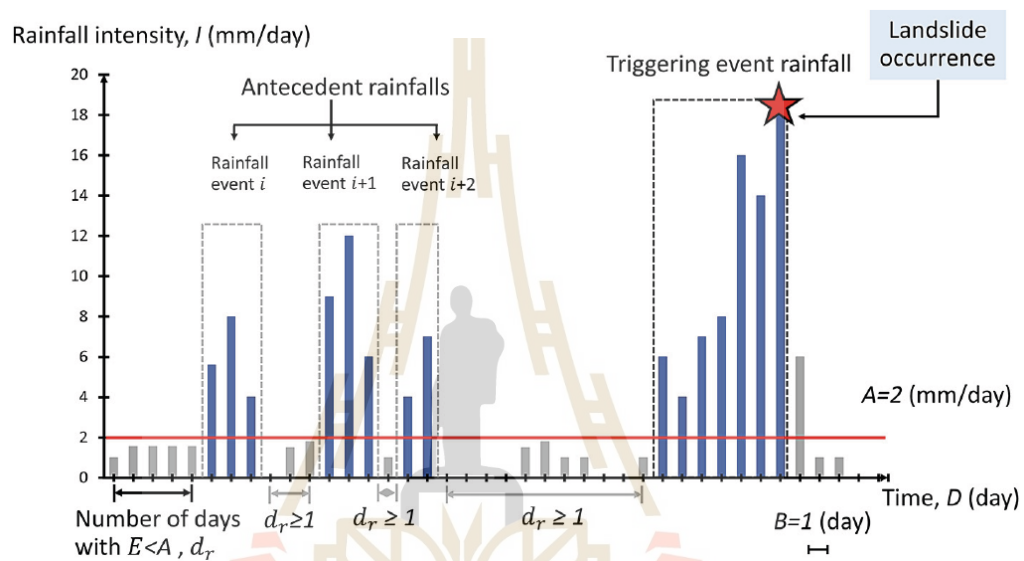


Figure 3.2 Definition of inter-event criteria used to separate two consecutive rainfalls in this study

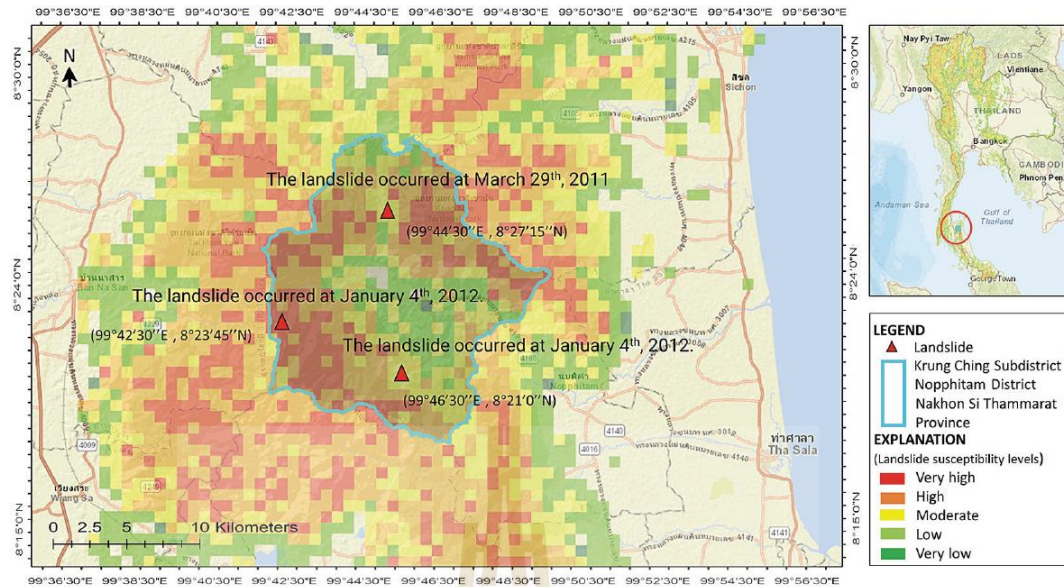


Figure 3.3 Landslide susceptibility map for Krung Ching subdistrict, Nopphitam district, Nakhon SiThammarat and locations of landslide took place in this area (<https://gis.dmr.go.th/DMR-GIS/gis>)

3.3 Landslide triggering rainfall thresholds and the assessment

Figure 3.4 presents the rainfall event (E) and rainfall duration (D) data points of non-triggering-rainfalls (open circles) and triggering-rainfalls (gray circles) plotted on a double logarithmic scale. On the basis of Eq. 1, the landslide rainfall threshold was analyzed from rainfall event (E) and duration (D) of triggering-rainfalls,

$$\log_{10} E = a + b \log_{10} D \tag{3.1}$$

where: a and b are regression coefficients.

With the above-mentioned relationship, the threshold gave a straight line in double logarithmic scale. Quantile regression (Koenker and Bassett, 1978; Koenker and Hallock, 2001; Koenker, 2009) was employed to fit the specified percentiles of the triggering events. The ED threshold given at various probability levels from 5–90% was presented in Figure 3.4. The corresponding magnitudes of parameters a and b for the ED threshold are given in Table 3.2.

For ease of incorporating the landslide susceptibility level to the rainfall threshold, the susceptibility level was re-categorized from five levels to two levels; termed as the modest susceptibility level and the huge susceptibility level. The modest level is the combination of the very low, low, and moderate susceptibility levels indicated in the landslide susceptibility maps. The huge level is the combination of the high, and very high susceptibility levels indicated in the landslide susceptibility maps. Among eighty events, thirty-three and forty-seven events occurred at the locations classified as the modest level and the huge level, respectively. Figure 3.5a presents rainfall event (E) and rainfall duration (D) data points of non-triggering-rainfalls (open circle) and triggering-rainfalls (colored circle) plotted on a double logarithmic scale. Indeed, this plot is Figure 3.4 modified by grouping the data with susceptibility levels (the modest level and the huge level). The green color plots are for the rainfalls that took place at the modest susceptibility places and the red color plots are for the rainfalls that took place at the huge susceptibility places. The ED threshold for the modest level places (ED^m threshold) and that for the huge level places (ED^h threshold) at various probability levels together with scatter plots, in double logarithmic rainfall event–duration plane, of non-triggering and triggering-rainfalls are given in Figure 3.5b. The threshold parameters a and b for exceedance probabilities from 5 to 90% of the ED^m and ED^h thresholds are given in Table 3.2.

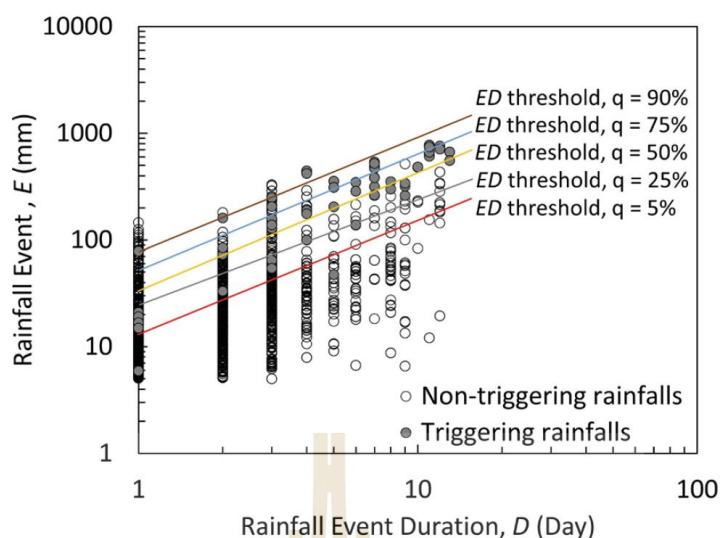


Figure 3.4 Relationship between rainfall event (E) and its duration (D) form triggering rainfalls and non-triggering rainfalls in the Southern Thailand. Gray circles represent the triggering rainfalls that caused landslides and open circles represent the non-triggering rainfall events. The ED threshold drawn from quantile regression at various probability levels of triggering rainfall events

Table 3.2 Threshold parameters a and b for the ED , ED^m , and ED^h thresholds at exceedance probabilities from 5 to 90%

Probabilistic level (%)	ED parameters		ED^m parameters		ED^h parameters	
	a	b	a	b	a	b
5	3.322	1.130	1.283	1.188	1.065	1.508
10	1.992	1.689	1.223	1.342	1.081	1.523
25	0.773	1.932	1.650	0.922	1.226	1.455
50	1.322	1.444	1.565	1.206	1.555	1.204
75	1.833	1.008	1.626	1.197	1.943	0.870
80	1.893	0.941	1.827	1.019	2.004	0.805
85	1.965	0.888	1.827	1.020	1.962	0.892
90	2.045	0.810	2.260	0.604	1.962	0.908

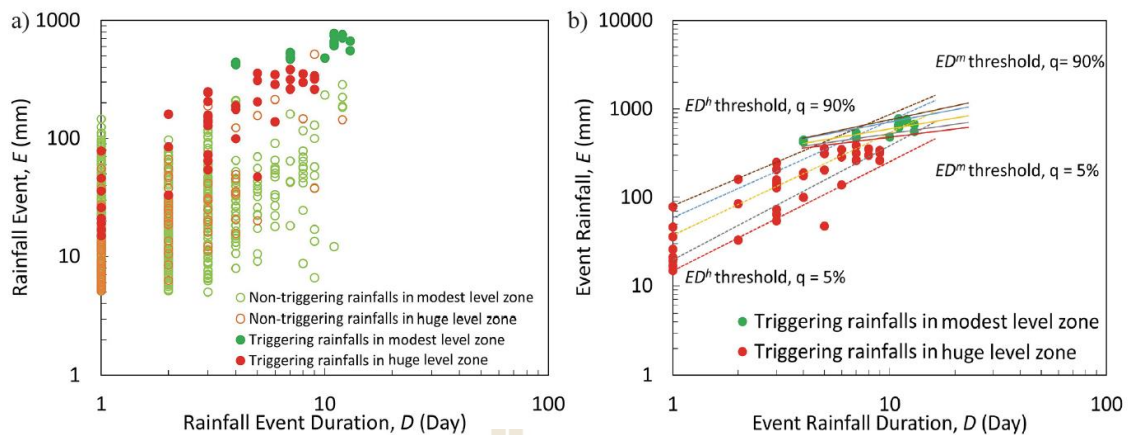


Figure 3.5 a) Relationship between rainfall event (E) and its duration (D) from triggering rainfalls and non-triggering rainfalls in the Southern Thailand. Red circles represent the triggering rainfalls that caused landslides at the huge susceptibility places and green circles represent that at the modest susceptibility places. In turn, open green circles and open red circles are for the non-triggering rainfalls in the modest and huge susceptibility places, respectively. b) The ED^m and ED^h thresholds drawn from quantile regression at various probability levels of triggering rainfalls at the modest and the huge susceptibility places, respectively

3.4 Assessment of the thresholds

The aforementioned thresholds were assessed through a contingency table and a receiver operating characteristic (ROC) curve. There are four scenarios in contingency table; including (1) true positives (TP), (2) true negative (TN), (3) false positive (FP), and (4) false negative (FN). Figure 3.6 presents TP, FN, FP, and TN defined from threshold value and distribution curve of triggering rainfall events and those of non-triggering rainfall events. TP indicated the cases in which landslides were correctly predicted, FN indicated the cases in which landslides took place without prediction, FP indicated the cases in which landslides were forecasted but did not take place, and TN stood for the correct prediction of a rainfall event without a landslide. These contingencies were employed to calculate the following skill scores; i) a hit rate (HR) which is defined as number of correct prediction per total number of

event rainfall: $HR = TP / (TP + FN)$, ii) a false alarm rate (FAR) which is defined as number of false alarm per the total number of non-event rainfall: $FAR = FP / (FP + TN)$, and iii) Hanssen and Kuipers skill score (HK): $HK = HR - FAR$. HK is proportional to the frequency of events being forecast by equal emphasis on ability to forecast both events and nonevents. The receiver operating characteristic curves (ROC curve), HR against FAR , was plotted at various probabilistic levels of landslide threshold and the areas under the ROC curves (AUC) were determined. At each threshold probabilistic level, the Euclidean distance δ was calculated from the distance between the point corresponding to the threshold on the ROC curve and the perfect point of coordinate (0,1).

Assessment of the thresholds was conducted by considering triggering and non-triggering rainfall events that took place at the places corresponding to the established thresholds. For the ED threshold, the rainfall events that took place in the whole study area were employed for the assessment. In turn, for the assessment of the ED^m and ED^h thresholds, only the rainfall events at the places classified to the corresponding susceptibility levels were employed. Furthermore, the considered data indicated that the rainfall events that caused landslides at the modest level places had duration no shorter than 4 days; the authors of this paper implied that the rainfall events of their duration shorter than 4 days did not cause landslides at the modest level places. Hence, for the rainfalls at the modest level places, only the rainfall events having their duration no shorter than 4 days were used for the assessment of ED^m threshold.

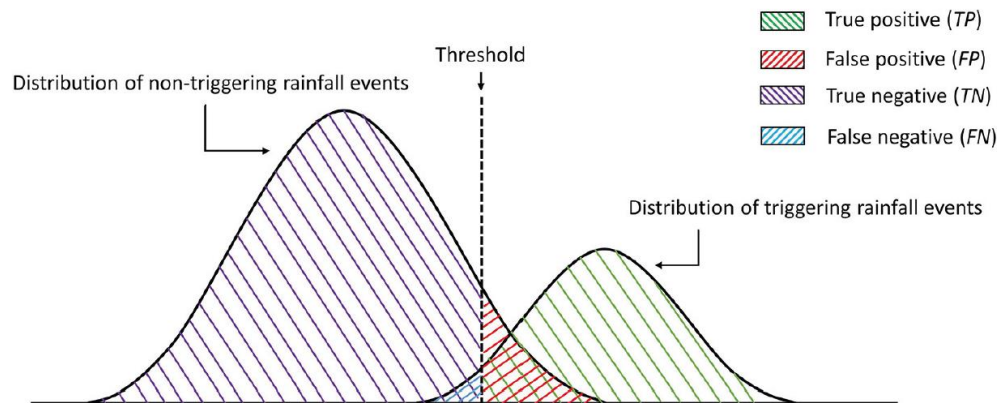


Figure 3.6 Distribution of triggering and non-triggering rainfalls and the threshold to define the meaning of true positive (TP), true negative (TN), false positive (FP), and false negative (FN)

3.5 Results and discussions

Table 3.3 summarizes the four contingencies (TP , FP , FN , TN) and the four skill scores (HR , FAR , HK , δ) for ten probabilistic levels (from 5 to 90%) from the ED , the ED^m and the ED^h thresholds. The best compromise between the minimum number of incorrect landslide predictions (FP , FN) and the maximum number of correct predictions (TP , TN), indicated by combination of the largest values for the HK and the smallest value of the δ , were obtained at 15%, 5%, and 10% for the ED , the ED^m , and the ED^h thresholds, respectively. Since the assessment of ED^m threshold was conducted by considering only the rainfall events having a duration no shorter than 4 days, the number of rainfall in contingency table for the ED^m threshold was not as high as that reported in the contingency table for the ED^h threshold.

Figure 3.7 presents the ROC curves obtained from the ED , ED^m , and ED^h thresholds. The areas under the ROC curves (AUC), indicating prediction capability, are also reported in Figure 3.7. Incorporating landslide susceptibility into the threshold resulted in an improvement of the threshold performance. Even at very high and high landslide susceptibility places, the threshold established particularly these zones (ED^h threshold) which exhibited significantly better performance ($AUC = 0.89$) than the ED threshold ($AUC = 0.71$). Since there was no non-triggering rainfall

event laid above the ED^m threshold, this threshold yielded FAR of 0.0 at every probabilistic level. This character was expressed through the ROC curve of the ED^m threshold that indicated perfect performance with AUC of 1.00. The years in which landslides occurred at very low to moderate landslide susceptibility places are presented in Table 3.4. Twenty landslides from thirty-three landslides took place in two periods (gray shaded rows in Table 4.4); 1) the period from the late 2010 to the early 2011, and 2) the year 2017. During the period from late 2010 to the early 2011, there were fourteen landslides were reported in this study. For late 2010, a tropical depression in November over Southern Thailand caused very heavy rain occupied widely over southern east-coast. Lastly, the daily maximum rainfall recorded 396 mm/day at Don Sak, Surat Thani. Thereafter in March 2011, an active low pressure cell caused intense rainfall over the Southern Region of Thailand, resulting in unprecedented flash floods and landslides in many provinces in Southern of Thailand. It was noted that in 2011, Thailand experienced the worst flood in over fifty years, as volume of flood water occupied more than half the country. For the 2017, there were six landslides reported in our study. In this year, a significantly strong southwest monsoon extended over Southern Thailand in January resulting in series of torrential rainfalls. The total amount of rainfall from December 30th to January 31st exceeded 1,000 mm in many provinces. According to Jin and Fu (2019), the maximum 24-h accumulated precipitation of up to 330 mm appeared around Nakhon Si Thammarat province on January 5th and the maximum 24-h accumulated precipitation of up to 420 mm appeared around the Pattani province on January 7th. In short, the locations classified to the zone of very low to moderate landslide susceptibility could suffer from landslide only if they experience unusual torrential rainfalls. The ED^m threshold established in this study laid above rainfall event of 400 mm which could represent unusual torrential rainfalls, and hence 100% of usual rainfalls were not predicted.

Table 3.3 Summary of the four contingencies (TP , FP , FN , TN) and the four skill scores (HR , FAR , HK , δ) obtained from the ED , ED^m , and ED^h thresholds for nine probabilistic levels

Threshold	Probabilistic level (%)	Contingencies and skill scores							
		TP	FN	TN	FP	HR	FAR	HK	δ
ED	5	77	3	848	1312	0.96	0.61	0.36	0.61
	10	72	8	884	1276	0.9	0.59	0.31	0.6
	15	62	18	1299	861	0.78	0.4	0.38	0.46
	25	40	40	1358	802	0.5	0.37	0.13	0.62
	50	21	59	2026	134	0.26	0.06	0.2	0.74
	75	15	65	2046	114	0.19	0.05	0.13	0.81
	80	12	68	2091	69	0.15	0.03	0.12	0.85
	85	8	72	2123	37	0.1	0.02	0.08	0.9
	90	4	76	2149	11	0.05	0.01	0.04	0.95
ED^m	5	28	3	151	0	0.9	0	0.9	0.1
	10	26	5	151	0	0.84	0	0.84	0.16
	15	26	5	151	0	0.84	0	0.84	0.16
	25	23	8	151	0	0.74	0	0.74	0.26
	50	17	14	151	0	0.55	0	0.55	0.45
	75	8	23	151	0	0.26	0	0.26	0.74
	80	5	26	151	0	0.16	0	0.16	0.84
	85	6	25	151	0	0.19	0	0.19	0.81
	90	4	27	151	0	0.13	0	0.13	0.87
ED^h	5	46	1	800	301	0.98	0.27	0.71	0.27
	10	43	4	846	255	0.91	0.23	0.68	0.25
	15	41	6	859	242	0.87	0.22	0.65	0.25
	25	35	12	900	201	0.74	0.18	0.56	0.31
	50	24	23	1052	49	0.51	0.04	0.47	0.49
	75	11	36	1069	32	0.23	0.03	0.2	0.77
	80	11	36	1078	23	0.23	0.02	0.21	0.77
	85	6	41	1081	20	0.13	0.02	0.11	0.87
	90	3	44	1086	15	0.06	0.01	0.05	0.94

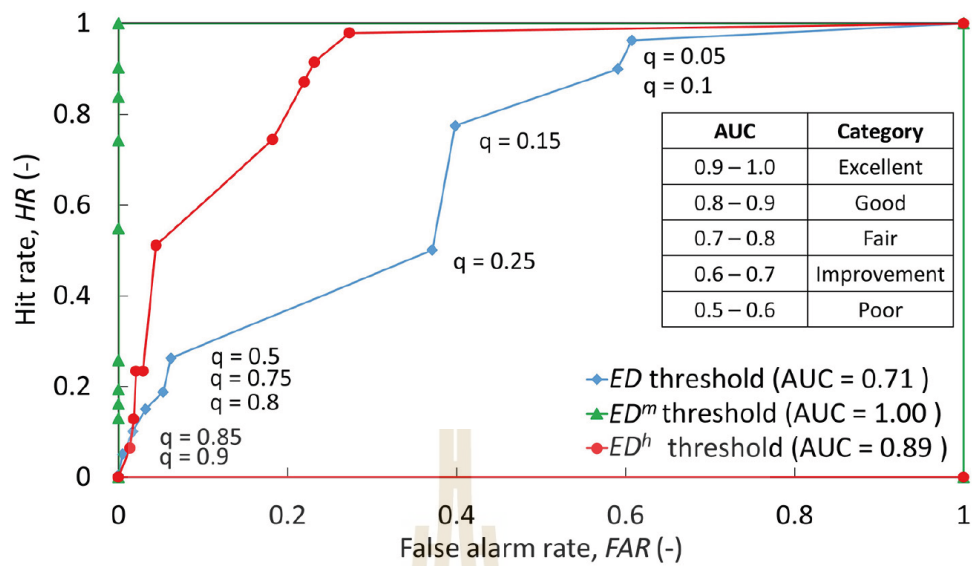


Figure 3.7 Receiver operating characteristic (ROC) and corresponding area under the ROC curve (AUC) of the ED , ED^m and ED^h thresholds

Table 3.4 Number of landslides with respect to time that landslide occurred at the very low to moderate susceptibility places

Month	Year	Number of landslides in modest susceptibility places		
		Moderate	Low	Very low
1988–2009		4	2	-
Nov.	2010	3	3	-
Mar.	2011	3	5	-
Jan.	2012	2	1	-
Jul.	2013	1	-	-
Nov.	2013	-	-	-
Oct.	2014	-	1	-
Jan.	2017	4	2	-
Jul.	2017	-	-	-
Sep.	2017	-	1	-
Nov.	2017	1	-	-
Dec.	2017	-	-	-
Mar.	2018	-	-	-
Jul.	2018	-	-	-
Aug.	2018	1	-	-

3.6 Conclusions

Landslide rainfall threshold based on rainfall event and rainfall duration (ED threshold) was proposed for landslide prediction in the Southern Thailand. Other than rainfall characteristic, a landslide can be influenced by various spatial factors, such as slope conditions, lithology, soil type, and hydrologic conditions. Incorporation of such factors to the rainfall threshold might enhance the predictability of the rainfall threshold. For this purpose, the landslide susceptibility maps at provincial level published by the Department of Mineral Resources (<https://gis.dmr.go.th/DMR-GIS/gis>) were used as a proxy to allow the connection between the ED threshold and the spatial factors. To facilitate the process, five susceptibility levels, ranging from very low to very high, indicated in the landslide susceptibility maps, were regrouped to two susceptibility levels (the modest and the huge susceptibility levels). The modest susceptibility level was a combination of very low, low, and moderate susceptibility levels indicated in the maps. The huge susceptibility level was a combination of high and very high susceptibility levels indicated in the map. Two ED thresholds, namely ED^m and ED^h thresholds, were introduced, each for different susceptibility level. The ED^m threshold was established for landslide warning at the places classified as very low to moderate susceptibility levels, while the ED^h threshold was established for the places classified as high and very high susceptibility levels. The following conclusions were drawn from this study:

1) On the basis of the rainfall event that triggered 99 landslides in Southern Thailand in 1988– 2018, a rainfall event-duration (ED) threshold was introduced for landslide warning in the whole Southern Thailand. However, the predictability of the ED threshold was fair with an area under a receiver operating characteristic curve (AUC) of 0.71.

2) Integration of the landslide rainfall threshold and the landslide susceptibility map gave a new set of ED thresholds (ED^m and ED^h thresholds). These thresholds provided much better predictions than the original ED threshold. The AUC for the ED^h threshold was 0.89 comparing with AUC of 0.71 for the ED threshold. In turn, the ED^m threshold provided perfect prediction with AUC of 1.00.

3) For the landslides reported in this study, it was found that the landslides in very low to moderate landslide susceptibility level zones were triggered only by the rainfall events having duration no shorter than 4 days. Under these conditions, many rainfall events with their duration shorter than 4 days were filtered out before the assessment of the ED^m threshold. Furthermore, the cumulated rainfall of triggered events was found greater than 400 mm, indicating that landslides in such places would be triggered by unusual torrential rainfall.

3.7 References

- Aleotti P. 2004. **A warning system for rainfall-induced shallow failures.** Eng Geol.,73, 247–265. <https://doi.org/10.1016/j.enggeo.2004.01.007>
- Bonta J.V., Rao A.R. 1988. **Factors affecting the identification of independent storm events.** Journal of Hydrology, 98(3–4), 275–293. [https://doi.org/10.1016/0022-1694\(88\)90018-2](https://doi.org/10.1016/0022-1694(88)90018-2)
- Caine, N. 1980. **The Rainfall Intensity: Duration Control of Shallow Landslides and Debris Flows.** Geografiska Annaler. Series A, Physical Geography, 62(1/2), 23–27. <https://doi.org/10.2307/520449>
- Chinkulkijniwat A., Salee R., Horpibulsuk S., Arulrajah A., Hoy M. 2022 **Landslide rainfall threshold for landslide warning in Northern Thailand,** Geomatics, Natural Hazards and Risk, 13(1), 2425–2241. <https://doi.org/10.1080/2022.2120833>
- Department of Mineral Resources 2019. **Department of Mineral Resources,** 75/10 Rama 6 Road, Thung Phayathai Sub-district, Ratchathewi District, Bangkok 10400, Thailand. webmaster@dmr.mail.go.th
- Department of Mineral Resources 2022. **Landslide susceptibility map** (last assess September 15th, 2022). <https://gis.dmr.go.th/DMR-GIS/gis>
- Gariano S.L., Melillo M., Peruccacci S., Brunetti M.T. 2019. **How much does the rainfall temporal resolution affect rainfall thresholds for landslide triggering?** Natural Hazards, 100, 655–670. <https://doi.org/10.1007/s11069-019-03830-x>.

- Guzzetti F., Peruccacci S., Rossi M., Stark C.P. 2008. **The rainfall intensity-duration control of shallow landslides and debris flows: an update.** *Landslides*, 5, 3–17. <https://doi.org/10.1007/s10346-007-0112-1>
- He S., Wang J., Liu S. 2020. **Rainfall Event–Duration Thresholds for Landslide Occurrences in China.** *Water* 12(2), 494. <https://doi.org/10.3390/w12020494>
- Jemec Auflič M., Šinigoj J., Krivic M., Podboj M., Peternel T., Komac M. 2016. **Landslide prediction system for rainfall induced landslides in Slovenia (MaspremGeologija, 59, 259–271.** <https://doi.org/10.5474/geologija.2016.016>
- Jin S., Fu S. 2020. **Mechanisms accounting for the repeated occurrence of torrential rainfall over South Thailand in early January 2017,** *Atmospheric and Oceanic Science Letters*, 13(2), 155–162. <https://doi.org/10.1080/16742834.2019.1706427>
- Koenker R., Bassett G. 1978. **Regression Quantiles.** *Econometrica* 46(1), 33. <https://doi.org/10.2307/1913643>
- Koenker R. 2009. **Quantile Regression in R: A Vignette.** Available at <http://www.econ.uiuc.edu/~roger/research/rq/vig.pdf>.
- Koenker R., Hallock K. F. 2001. **Quantile regression.** *Journal of Economic Perspectives*, 15(4), 143–156. <https://doi.org/10.1257/jep.15.4.143>
- Salee R, Chinkulkijniwat A., Yubonchit S., Horpibulsuk S., Wangfaoklang C., Soisompong S. 2022. **New threshold for landslide warning in the southern part of Thailand integrates cumulative rainfall with event rainfall depth-duration.** *Natural Hazards*, 113(1), 125–141. <https://doi.org/10.1007/s11069-022-05292-0>
- Schmidt-Thomé P., Tatong T., Kunthasap P., Wathanaprida S. 2018. **Community based landslide risk mitigation in Thailand.** *Episodes*, 41(4), 225–233. <https://doi.org/10.18814/epiiugs/2018/018017>
- Segoni S., Lagomarsino D., Fanti R., Moretti S., Casagli N. 2015. **Integration of rainfall thresholds and susceptibility maps in the Emilia Romagna (Italy) regional - scale landslide warning system.** *Landslides*, 12, 773–785. <https://doi.org/10.1007/s10346-014-0502-0>.

- Segoni S., Tofani V., Rosi A., Catani F., Casagli N. 2018. **Combination of Rainfall Thresholds and Susceptibility Maps for Dynamic Landslide Hazard Assessment at Regional Scale**. *Front. Earth Sci.*, 6, 85. <https://doi.org/10.3389/feart.2018.00085>
- Vennari C., Gariano S.L., Antronico L., Brunetti M.T., Iovine G., Peruccacci S., Guzzetti F. 2014. **Rainfall thresholds for shallow landslide occurrence in Calabria, southern Italy**. *Natural Hazards and Earth System Sciences*, 14(2), 317–330. <https://doi.org/10.5194/nhess-14-317-2014>.
- Vessia G., Parise M., Brunetti M.T., Peruccacci S., Rossi M., Vennari C., Guzzetti F. 2014. **Automated reconstruction of rainfall events responsible for shallow landslides**. *Natural Hazards and Earth System Sciences*, 14(9), 2399–2408. <https://doi.org/10.5194/nhess-14-2399-2014>.



CHAPTER IV

NEW THRESHOLD FOR LANDSLIDE WARNING IN THE SOUTHERN PART OF THAILAND INTERGRATES CUMULATIVE RAINFALL WITH EVENT RAINFALL DEPTH-DURATION

4.1 Introduction

Landslides are considered as one of major natural hazards that result in economic and human losses every year. Risk analysis and assessment is an important tool for landslides management. In fact, risk assessment has been broadly applied in various geotechnical works (Lyu et al. 2020; Lin et al. 2021a, b, c; Kardani et al. 2021; Zheng et al. 2021). As for risk assessment in landslides, reliable landslides early warning system (LEWS) is one of the vital components. Because of ease in measurement of their monitoring variables, landslide rainfall thresholds are extensively used as part of developing an efficient LEWS. Since Thailand is not among the world's landslide hotspots, limited attempts have been devoted to establish landslide rainfall threshold in Thailand. According to Segoni et al. (2018), there is only one landslide rainfall threshold in Thailand (Kanjanaikul et al. 2016) published in journals indexed in Scopus or ISI Web of Knowledge database during 2008–2016. It is a threshold, which was defined using monthly rainfall measures, established for a very specific place, i.e., at Sichon District in Nakhon Si Thammarat Province, Southern Thailand. However, landslide events in Thailand have caused significant damage to residents and infrastructure, and loss of human life as reported in Phien-Wej et al. (1993), Yumuang (2006). Accordingly, this study aims to determine the appropriate landslide-triggering rainfall threshold for the south of Thailand. The south of Thailand sits on a narrow peninsula between the Gulf of Thailand to the east and the Andaman Sea to the west. As reported by Arai et al. (2019), the mean annual rainfall in the south during 1981–2017 was more than 2000 mm, versus about 1500 mm from the center to the northern and northeastern regions in this country.

According to Department of Mineral Resources (2019), this region experiences rainfall-triggered landslides most frequently comparing to other regions of Thailand.

There are ways the threshold can be determined: using a physical approach or an empirical approach. Since the physical approach requires high-resolution images and relevant data such as groundwater conditions, shear strength of sloping soils, and geological soil profiles, it is more suitable for the assessment of conditions over small areas (Guzzetti et al. 2007a, b). The empirical approach, which is more widely employed, uses the statistical analysis of rainfall datasets collected in the area that experienced the rainfall-triggered landslide. The thresholds established by the empirical approach can be grouped into three categories: (1) thresholds obtained from precipitation measurements for specific landslide events, (2) thresholds based on cumulative or antecedent rainfall conditions, and (3) other thresholds, incorporating hydrological thresholds (Guzzetti et al. 2007a, b). Thresholds in the first category are the most widely used since they are easy to establish and require few input data (Rosi et al. 2020). The most commonly used type of rainfall threshold is the intensity–duration (*ID*) threshold. Since the introduction of the first global *ID* threshold by Caine (1980), reports have been published about the threshold by Peruccacci et al. (2012); Segoni et al. (2014); Gariano et al. (2015); Peruccacci et al. (2017); and Guzzetti et al. (2005a) and (2005b). The literature also contains reports about the rainfall eventduration (*ED*) threshold (Vennari et al. 2014; Vessia et al. 2014; He et al. 2020; Gariano et al. 2020; Peruccacci et al. 2017). Gariano et al. (2020) pointed out that the two rainfall variables in the *ED* threshold are not dependent on each other, whereas in the case of the *ID* threshold, the average rainfall intensity depends on the rainfall duration. For this reason, the *ED* threshold was preferred in this study since two rainfall parameters must be considered independently.

One key important of determining a threshold based on a precipitation event is the identification of the starting point of the rainfall event (Guzzetti et al. 2008). To resolve this problem, studies by Kim et al. (1991); Dahal and Hasegawa (2008); Glade (2000); Hasnawir and Kubota (2008); Giannecchini et al. (2012); and Khan et al. (2012), focused either on the relationship between daily rainfall and cumulative rainfall or used *ID* thresholds established from continuous rainfall events. This approach avoids

the need to identify the start point of a rainfall event. Furthermore, the rainfall event and the cumulative rainfall are implicitly incorporated. Although this approach underpins reports that both event and antecedent rainfalls influence slope stability (Rahardjo et al 2011; Rahimi et al. 2011; Wicki et al. 2020; Rosi et al. 2020; Kim et al. 2020; Yang et al. 2020), it might lead to misinformation in some magnitudes of event rainfall. Based on the aforementioned concerns, this paper aims to: (1) establish an *ED* threshold for the south of Thailand through a suitable criterion that identifies the starting point of event rainfall and (2) explicitly incorporate a cumulative rainfall variable to the event rainfall threshold.

4.1.1 Data collection

Ninety-two landslide events that took place in the south of Thailand from 1988 to 2018 were considered. Data were collected mainly from scientific papers published by the Department of Mineral Resources, Ministry of Natural Resources and Environment and partly from local newspapers. Landslide information had to convey at least the following details: (1) the date of the occurrence of the landslide, (2) the location of the landslide event, and (3) consequential damages. Among 92 events, 50 events took place on the east side of the study area and the 42 events took place on the west side. The rainfall data associated with each landslide were gathered from Thai Meteorological Department (TMD) rain gage stations located in the catchment area where the considered landslide is located. The locations of landslide events and TMD rain gage stations in the study area are indicated in Figure. 4.1. Inverse distance weighting (*IDW*), which assigned a larger weight, based on inverse functions of distance, to a station closer to a landslide location than a station further away, is most commonly used method and usually used as standard method for comparison (Li et al. 2011). Although it is deterministic or non-geostatistic modeling, number of literatures reports that *IDW* is one of reliable methods for spatial interpolation in various applications, i.e., point spread function (Gentile et al. 2012), baseflow and baseflow index (Ditthakit et al. 2021). As for interpolation of rainfall data, Kong and Tong (2008), Kurtzman et al. (2009), Chen et al. (2010), Yang et al. (2015), among others, reported successful application of *IDW* in various locations. Accordingly, *IDW* was employed in this study to approximate

rainfall data at the landslide locations. Figure 4.2 presents the distribution of landslide events on the west side (Figure. 4.2a) and the east side (Figure. 4.2b) with respect to the different monsoon periods: southwest, northeast, and pre-monsoons. The southwest monsoon blows from the Indian Ocean during June to September. It brings more rain to the west side than the east. During November to January, northeasterly winds bring heavy rainfall to the east side. As expected, on the east side, more landslides (46%) occurred during the northeast monsoon than at any other time, while more landslides (43%) on the west side occurred during the southwest monsoon. On the west side, 36% of landslides took place during the pre-monsoon period compared to 16% on the east side.

4.1.2 Geological setting of the study area

Southern Thailand lies on the narrow part of the Malay Peninsula whose landforms comprise two parallel mountain chains running north–south: the Phuket and Nakhon Srithammarat ranges; situated to the west and east, respectively. Alluvial fans, foothills, alluvial plains, and coastal plains can be found alongside the ranges. Geologically, the southern part of Thailand consists of a succession of Paleozoic and Mesozoic sedimentary and metamorphic rocks, intruded by Late Paleozoic to Mesozoic igneous rocks, and covered by Cenozoic sedimentary rock or sediments. According to Ridd et al. (2011), the upper part of the study area is dominated by upper Paleozoic sedimentary rock, which is intruded by chains of granitic bodies rising up to 1000 m in height through forested mountains. The lower part of the study area comprises a main chain of granitic mountains which continues north into the Gulf of Thailand, forming islands such as Koh Samui, Koh Phangang, and Koh Tao. Khao Luang, where the worst landslide disaster in Thailand took place in 1988, belongs to this chain of granite bodies. Since many landslides have occurred on Khao Luang, reports of landslide investigations in this area have indicated that most landslides developed within a thin layer of residual soil even though the weathering of granite was more than 10 m deep

Due to the tropical temperatures and high annual precipitation, weathering of granitic rocks in the study area is generally deep. The residual soils consist of a thin capping veneer of sandy to silty clay which changes transitionally to

a clayey to silty, coarse sand layer that preserves some relics of the rock structure. This layer, which is very hard but friable when dry, becomes weak when wet. Its medium permeability permits easy water filtration and a build-up of high-water pressure underneath the capping layer. These physical characteristics of the weathered materials make them susceptible to slide or flow on steep slopes.

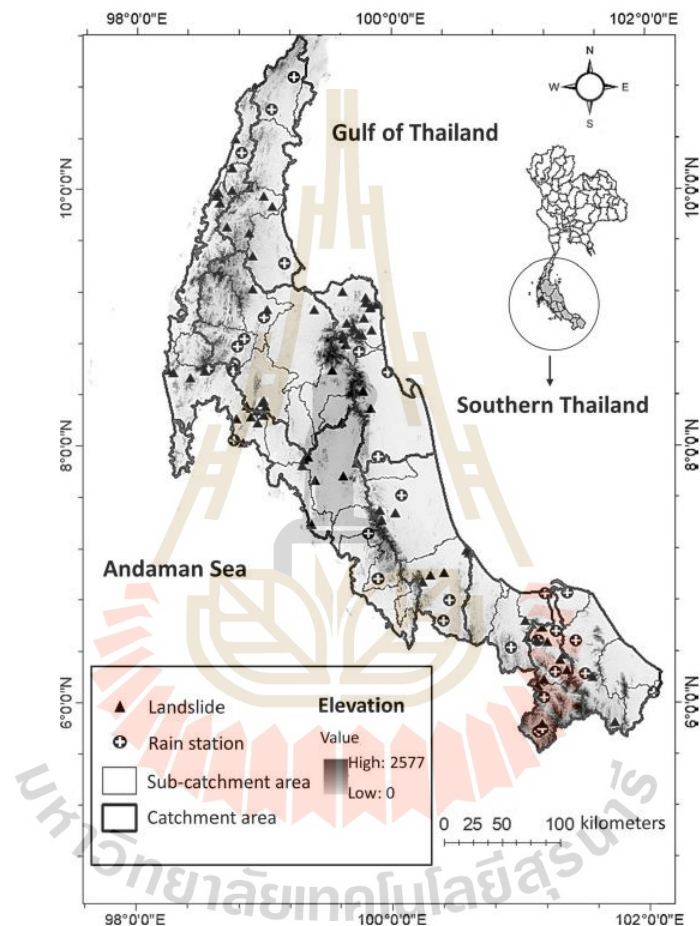


Figure 4.1 Location of the landslide as depicted by the black triangle, and location of the Rain station shown by the black circle. The area in thick black line represents catchment area locations. The thin black line area is a representation of sub catchment area locations. The gradient black and white area will show the elevation value of the area. (Figure created using ESRI ArcGIS 10.5 software, <https://www.esri.com/en-us/arcgis/about-arcgis/overview>)

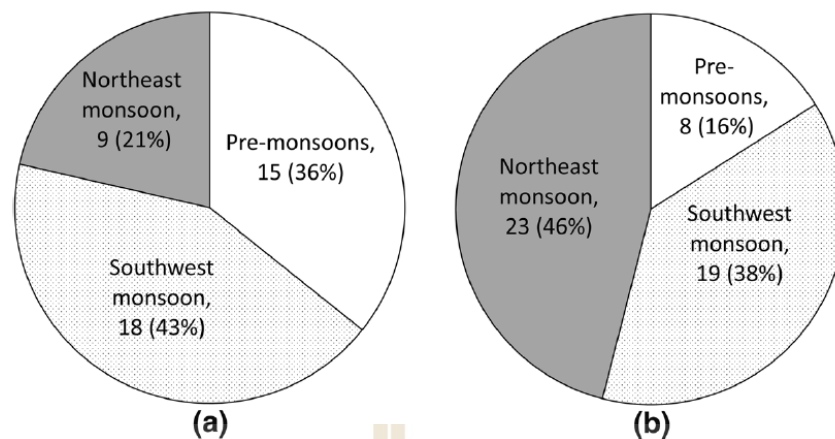


Figure 4.2 Number of landslide events (the proportion is presented in parenthesis) associated with different monsoon periods; including southwest, northeast, and pre-monsoons, on the west side (Figure. 4.2a) and on the east side (Figure. 4.2b) of the study area

4.1.3 Rainfall characterization

In order to characterize a rainfall event in the study area, criteria must be identified that enable distinction between two consecutive rainfalls. The inter-event criterion (*IEC*) used in this study to separate two consecutive rainfalls is shown in Figure. 4.3. The inter-event criterion $IEC_{A,B}$ is a combination of the rainfall intensity threshold *A* and rainfall duration *B*. In Figure. 4.3, if rainfall intensity is no greater than *A* mm/day for at least *B* consecutive days, two consecutive rainfall events were considered to have occurred, defined by two different results. Conversely, if the rainfall intensity and duration between two rainfalls do not meet the *IEC*, these two rainfalls are not separate and are considered as one continuous rainfall. Determination of a suitable *IEC* is crucial for establishing the landslide-triggering rainfall threshold. An *IEC* which is easy to meet might result in the rejection of some continuous rainfall, and an *IEC* which is hard to meet might produce too long a rainfall duration that includes independent rainfall events. Saito et al. (2010) used a 24-h duration to define a rainfall event in Japan; Brunetti et al. (2010) proposed different periods without rainfall for late spring and summer (2 days) and for the other seasons (4 days). In South Korea, Hong et al. (2017) analyzed *ID* thresholds

through skill scores; including receiver operating characteristic (*ROC*) plots and threat scores (*TS*), and concluded that 12 h was a suitable interevent time for separating two different rainfall events for landslide prediction. In this study, the suitable *IEC* was identified using rainfall data from the years in which landslide events occurred in the study areas.

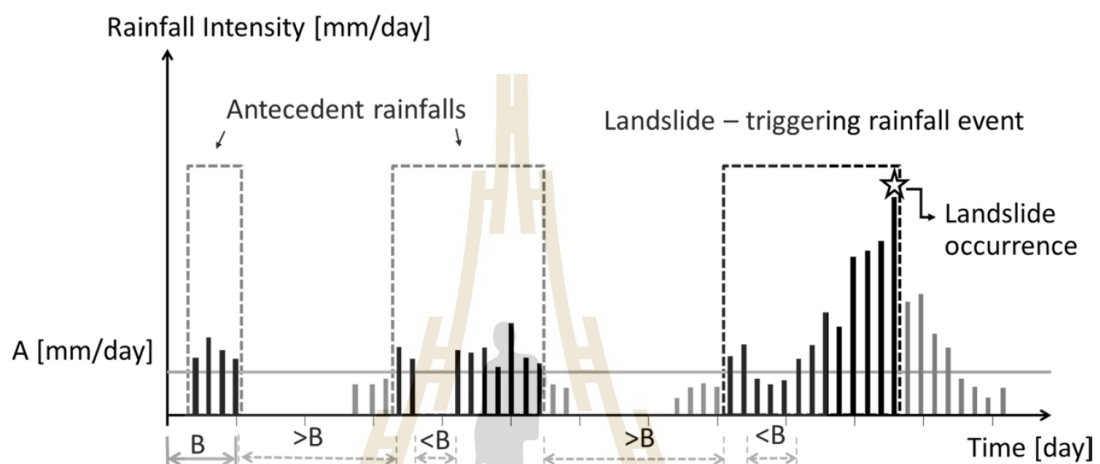


Figure 4.3 Definition of inter-event criteria used to separate two consecutive rainfalls in this study

Table 4.1 A set of inter-event criteria used to characterize rainfall data in the study area

Rainfall intensity, A (mm/day)	Number of days, B (day)		
	1	2	3
0	$IEC_{0,1}$	$IEC_{0,2}$	$IEC_{0,3}$
1	$IEC_{1,1}$	$IEC_{1,2}$	$IEC_{1,3}$
2	$IEC_{2,1}$	$IEC_{2,2}$	$IEC_{2,3}$
5	$IEC_{5,1}$	$IEC_{5,2}$	$IEC_{5,3}$

A set of twelve variables examined to identify the suitable $IEC_{A,B}$ is given in Table 4.1. Statistics of rainfall characteristics including rainfall depth, rainfall intensity, and rainfall duration, calculated from the different *IEC* are given in Table 4.2. The

max, mean and standard deviation for rainfall depth more than doubled, as rainfall duration increased from 1 to 3 days, except when the rainfall intensity threshold was equal to 5 mm/day. We inferred that setting rainfall intensity threshold A at 5 mm/day reduced the sensitivity of the rainfall depth to the B variable. From the data for years corresponding to studied landslide events, the average rainfall intensity ranged from 7.4 mm/day at $IEC_{0,3}$ to 15.3 mm/day at $IEC_{5,1}$. The average rainfall intensity was more sensitive to variation of A than variation of B. A greater value of A resulted in a higher average rainfall intensity. As for the rainfall duration, the average rainfall duration varied widely from 2.6 days at $IEC_{5,1}$ to 21.9 days at $IEC_{0,3}$. The max, mean and standard deviation of rainfall duration became lower with the increasing magnitude of A. Furthermore, at low magnitudes of A, the max, mean and standard deviation for rainfall duration were more sensitive to variation in B than the max, mean and standard deviation for rainfall duration at high magnitudes of A.

In order to determine a suitable IEC , two consecutive rainfalls were identified for each IEC . All inter-event times between the two consecutive rainfalls were read and then employed to calculate the variation coefficient (CV) of inter-event times, where the CV was the ratio of the standard deviation to the mean. Based on an assumption that inter-event times have an exponential distribution for which the mean equals the standard deviation (Bonta and Rao. 1988), the suitable IEC was identified on the basis of a variation coefficient (CV) of inter-event times equal to 1.0. Since the suitable IEC can vary depending on seasonal and climatic conditions, and there is a clear distinction between two consecutive rainfalls in the pre-monsoon period, the determination of the suitable IEC was based on a dataset that excluded rainfall events in the pre-monsoon period. The $IECs$ that returned a CV near 1.0 were selected as candidate suitable criteria. Based on Table 4.3, which presents statistics of rainfall inter-event time, there were two inter-event criteria that gave a CV close to 1.0: $IEC_{2,1}$ and $IEC_{5,1}$.

Table 4.2 Basics statistics of rainfall depth corresponding to various inter-event criteria

$IEC_{A,B}$	Rainfall depth (mm)			Rainfall intensity (mm/day)			Rainfall duration (day)		
	Max	Mean	SD	Max	Mean	SD	Max	Mean	SD
$IEC_{0,1}$	1916.9	58.3	133.1	115.9	7.9	11.1	67.0	6.3	7.6
$IEC_{0,2}$	4007.8	124.5	256.2	101.4	7.7	10.7	190.0	14.1	18.8
$IEC_{0,3}$	4019.7	197.7	349.8	63.4	7.4	9.1	196.0	21.9	28.3
$IEC_{1,1}$	1351.1	44.7	101.8	142.6	9.5	12.0	53.0	4.0	4.0
$IEC_{1,2}$	1916.6	85.6	167.7	142.6	9.2	12.0	65.0	8.4	9.1
$IEC_{1,3}$	2739.0	146.3	257.6	142.6	9.2	12.0	195.0	15.2	18.0
$IEC_{2,1}$	1351.1	41.2	97.5	153.9	11.0	13.1	26.0	3.1	3.0
$IEC_{2,2}$	1881.1	66.9	145.4	142.6	10.2	12.4	61.0	5.8	6.3
$IEC_{2,3}$	2125.8	116.6	213.1	142.6	10.4	13.1	92.0	11.1	12.4
$IEC_{5,1}$	1311.6	43.6	102.0	145.8	15.3	16.1	24.0	2.6	2.6
$IEC_{5,2}$	1323.9	54.1	128.1	145.8	13.3	13.1	32.0	3.5	3.5
$IEC_{5,3}$	1397.1	72.1	165.7	125.0	12.9	12.8	57.0	5.1	6.4

Table 4.3 Basic statistics of interevent duration corresponding to various inter-event criteria

Inter-event criteria	Max. (day)	Mean (day)	SD (day)	CV
$IEC_{0,1}$	30	4.1	5.1	1.23
$IEC_{0,2}$	26	5.0	4.5	0.9
$IEC_{0,3}$	25	6.7	4.2	0.64
$IEC_{1,1}$	29	3.5	3.9	1.13
$IEC_{1,2}$	30	5.1	4.8	0.93
$IEC_{1,3}$	28	6.8	4.8	0.71
$IEC_{2,1}$	28	4.3	4.4	1.03
$IEC_{2,2}$	30	6.1	5.6	0.92
$IEC_{2,3}$	30	8.0	6.3	0.79
$IEC_{5,1}$	30	5.7	6	1.05
$IEC_{5,2}$	29	7.0	5.6	0.79
$IEC_{5,3}$	30	7.4	5.5	0.73

4.2 Event rainfall depth–duration (*ED*) threshold

The event rainfalls that corresponded to the 92 landslides studied were established based on the inter-event criteria $IEC_{2,1}$ and $IEC_{5,1}$. They are presented in double logarithmic rainfall event depth–duration planes in Figure 4a, b, respectively. Rainfall events that took place on the west side are represented by an open triangle and those on the east side are represented by a cross. To determine whether there were any differences between the distributions of the two plots, we conducted a 2-

dimensional Kolmogorov Smirnov test, which extends an earlier idea due to Peacock (1983) and an implementation proposed by Fasano and Franceschini (1987). Table 4.4 presents the Kolmogorov–Smirnov statistic D with significance level for the event rainfall depth versus duration established using $IEC_{2,1}$ and $IEC_{5,1}$. The significance levels for both inter-event criteria were greater than 0.90. These results indicated that there was no significant difference between the event rainfall depth and duration that satisfied the criteria $IEC_{2,1}$ and $IEC_{5,1}$ for landslides studied on the east side and those studied on the west side. Therefore, the ED threshold could be established by combining rainfall data corresponding to landslides on both sides of the study area. The landslide-triggering rainfall threshold was analyzed using rainfall event depth and duration based on Eq. 4.1.

$$\log_{10} E = a + b \log_{10} D \quad (4.1)$$

where a and b are regression coefficients. With the above relationship, the threshold gave a straight line in double logarithmic scale. ED thresholds are given at a probability level of 5% corresponding to landslide-triggering rainfalls defined by inter-event criteria $IEC_{2,1}$ (Figure. 4.4a) and $IEC_{5,1}$ (Figure. 4.4b). Quantile regression, which was introduced by Koenker and Bassett (1978), to fit specified percentiles of a response, was performed in the R program using the package “quantreg” (Koenker et al. 2001; Koenker 2009).

Table 4.4 Two-dimensional Kolmogorov–Smirnov test results determined the variation in the distributions of the scatter plots (in double logarithmic rainfall event depth–duration plane) for event rainfalls corresponding to landslides on the west and east sides of the study area

Inter-event criteria	Kolmogorov–Smirnov statistic D	Corresponding probability (Significant level)
$IEC_{2,1}$	0.383	0.936
$IEC_{5,1}$	0.445	0.976

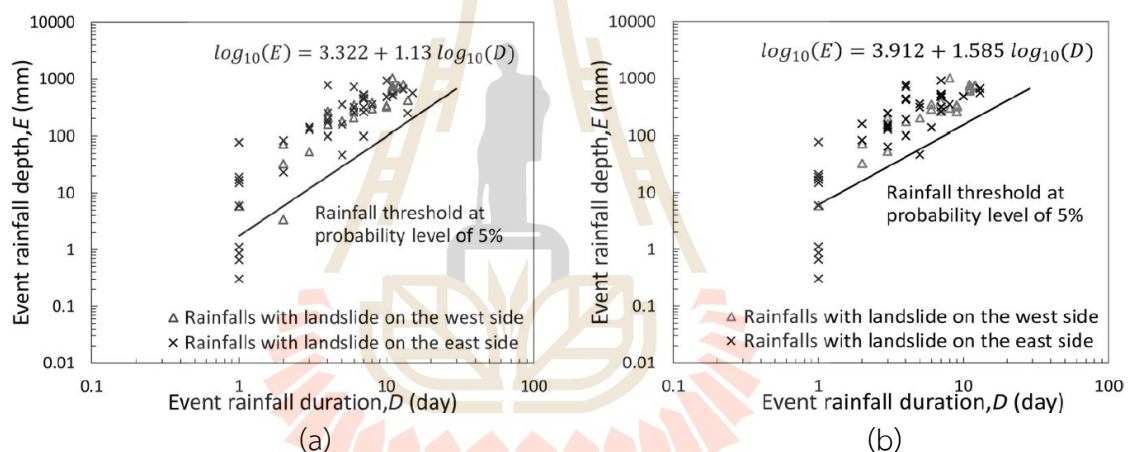


Figure 4.4 Scatter plot, in double logarithmic rainfall event depth–duration plane, of 92 triggering events established using (a) $IEC_{2,1}$ and (b) $IEC_{5,1}$. Rainfall thresholds at probability level of 5% based on triggering events defined by inter-event criteria (a) $IEC_{2,1}$ and (b) $IEC_{5,1}$

The performances of these thresholds were assessed through analysis of the contingency matrix, skill scores, and the receiver operating characteristic (ROC). The contingency matrix comprised four scenarios; including true positive (TP), true negative (TN), false positive (FP), and false negative (FN). These scenarios were based on two conditions (1) whether rainfall triggers a landslide or not, and (2) whether the threshold gives a warning or not. As depicted in Figure. 4.5a, true positive (TP) stood

for the outcome that the landslide was correctly predicted, false negative (*FN*) indicated a missed alarm in which case a landslide took place without prediction, false positive (*FP*) indicated a false alarm in which case a landslide was forecasted but did not take place, and true negative (*TN*) stood for the correct prediction of a rainfall event without a landslide. Skill scores, including hit rate (*HR*) and false alarm rate (*FAR*), were calculated according to Equation. 2, and 3, respectively. The optimal prediction was one that yielded an *HR* of 1 and an *FAR* of 0. The distance between the optimal prediction and the prediction result could indicate the performance of the prediction: the closer the prediction result to the perfect point, the better the prediction performance. The receiver operating characteristic (*ROC*) curve, *HR* against *FAR*, was plotted at various probabilistic levels of landslide threshold and the areas under the *ROC* curves (*AUC*) were determined. The larger the *AUC*, the better the predictive capability.

$$HR = \frac{TP}{TP + FN} \quad (4.2)$$

$$FAR = \frac{FP}{FP + TN} \quad (4.3)$$

มหาวิทยาลัยเทคโนโลยีสุรนารี

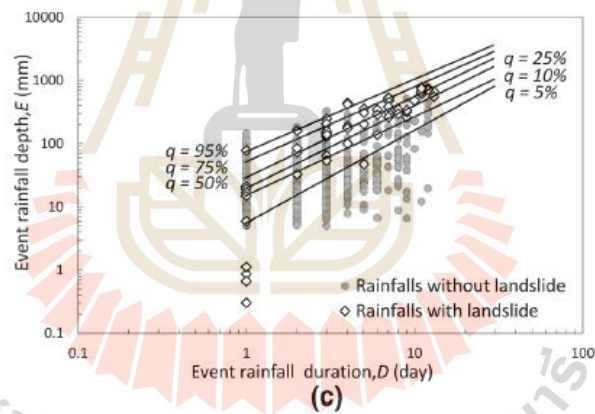
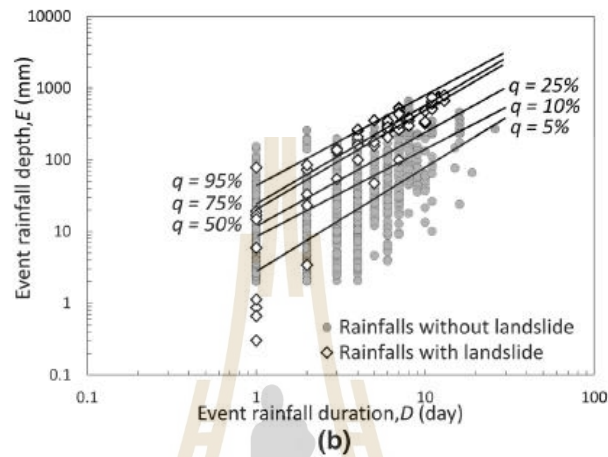
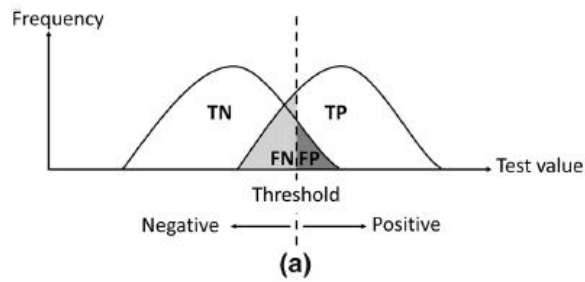


Figure 4.5 (a) Definition of true positive (TP), true negative (TN), false positive (FP), and false negative (FN) in the contingency matrix. Results from quantile regression at various probability levels and scatter plot, in double logarithmic rainfall event depth–duration plane, of triggering events and non-triggering events in established using (b) $IEC_{2,1}$ and (c) $IEC_{5,1}$

Figure 4.5b, c depicts scatter plots, in double logarithmic rainfall event depth–duration plane, of triggering and non-triggering rainfall events together with thresholds at various probabilistic levels from 5 to 95% for the inter-event criteria

$IEC_{2,1}$ and $IEC_{5,1}$, respectively. The ROC curves are given in Figure. 4.6. Each curve was drawn for rainfall data created using each IEC and the dots on each curve represent the variation of the threshold setting. The area under ROC curve (AUC) for the inter-event criteria $IEC_{5,1}$ was slightly greater than the AUC for the inter-event criteria $IEC_{2,1}$. However, at high HR , the ROC curve for $IEC_{2,1}$ possesses the notable lower FAR than the ROC curve for $IEC_{5,1}$ does. The ED threshold based on $IEC_{2,1}$ is preferable to the ED threshold based on $IEC_{5,1}$. Hence the ED threshold based on $IEC_{2,1}$ will be further elaborated and proposed as the threshold for the study area. This ED threshold could be written as:

$$\log_{10}(E) = 3.322 + 1.13 \log_{10}(D) \quad (4.4)$$

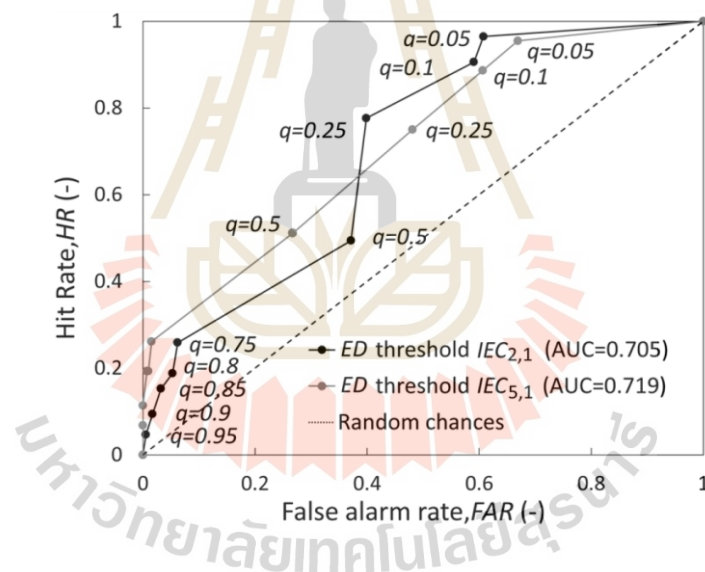
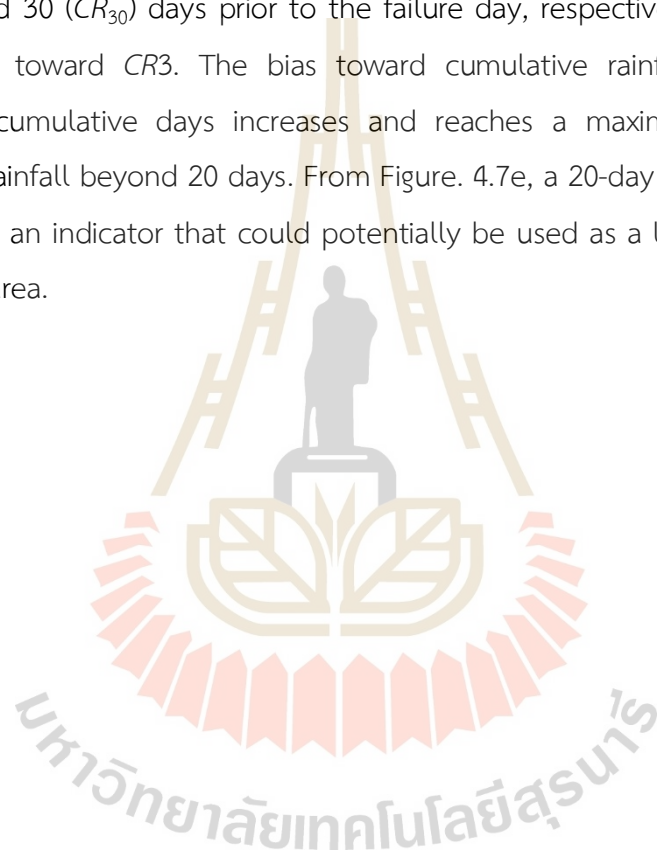


Figure 4.6 Receiver operating characteristic (ROC) curves for ED thresholds established based on inter-event criteria $IEC_{2,1}$ and $IEC_{5,1}$

4.3 CED Threshold: an integrated cumulative rainfall with event rainfall depth - duration threshold

Figure 4.7a presents rainfall depth on a failure day (DR_f) with respect to cumulative rainfall over various periods prior to the failure day. A 1:1 line divides the plots into two zones to clarify bias in the scattering toward either rainfall depth on a

failure day (y -axis) or cumulative rainfall prior to failure (x -axis). The plot reveals that the occurrence of landslide events was biased toward cumulative rainfall prior to failure rather than rainfall depth on a failure day. In other words, out of 92 landslide events, most took place under the influence of cumulative rainfall prior to failure. The plots confirm that cumulative rainfall prior to failure plays a bigger role in the occurrence of landslides than the rainfall depth on a failure day. Figure 4.7b–f are the plots of DR_f with respect to cumulative rainfall over 3 (CR_3), 10 (CR_{10}), 15 (CR_{15}), 20 (CR_{20}), and 30 (CR_{30}) days prior to the failure day, respectively. Seventy-six cases were biased toward CR_3 . The bias toward cumulative rainfall increases as the number of cumulative days increases and reaches a maximum of 91 cases at cumulative rainfall beyond 20 days. From Figure. 4.7e, a 20-day cumulative rainfall of 100 mm was an indicator that could potentially be used as a landslide threshold in the studied area.



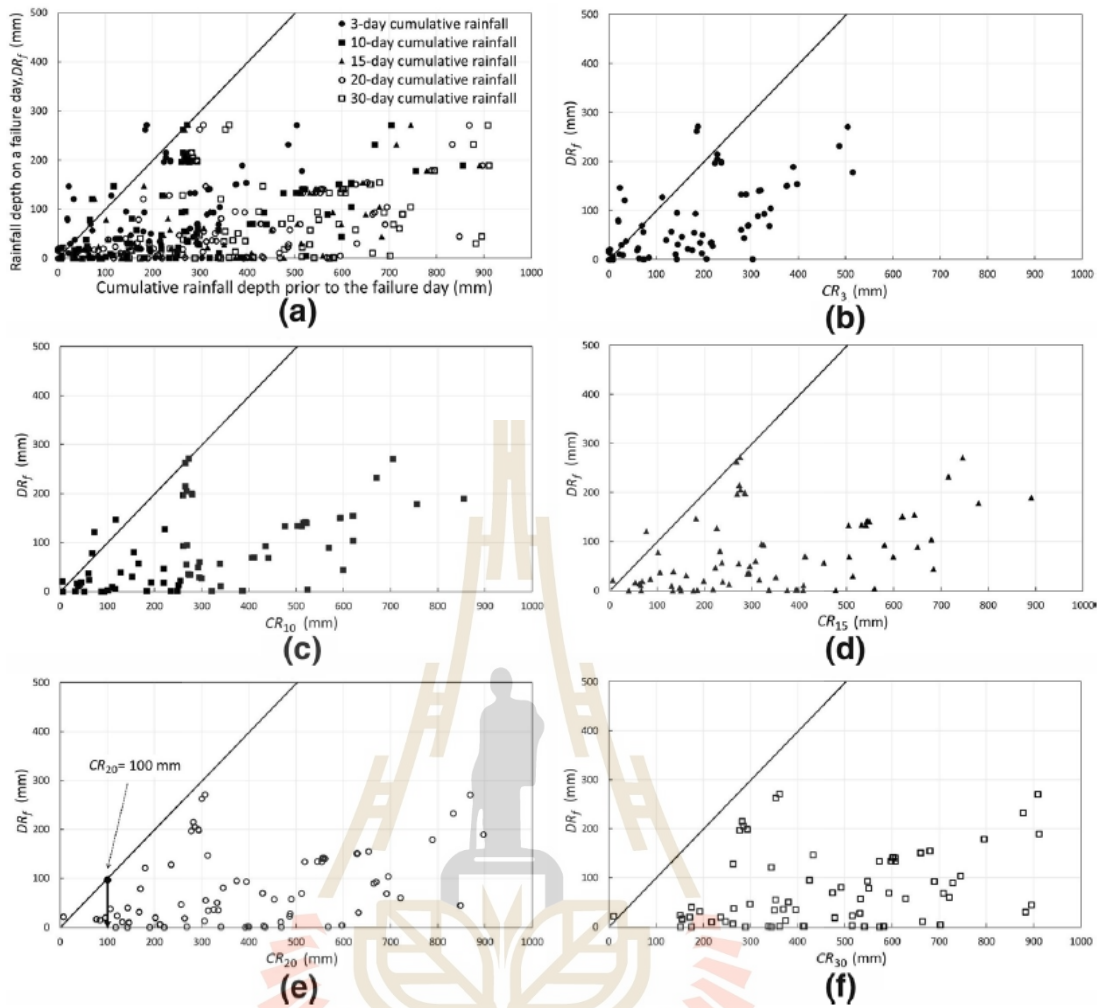


Figure 4.7 Rainfall depth on a failure day is plotted with respect to cumulative rainfall depth (3, 10, 15, 20, 30 days) before the failure day (a). CR_3 (b), CR_{10} (c), CR_{15} (d), CR_{20} (e), and CR_{30} (f) show relationships between rainfall depth on a failure day and 3-, 10-, 15-, 20-, and 30-day cumulative rainfall depth before the failure day

The variable CR_{20} then had to be integrated to the ED threshold. To do so, three rainfall variables, CR_{20} , E , and D , were plotted in three-dimensional space (Figure. 4.8). This threshold was named the CED threshold, standing for cumulative rainfall integrated with event rainfall depth-duration threshold. Setting CR_{20} on the z-axis, the warning zone was defined by shifting the ED threshold 100 mm along the z-axis. The warning zone in Figure. 4.8 is the zone above the gray-shaded area. The

performance of the 3D threshold was compared with that of the *ED* threshold through *ROC* curves and skill scores. The *ROC* curves are given in Figure. 4.9. For the *ED* threshold and the *CED* threshold, the areas under the *ROC* curves (*AUC*) were 0.705 and 0.944, respectively, indicating that the predictive capability of the *CED* threshold was much better than the predictive capability of the *ED* threshold. Since many rainfall events having CR_{20} lower than 100 mm were excluded from the *FP* score, the false alarm rate produced by the *CED* threshold is much lower than the false alarm rate produced by the *ED* threshold. Since 4 out of 92 landslide events had CR_{20} lower than 100 mm (Figure. 4.7e), at low probabilistic levels, four fewer true positive (*TP*) events were indicated by the *CED* threshold than by the *ED* threshold. Accordingly, at low probabilistic levels, the *HR* of the *CED* threshold was a bit lower than the *HR* of the *ED* threshold. At a 5% probabilistic level, the *HR* of the *CED* threshold was 0.918 compared with an *HR* of 0.965 for the *ED* threshold.

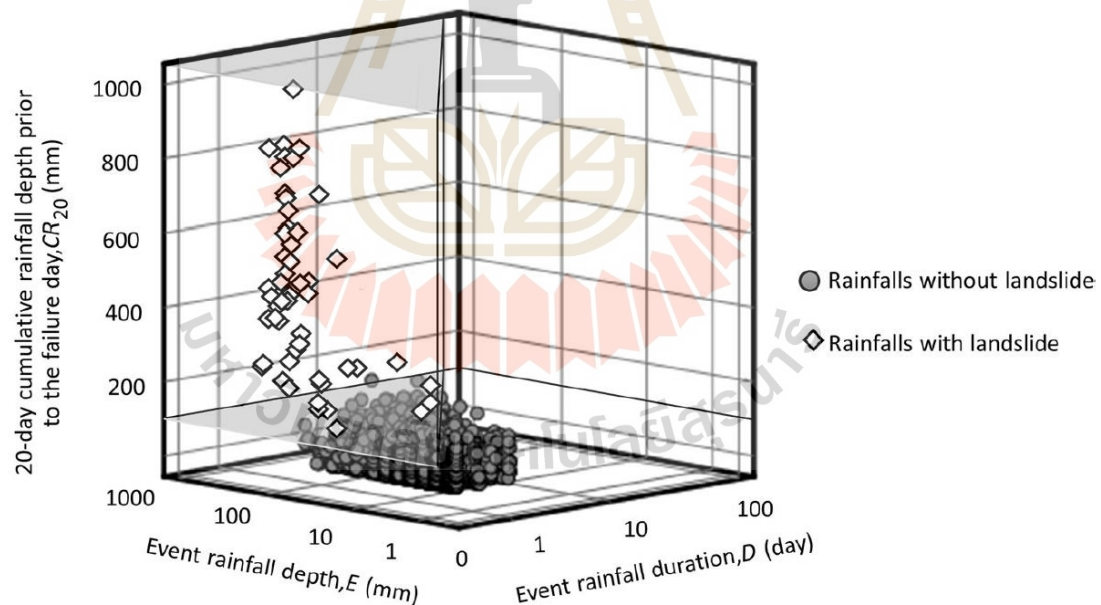


Figure 4.8 *CED* threshold plotted in three -dimensional space

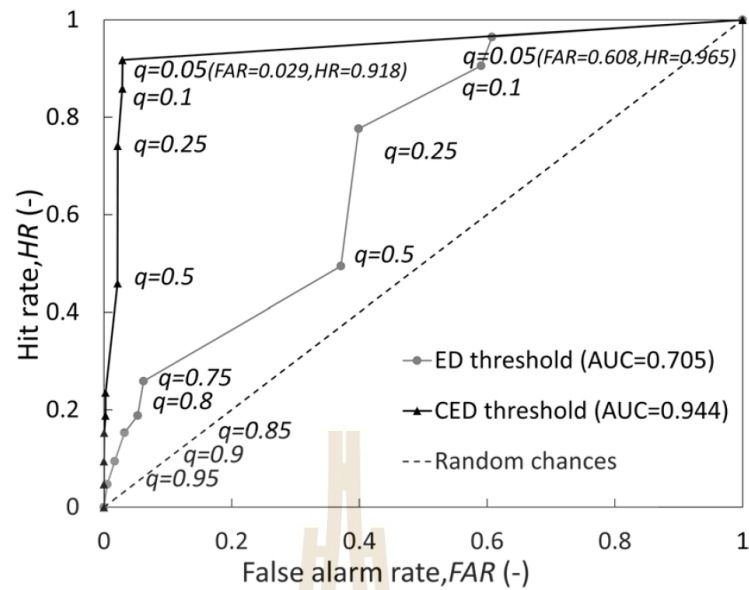


Figure 4.9 Receiver operating characteristic (ROC) curves for *ED* and *CED* thresholds

4.4 Conclusions

Rainfall events corresponding to 92 landslides in the south of Thailand were used to establish a landslide-triggering rainfall threshold. Event rainfall and cumulative rainfall were found to play important roles in landslide initiation in the study area. Event rainfall depth (*E*), duration of event rainfall (*D*), and cumulative rainfall depth of 20 days prior to the failure day (CR_{20}), were explicitly included in the threshold in a 3-dimensional plot. The following conclusions were drawn from this study.

- The suitable inter-event criterion to separate two consecutive rainfalls (*IEC*) was identified using three parameters: (1) an inter-event criterion (*IEC*) that returned the variation coefficient (*CV*) of inter-event times closest to 1.0, (2) an *IEC* that returned the highest value of the *AUC* of receiver operating characteristic curves, and (3) an *IEC* that, at high *HR*, possess the lower *FAR*.
- Based on the procedure stated above, the suitable inter-event criterion was $IEC_{2,1}$. This variable describes a rainfall condition having an intensity no greater than 2 mm/day for at least 1 consecutive day. Event rainfalls based on $IEC_{2,1}$ was used to draw an *ED* threshold. The

proposed *ED* threshold was based on quantile regression at a probability level of 5% and it is written as: $\log_{10}(E) = 3.322 + 1.13 \log_{10}(D)$.

- Cumulative rainfall of 100 mm for 20 days prior to a failure day (CR_{20}) was chosen as an extra rainfall variable added to the proposed *ED* threshold. The new threshold, namely the *CED* threshold, was plotted in 3-dimensional space integrating two rainfall variables from event rainfall and one variable from cumulative rainfall.
- The new *CED* threshold is implemented by assessing of the CR_{20} first followed by assessment of the event rainfall using the *ED* threshold. The implementation is conducted in the following manner:
 - The CR_{20} assessment determines whether cumulative rainfall exceeds 100 mm.
 - If the CR_{20} is not over 100 mm, it is presumed that land sliding will not happen. If CR_{20} is equal to or more than 100 mm, the event rainfall will be assessed through the *ED* threshold. If the event rainfall returns a rainfall depth and duration above the *ED* threshold, the landslide warning will be activated.
- Although the *CED* threshold provides a little lower hit rate (*HR*) than the *ED* threshold does, the *CED* threshold performs much better in terms of false alarm rate (*FAR*) than the *ED* threshold does since many rainfalls are filtered by the 20-day cumulative rainfall (CR_{20}) lower limit of 100 mm prior to the assessment of the event rainfall.
- The area under the receiver operating characteristics curve (*AUC*) was significantly bigger for the *CED* threshold than for the *ED* threshold. This result indicates the superiority of the *CED* threshold, particularly in the view of the respective false alarm rates.

4.5 References

- Arai S, Urayama K, Tebakari T, Archvarahuprok B (2019) **Characteristics of gridded rainfall data for Thailand from 1981–2017**. Eng J 23(6):461–468. <https://doi.org/10.4186/ej.2019.23.6.461>
- Bonta JV, Rao AR (1988) **Factors affecting the identification of independent storm events**. J Hydrol 98(3–4):275–293. [https://doi.org/10.1016/0022-1694\(88\)90018-2](https://doi.org/10.1016/0022-1694(88)90018-2)
- Brunetti MT, Peruccacci S, Rossi M, Luciani S, Valigi D, Guzzetti F (2010) **Rainfall thresholds for the possible occurrence of landslides in Italy**. Nat Hazards Earth Syst Sci 10(3):447–458. <https://doi.org/10.5194/nhess-10-447-2010>
- Caine N (1980) **The Rainfall intensity: duration control of shallow landslides and debris flows**. Geogr Ann Series A Phys Geogr 62(1/2):23. <https://doi.org/10.2307/520449>
- Chen D, Ou T, Gong L, Xu CY, Li W, Ho CH, Qian W (2010) **Spatial interpolation of daily precipitation in China: 1951–2005**. Adv Atmos Sci 27: 1221–1232. <https://doi.org/10.1007/s00376-010-9151-y>
- Dahal RK, Hasegawa S (2008) **Representative rainfall thresholds for landslides in the Nepal Himalaya**. Geomorphology 100(3–4):429–443. <https://doi.org/10.1016/j.geomorph>
- Department of Mineral Resources (2019) **The Best practices for landslide risk management in Thailand**. Department of Mineral Resources, 75/10 Rama 6 Road, Thung Phayathai Sub-district, Ratchathewi District, Bangkok 10400, Thailand. webmaster@dmr.mail.go.th
- Ditthakit P, Nakrod S, Viriyanantavong N, Tolche AD, Pham QB (2021) **Estimating baseflow and baseflow index in ungauged basins using spatial interpolation techniques: a case study of the southern river basin of Thailand**. Water 13:3113. <https://doi.org/10.3390/w13213113>
- Fasano G, Franceschini A (1987) **A multidimensional version of the Kolmogorov–Smirnov test**. Mon Not R Astron Soc 225(1):155–170. <https://doi.org/10.1093/mnras/225.1.155>

- Gariano SL, Brunetti MT, Iovine G, Melillo M, Peruccacci S, Terranova O, Guzzetti F (2015) **Calibration and validation of rainfall thresholds for shallow landslide forecasting in Sicily, southern Italy.** *Geomorphology* 228:653–665. <https://doi.org/10.1016/j.geomorph.2014.10.019>
- Gariano SL, Melillo M, Peruccacci S, Brunetti MT (2020) **How much does the rainfall temporal resolution affect rainfall thresholds for landslide triggering?** *Nat Hazards*. <https://doi.org/10.1007/s11069-019-03830-x>
- Gentile M, Courbin F, Meylan G (2012) **Interpolating point spread function anisotropy.** *Astron Astrophys.* <https://doi.org/10.1051/0004-6361/201219739>
- Giannecchini R, Galanti Y, D'Amato Avanzi G (2012) **Critical rainfall thresholds for triggering shallow landslides in the Serchio river valley (Tuscany, Italy).** *Nat Hazard* 12(3):829–842. <https://doi.org/10.5194/nhess-12-829-2012>.
- Glade T (2000) **Applying probability determination to refine landslide-triggering rainfall thresholds using an empirical “antecedent daily rainfall model.”** *Pure Appl Geophys* 157(6–8):1059–1079. <https://doi.org/10.1007/s000240050017>.
- Guzzetti F, Salvati P, Stark CP (2005a) **Evaluation of risk to the population posed by natural hazards in Italy.** In: Hungr O, Fell R, Couture R, Eberhardt E (eds) *Landslide risk management*. Taylor, Francis Group, London, pp 381–389
- Guzzetti F, Stark CP, Salvati P (2005b) **Evaluation of flood and landslide risk to the population of Italy.** *Environ Manag* 36(1):15–36. <https://doi.org/10.1007/s00267-003-0257-1>
- Guzzetti F, Peruccacci S, Rossi M, Stark CP (2007a) **The rainfall intensity–duration control of shallow landslides and debris flows: an update.** *Landslides* 5(1):3–17. <https://doi.org/10.1007/s10346-007-0112-1>
- Guzzetti F, Peruccacci S, Rossi M, Stark C (2007b) **Rainfall thresholds for the initiation of landslides in central and southern Europe.** *Meteorol Atmos Phys* 98:239–267. <https://doi.org/10.1007/s00703-007-0262-7>

- Guzzetti F, Peruccacci S, Rossi M, Stark CP (2008) **The rainfall intensity-duration control of shallow landslides and debris flows: an update.** *Landslides* 5:3–17. <https://doi.org/10.1007/s10346-007-0112-1>
- Hasnawir KT (2008) **Analysis of critical value of rain-fall to induce landslide and debris-flow in Mt. Bawakaraeng Caldera, South Sulawesi, Indonesia.** *J Fac Agric Kyushu Univ* 53(2):523–527. <https://doi.org/10.5109/12868>
- He S, Wang J, Liu S (2020) **Rainfall event-duration thresholds for landslide occurrences in China.** *Water* 12(2):494. <https://doi.org/10.3390/w12020494>
- Hong H, Liu J, Zhu AX, Shahabi H, Pham BT, Chen W, Bui DT (2017) **A novel hybrid integration model using support vector machines and random subspace for weather-triggered landslide susceptibility assessment in the Wuning area (China).** *Environ Earth Sci.* <https://doi.org/10.1007/s12665-017-6981-2>
- Kanjanakul C, Chub-uppakarn T, Chalermyanont T (2016) **Rainfall thresholds for landslide early warning system in Nakhon Si Thammarat.** *Arabian J Geosci.* <https://doi.org/10.1007/s12517-016-2614-4>
- Kardani N, Zhou AN, Nazem M, Shen SS (2021) **Improved prediction of slope stability using a hybrid stacking ensemble method based on finite element analysis and field data.** *J Rock Mech Geotech Eng.* <https://doi.org/10.1016/j.jrmge.2020.05.011>
- Khan YA, Lateh H, Baten MA, Kamil AA (2012) **Critical antecedent rainfall conditions for shallow landslides in Chittagong city of Bangladesh.** *Environ Earth Sci* 67:97–106. <https://doi.org/10.1007/s12665-011-1483-0>.
- Kim SK, Hong WP, Kim YM (1991) **Prediction of rainfall-triggered landslides in Korea.** In: Bell DH (ed) *landslides*, 2nd edn. A.A Balkema Rotterdam, pp. 989–994
- Kim SW, Chun KW, Kim M, Catani F, Choi B, Seo JI (2020) **Effect of antecedent rainfall conditions and their variations on shallow landslide-triggering rainfall thresholds in South Korea.** *Landslides.* <https://doi.org/10.1007/s10346-020-01505-4>

- Koenker R, Bassett G (1978) **Regression quantiles**. *Econometrica* 46(1):33. <https://doi.org/10.2307/1913643>
- Koenker R, Hallock KF (2001) **Quantile regression**. *J Econ Perspect* 15(4):143–156. <https://doi.org/10.1257/jep.15.4.143>
- Koenker R (2009) **Quantile regression in R: A Vignette**. Available at <http://www.econ.uiuc.edu/roger/research/rq/vig.pdf>
- Kong YF, Tong WW (2008) **Spatial exploration and interpolation of the surface precipitation data**. *Geogr Res* 27(5):1097–1108
- Kurtzman D, Navon S, Morin E (2009) **Improving interpolation of daily precipitation for hydrologic modeling: spatial patterns of preferred interpolators**. *Hydrol Process* 23:3281–3329
- Li J, Heap AD, Potter A, Daniell JJ (2011) **Application of machine learning methods to spatial interpolation of environmental variables**. *Environ Model Softw* 26(12):1647–1659
- Lin SS, Shen SL, Zhou AN, Xu YS (2021a) **Risk assessment and management of excavation system based on fuzzy set theory and machine learning methods**. *Autom Constr* 122:103490. <https://doi.org/10.1016/j.autcon.2020.103490>
- Lin SS, Shen SL, Zhou AN, Xu YS (2021b) **Novel model for risk identification during karst excavation**. *Reliab Eng Syst Saf* 209:107435. <https://doi.org/10.1016/j.res.2021.107435>
- Lin SS, Shen SL, Zhang N, Zhou AN (2021c) **Comprehensive environmental impact evaluation for concrete mixing station (CMS) based on improved TOPSIS method**. *Sustain Cities Soc* 69:102838. <https://doi.org/10.1016/j.scs.2021.102838>
- Lyu HM, Zhou WH, Shen SL, Zhou AN (2020) **Inundation risk assessment of metro system using AHP and TFN-AHP in Shenzhen**. *Sustain Cities Soc* 56:102103. <https://doi.org/10.1016/j.scs.2020.102103>
- Peacock JA (1983) **Two-dimensional goodness-of-fit testing in astronomy**. *Mon Not R Astron Soc* 202(3):615–627. <https://doi.org/10.1093/mnras/202.3.615>

- Peruccacci S, Brunetti MT, Luciani S, Vennari C, Guzzetti F (2012) **Lithological and seasonal control on rainfall thresholds for the possible initiation of landslides in central Italy**. *Geomorphology* 139–140:79–90. <https://doi.org/10.1016/j.geomorph.2011.10.005>
- Peruccacci S, Brunetti MT, Gariano SL, Melillo M, Rossi M, Guzzetti F (2017) **Rainfall thresholds for possible landslide occurrence in Italy**. *Geomorphology* 290:39–57. <https://doi.org/10.1016/j.geomorph.2017.03.031>
- Phien-Wej N, Nutalaya P, Aung Z, Zhibin T (1993) **Catastrophic landslides and debris flows in Thailand**. *Bull Int Assoc Eng Geol* 48:93–100. <https://doi.org/10.1007/BF02594981>
- Rahardjo H, Melinda F, Leong EC, Rezaur RB (2011) **Stiffness of a compacted residual soil**. *Eng Geol* 120(1–4):60–67. <https://doi.org/10.1016/j.enggeo.2011.04.006>
- Rahimi A, Rahardjo H, Leong EC (2011) **Effect of Antecedent Rainfall Patterns on Rainfall-Induced Slope Failure**. *J Geotech Geoenviron Eng* 137(5):483–491. [https://doi.org/10.1061/\(asce\)gt.1943-5606.0000451](https://doi.org/10.1061/(asce)gt.1943-5606.0000451)
- Ridd MF, Barber AJ, Crow MJ (2011) **The Geology of Thailand**. *Geol Soc Lond*. <https://doi.org/10.1144/GOTH>
- Rosi A, Segoni S, Canavesi V, Monni A, Gallucci A, Casagli N (2020) **Definition of 3D rainfall thresholds to increase operative landslide early warning system performances**. *Landslides*. <https://doi.org/10.1007/s10346-020-01523-2>
- Saito H, Nakayama D, Matsuyama H (2010) **Relationship between the initiation of a shallow landslide and rainfall intensity-duration threshold in Japan**. *Geomorphology* 118:167–175. <https://doi.org/10.1016/j.geomorph.2009.12.016>
- Segoni S, Lagomarsino D, Fanti R, Moretti S, Casagli N (2014) **Integration of rainfall thresholds and susceptibility maps in the Emilia Romagna (Italy) regional-scale landslide warning system**. *Landslides* 12:773–785. <https://doi.org/10.1007/s10346-014-0502-0>

- Segoni S, Piciullo L, Gariano SL (2018) **A review of the recent literature on rainfall thresholds for landslide occurrence.** *Landslides* 15: 1483–1501. <https://doi.org/10.1007/s10346-018-0966-4>
- Vennari C, Gariano SL, Antronico L, Brunetti MT, Iovine G, Peruccacci S, Guzzetti F (2014) **Rainfall thresholds for shallow landslide occurrence in Calabria, southern Italy.** *Nat Hazard* 14(2):317–330. <https://doi.org/10.5194/nhess-14-317-2014>
- Vessia G, Parise M, Brunetti MT, Peruccacci S, Rossi M, Vennari C, Guzzetti F (2014) **Automated reconstruction of rainfall events responsible for shallow landslides.** *Nat Hazard* 14(9):2399–2408. <https://doi.org/10.5194/nhess-14-2399-2014>
- Wicki A, Lehmann P, Hauck C, Seneviratne SI, Waldner P, Stihli M (2020) **Assessing the potential of soil moisture measurements for regional landslide early warning.** *Landslides*. <https://doi.org/10.1007/s10346-020-01400-y>
- Yang X, Xie X, Liu DL, Ji F, Wang L (2015) **Spatial interpolation of daily rainfall data for local climate impact assessment over greater Sydney region.** *Adv Meteorol*. <https://doi.org/10.1155/2015/563629>
- Yang W, Liu L, Shi P (2020) **Detecting precursors of an imminent landslide along the Jinsha River.** *Nat Hazards Earth Syst Sci* 20:3215–3224. <https://doi.org/10.5194/nhess-20-3215-2020>
- Yumuang S (2006) **2001 debris flow and debris flood in Nam Ko area, Phetchabun province, Central Thailand.** *Environ Geol* 51:545–564
- Zheng Q, Lyu HM, Zhou AN, Shen SL (2021) **Risk assessment of geohazards along Cheng-Kun railway using fuzzy AHP incorporated into GIS.** *Geomat Nat Haz Risk* 12:1508–1531. <https://doi.org/10.1080/19475705.2021.1933614>

CHAPTER V

LANDSLIDE RAINFALL THRESHOLD FOR LANDSLIDE WARNING IN NORTHERN THAILAND

5.1 Introduction

Every year, landslides result in economic and human losses. Understanding, managing, monitoring, and preventing these major natural hazards can mitigate the human and economic impacts. Studies of the many different aspects of landslide hazards have investigated triggering factors and hydrological responses (Chinkulkijniwat, Yubonchit et al. 2016; Chinkulkijniwat, Horpibulsuk et al., 2016; 2019; Yang et al. 2021), biological stability (Indraratna et al. 2006), and landslide hazard assessment (Grozavu and Patriche 2021). Work carried out on landslide risk assessment has made some of the most vital contributions to landslide mitigation measures. Since rainfall is known to be an important factor in landslide events (Iida 2004; Fan et al. 2016), landslide rainfall thresholds are commonly utilized as an important component of landslide early warning systems (Guzzetti et al. 1994; Aleotti 2004; Wieczorek and Glade 2005; Ya'acob et al. 2019; Maturidi et al. 2020; Yang et al. 2020; Rosi et al. 2021). The most common parameters used to define landslide-triggering rainfall thresholds are based on event rainfall parameters, particularly the parameter that combines rainfall intensity and rainfall event duration, known as the *ID* threshold (Caine 1980; Crosta and Frattini 2001; Ahmad 2003; Aleotti 2004; Guzzetti et al. 2008; Yubonchit et al. 2017). Since the rainfall variables used to predict the *ID* threshold are not independent (Gariano et al. 2020), certain studies (Vennari et al. 2014; Vessia et al. 2014; Gariano et al. 2015; Peruccacci et al. 2017; Gariano et al. 2019; He et al. 2020; Germain et al. 2021; Lee et al. 2021) have preferred to use a threshold that takes into account event rainfall and rainfall duration, known as the *ED* threshold

Thailand's Northern Region regularly experiences rainfall-triggered landslides that cause tragedy, injuries and loss of life (Yumuang 2006; Teerarungsigul et al. 2016; Komolvilas et al. 2021). In 2001, 176 people lost their lives in rainfall-triggered landslide events in the area. In 2006, 87 fatalities were recorded, and in 2018, eight people died but 260 casualties were reported. In 2003, Thailand's Environmental Geology Division reported that 6563 villages, in 1084 rural subdistricts, in 54 provinces, mostly in Northern Thailand, were located in landslide hazard zones. According to Segoni et al. (2018), who conducted a review of the recent literatures on rainfall thresholds for landslide occurrence published in journals indexed in Scopus or ISI Web of Knowledge database during 2008–2016, there was only one report for landslide rainfall threshold in Thailand (Kanjanaikul et al. 2016) during the period of 2008–2016. The present work determines a landslide rainfall threshold at regional scale for Northern Thailand. The introduced threshold was modified from a landslide rainfall threshold for the Southern Thailand region that combined cumulative rainfall with rainfall event - duration, known as the *CED* threshold (Salee et al. 2022). The modification was achieved by portioning the *CED* threshold to two portions; one for short duration rainfall events and the other for long duration rainfall events. In general, the short duration, high intensity rainfall events involved shallow landslides, while the long duration, low to medium intensity rainfall events caused deep seat landslides (Caine 1980; Giannecchini et al. 2012, 2015; Zhang et al. 2019). Taking rainfall duration into account in an established landslide rainfall threshold, the difference mechanism of landslide formation might be incorporated to the threshold. Contingency tables and sets of skill scores were used to assess the performances of the thresholds. The threshold introduced in this study will be useful for rainfall-triggered landslide warning in Northern Thailand. Furthermore, this study shows the first attempt to incorporate the difference mechanism of landslide formation by dividing the *CED* threshold to two portions for difference durations of rainfall event.

5.2 Background of the study area

The Northern Thailand region (Figure 5.1) consists of nine administrative provinces, namely Chiang Rai, Mae Hong Son, Chiang Mai, Lamphun, Lampang,

Phayao, Nan, Phrae, and Uttaradit. The region covers approximately 93,691 km². The landscape of Northern Thailand is dominated by mountain ranges in the western and northeastern parts of the region. These ranges are part of the wider system that covers neighboring Burma and Laos. Broadly defined based on geological composition, there are two mountainous subsystems in the study area. In the western part of the region, mountains run southwards from the Daen Lao Range with the two parallel chains of the Thanon Thong Chai Range, which includes the highest mountain in Thailand, Doi Inthanon (2,565m above mean sea level). In the northeastern part of the region, parallel ranges extending into northern Laos include the Khun Tan Range, the Phi Pan Nam Range, the Phlueng Range, and the western part of the Luang Prabang Range. There also exists a set of strike-slip faults in this region. However, landslides triggered by seismic events are rare in Thailand, and the most recent earthquakes in 2006 and 2014 did not lead to significant landslides (Schmidt-Thom_e et al. 2018). The annual average minimum and maximum temperatures are 4 and 40 °C, respectively. The average annual rainfall of 943.2mm is spread over 122 days on average. Rainfall in this area is under the influence of the southwest monsoon, which starts in May and ends in October. Streams of warm moist air from the Indian Ocean bring abundant rain to the region, especially to the windward side of mountain ranges. However, the southwest monsoon is not the only source of precipitation during this period. The influence of the Inter Tropical Convergence Zone and tropical cyclones can also deposit large amounts of rain. Based on the available records, all major landslides in this area have been triggered by heavy rainfall caused by tropical cyclones. Landslides in Phrae and Phetchabun provinces in 2001 were triggered by continuous heavy rain that fell during Typhoon Usagi. Several landslides in Uttaradit, Sukhothai, Phrae, Lampang and Nan provinces in 2006 were caused by continuous heavy rainfall in the wake of Typhoon Xangsane. More recently, in 2018, landslides at Huay Khab village in Nan province followed ten days of continuous rainfall caused by Typhoon Son-Tinh.

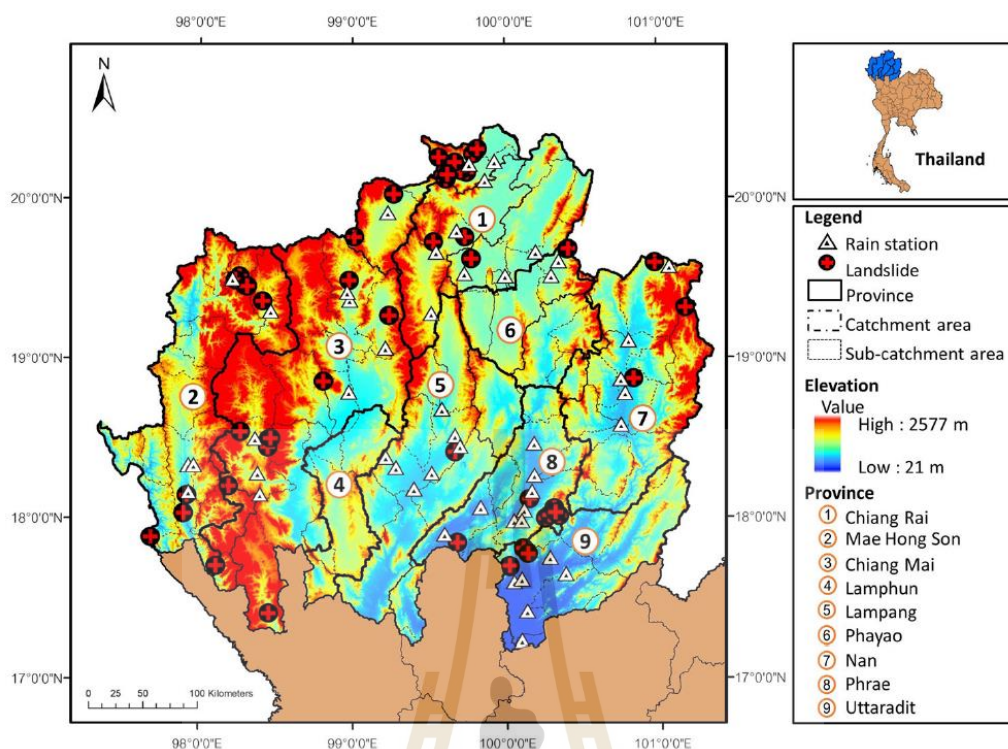


Figure 5.1 Location of the landslide as depicted by the red cross on black circle, and location of the Rain station shown by the white triangle. The area in dot-dash line represents boundary of catchment area. The thin dot line represents boundary of sub catchment area. The gradient color shows the elevation value of the area.

5.3 Data collection and rainfall characterization

This study considered 59 landslide events recorded in Northern Thailand during the years 2002 to 2018. Data were collected mainly from scientific papers published by the Department of Mineral Resources, Ministry of Natural Resources and Environment and partly from local newspapers. For an event to be taken into consideration, the available information had to convey at least the following details: (1) the date of the occurrence of the landslide, (2) the location of the landslide event, and (3) consequential damages. Triggered and non-triggered rainfall data from the years when these landslide events occurred were gathered from Thai Meteorological Department (TMD) rain gauge stations. These rain gauge stations

located in the catchment area where the considered landslides were located. The locations of landslide events and TMD rain gauge stations in the study area are indicated in Figure 5.1. To estimate rainfall at landslide locations, rainfall data from TMD rain gauge stations was processed by use of Inverse Distance Weighting (IDW). Based on inverse functions of distance, IDW assigned a larger weight to a station closer to a landslide location than it assigned to a station further away. Although, IDW is a deterministic model, it has been considered a reliable method of spatial interpolation in applications such as point spread function (Gentile et al. 2013), and baseflow measurement and baseflow index calculation (Ditthakit et al. 2021). IDW has also been successfully applied to the interpolation of rainfall data in various locations by Kong and Tong (2008), Kurtzman et al. (2009), Chen et al. (2010), and Yang et al. (2015) among others.

In order to characterize rainfall in this region, criteria must be identified that enable distinction between two consecutive rainfalls. The inter - event criterion (*IEC*) used in this study to separate two consecutive rainfalls is shown in Figure 5.2.

In Figure 5.2, the inter-event criterion $IEC_{A,B}$ is a combination of the rainfall intensity threshold *A* and duration *B*. The condition that distinguished two consecutive rainfall events had to satisfy the combined criterion. If rainfall intensity was no greater than *A* mm/day for at least *B* consecutive days, two consecutive rainfall events were considered to have occurred. Conversely, if the rainfall intensity and duration of two rainfalls did not meet the $IEC_{A,B}$, these two rainfalls were considered as one continuous rainfall. The determination of a suitable *IEC* was crucial to establishing a suitable landslide-triggering rainfall threshold. An *IEC* which is easy to meet might result in the rejection of a continuous rainfall, and an *IEC* which is hard to meet might produce too long a rainfall duration that includes independent rainfall events.

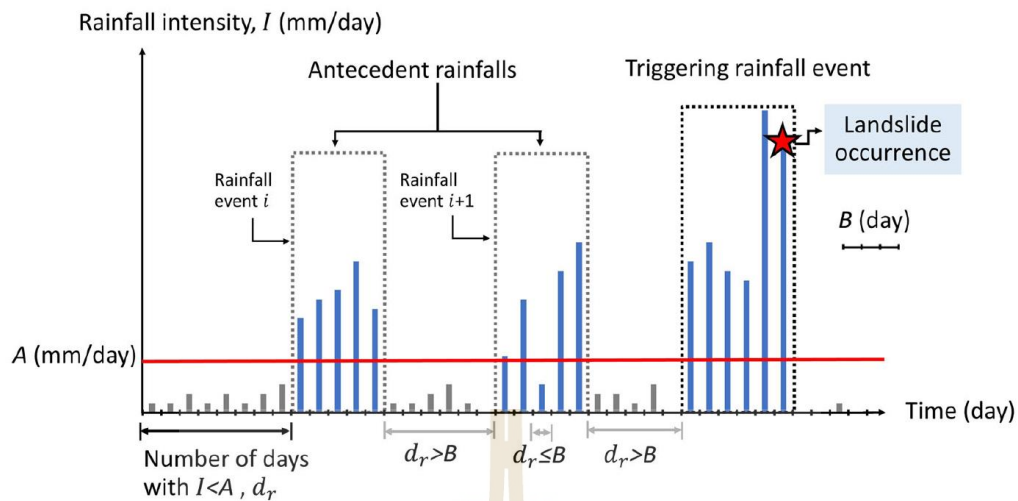


Figure 5.2 The chart shows how consecutive rainfall events were determined to have satisfied both conditions of the inter-event criterion used to define a single rainfall event in this study.

In this study, the suitable IEC was identified using all rainfall data (both triggered and non-triggered rainfall events) from the years in which landslide events occurred in the study areas. Since the suitable IEC can vary depending on seasonal and climatic conditions, and there is a clear distinction between two consecutive rainfalls in the pre-monsoon period, the determination of the suitable IEC in this study was based on a dataset that excluded inter-event rainfall in the pre-monsoon period. Twelve sets of variables A and B were examined to identify the suitable $IEC_{A,B}$. For each $IEC_{A,B}$, all inter-event times between every consecutive rainfalls were read and then employed to calculate the mean and the standard deviation of the inter-event times. Based on an assumption that inter-event times have an exponential distribution for which the mean equals the standard deviation (Bonta and Rao 1988), the suitable IEC was identified on the basis of a variation coefficient (CV) of inter-event times equal to 1.0. The variation coefficient (CV), defined as the ratio of the standard deviation to the mean, was calculated and presented in Table 5.1. As expressed in Table 1, the IEC that returned the CV closest to 1.0 was the $IEC_{5,1}$, which stands for the condition that rainfall intensity was no greater than 5 mm/day for at least 1 days.

Table 5.1 Basic statistics of inter-event duration corresponding to various inter-event criteria.

Inter-event criteria	Mean [day]	SD [day]	CV [-]
IEC _{0,1}	3.00	3.49	1.16
IEC _{0,2}	5.32	4.02	0.75
IEC _{0,3}	6.81	4.03	0.59
IEC _{1,1}	3.19	3.64	1.14
IEC _{1,2}	5.79	4.60	0.79
IEC _{1,3}	7.25	4.62	0.64
IEC _{2,1}	3.30	3.64	1.10
IEC _{2,2}	5.06	4.07	0.80
IEC _{2,3}	6.67	4.21	0.63
IEC _{5,1}	3.64	3.79	1.04
IEC _{5,2}	5.10	4.04	0.79
IEC _{5,3}	6.52	4.18	0.64

Table 5.2 Frequency distribution of rainfall duration.

Duration [day]	Number of rainfall events [-]	Number of rainfall events [%]
1	881	46.8
2	410	21.8
3	298	15.8
4	121	6.4
5	56	3
6	48	2.6
7	37	2
8	14	0.7
9	9	0.5
11	2	0.1
12	2	0.1
13	1	0.1
15	2	0.1
17	1	0.1

Remark: The rainfall events were defined by IEC_{5,1}.

Table 5.3. Frequency distribution of rainfall event in mm.

Rainfall events [mm]	Number of rainfall events [-]	Number of rainfall events [%]	Cumulated number of rainfall event [%]
0 - 10	658	35.0	35.0
11 - 20	356	18.9	53.9
21 - 30	250	13.3	67.2
31 - 40	179	9.5	76.7
41 - 50	114	6.1	82.8
51 - 60	46	2.4	85.2
61 - 70	62	3.3	88.5
71 - 80	33	1.8	90.3
81 - 90	44	2.3	92.6
91 - 100	24	1.3	93.9
101 - 110	36	1.9	95.8
111 - 120	12	0.6	96.4
121 - 130	14	0.7	97.1
131 - 140	10	0.5	97.6
141 - 150	2	0.1	97.7
150 - 200	24	1.3	99.0
>200	18	1.0	100.0

Remark: The rainfall events were defined by $IEC_{5,1}$.

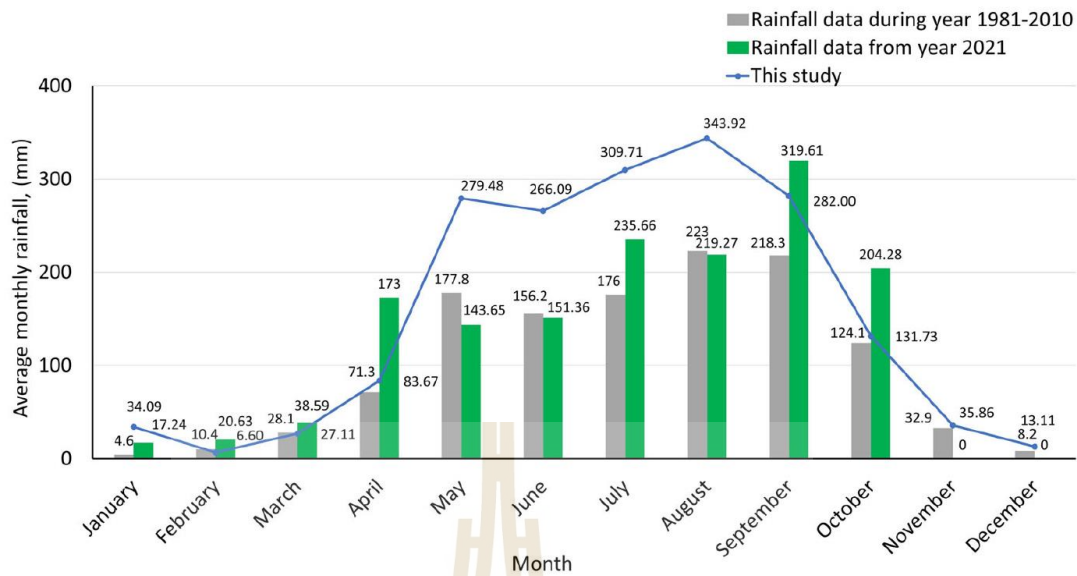


Figure 5.3 Average monthly rainfall in mm derived from gauge data for 30-year period from 1981 to 2010 (gray column) and for the recent year 2021 (green column). The blue line represents average monthly rainfall from data extracted in years when landslides occurred and from rain gauges located in the catchment areas where landslides had occurred.

Based on rainfall events defined by $IEC_{5,1}$, frequency distributions tables were produced of rainfall duration in days (Table 5.2) and rainfall event in mm (Table 5.3) for rainfall events from the years in which landslide events occurred in the study areas. Eighty-four percent of the collected rainfalls lasted no longer than 3 days. With regard to a depth of rainfall, it was found that eighty-three percent of the collected rainfalls fell to a depth no greater than 50 mm. Figure 5.3 presents average monthly rainfall in mm (blue line) calculated from rainfall data in this study compared with 30-year average monthly rainfall from years 1981–2010 (gray column) and monthly rainfall of the recent year 2021 (green column) sourced from Thai Meteorological Department (2022). The rainfall data gathered in this study produced a similar distribution to the results from gauge readings throughout the Northern Thailand. Since the rainfall data in this study were collected from the years when the landslide events occurred and from selected rain gauge stations located in the same

catchments with the considered landslides, the average monthly rainfall from rainfall data in this study was surely higher than the 30-year average and the recent year.

5.4 Measures of evaluation

In the evaluation of the performance of the thresholds to be established in this study, we considered various measures that are applied in the contingency table, comprising numbers of true positives (TP), true negatives (TN), false positives (FP), and false negatives (FN), and were employed in diagnosing landslide rainfall threshold in the study area. A hit rate (HR) in Eq. 1 indicates the proportion of the correctly predicted landslide triggered rainfall events among all triggered rainfall events. The HR ranges from zero (0) at the poor end to one (1) at the good end. A false alarm rate (FAR) in Eq. 2 measures the number of false alarms per total number of non-triggering rainfalls. A false alarm ratio (FA) in Eq. 3 measures the fraction of forecasted events that did not occur. The FAR and FA range from zero (0) at the good end to one (1) at the poor end. A Hanssen-Kuiper skill score (KH) in Eq. 4 represents the hit rate with respect to the false alarm rate and remain positive while the hit rate is higher than the false alarm rate. The best possible KH score is 1, which is returned when the HR is 1 and the FAR is 0. The worst possible HK is 0, which is returned when $HR = FA$. A critical success index (CSI) in Eq. 5 combines HR and FA into one score for low frequency events. This score measures the fraction of observed and/or forecast events that were correctly predicted. It ranges from zero (0) at the poor end to one (1) at the good end.

$$HR = \frac{TP}{TP + FN} \quad (5.1)$$

$$FAR = \frac{FP}{FP + TN} \quad (5.2)$$

$$FA = \frac{FP}{TP + FP} \quad (5.3)$$

$$HK = HR - FAR \quad (5.4)$$

$$CSI = \frac{TP}{TP + FP + FN} \quad (5.5)$$

Other than the aforementioned scores, the receiver operating characteristic (ROC) curves of HR against FAR were plotted at various probabilistic levels of landslide threshold and the corresponding areas under the ROC curves (AUC) were calculated to determine predictability. Furthermore, for each probabilistic level, the Euclidean distance, δ , was calculated between the point corresponding to the threshold on the ROC curve and the ideal coordinate (0,1).

5.5 The event rainfall – duration thresholds

Based on rainfall events defined by $IEC_{5,1}$, rainfall event (E) and rainfall duration (D) data points of non-triggering- and triggering-rainfalls plotted on a double logarithmic scale were plotted on a double logarithmic scale in Figure 5.4a. The threshold was being established from rainfall event (E) and rainfall duration (D) of landslide-triggering rainfall events in Northern Thailand. Quantile regression (Koenker and Bassett 1978) was employed to generate sets of rainfall thresholds at various probabilistic levels using Eq. (5.6).

$$\log_{10} E = a + b \log_{10} D \quad (5.6)$$

where a and b are regression coefficients. Using the above relationship, the ED threshold gave a straight line in double logarithmic scale.

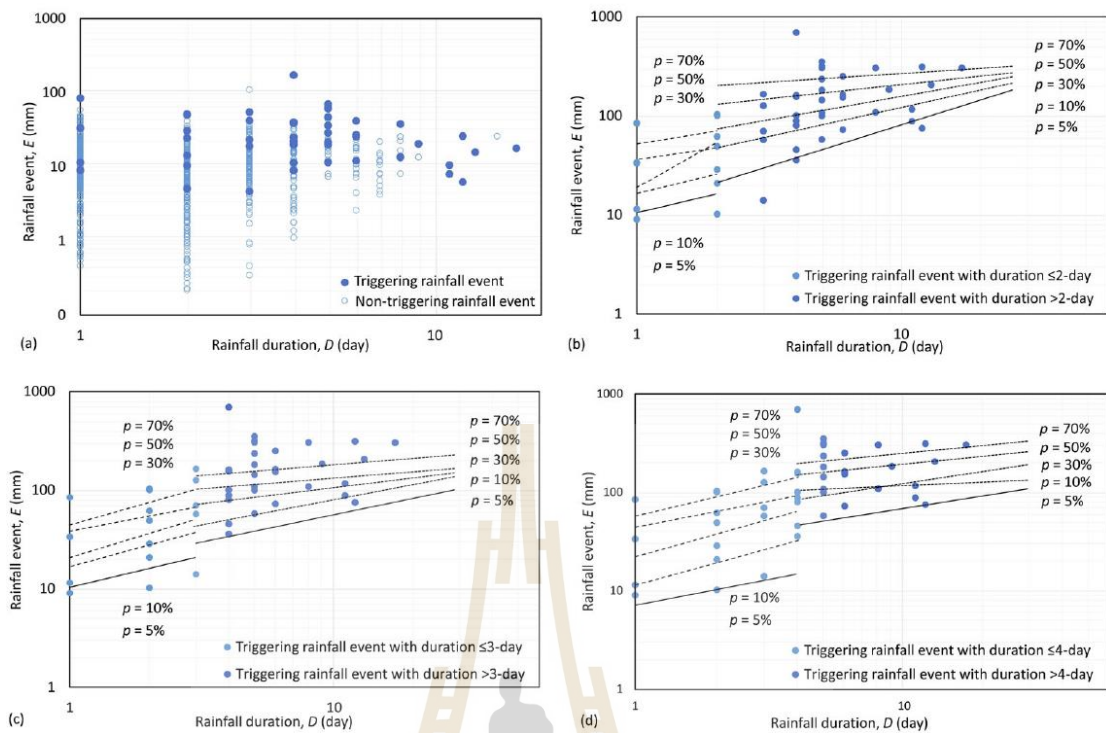


Figure 5.4 (a) From the data of non-triggering and triggering rainfalls, double logarithmic scatter plots were built from data points of rainfall event versus rainfall duration. The rainfall event – duration (ED) threshold was determined at various probability levels using quantile regression. (b) The ED threshold was divided to two categories; short duration rainfall threshold and log duration rainfall threshold, using a split point at 2 days, (c) The ED threshold using a split point at 3 days, (d) The ED threshold using a split point at 4 days.

To account for short- and long-duration rainfall events, the rainfall events were divided to two groups: short- and long- duration rainfall events. However, due to wide variety of hydrogeological conditions, a time at a split point between short- and long-duration rainfall thresholds lays over a range from many hours to few days. He et al. (2020) divided rainfalls to two groups; short- and long-duration rainfalls, using 48 hours as a split point to establish landslide rainfall threshold in China. Wicki et al. (2020) used rainfall duration of 6 hours to classified if the rainfall is short- or longduration rainfalls. Chen and Chen (2022) characterized rainfalls that triggered

landslide in Taiwan to three types; including high rainfall intensity over a short duration (<12 h), high-intensity and prolonged rainfall, and high cumulative rainfall over a long duration (>36 h). Based on distribution of rainfall duration presented in Table 5.2, most of the rainfall events (almost 70%) last no longer than 2 days and there are few rainfall events (less than 10%) last longer than 4 days. Therefore, a time at a split point between short- and long-duration rainfall thresholds could be within 2–4 days. In order to define a suitable split point, three sets of the *ED* thresholds having their split point at 2-day (Figure 5.4b), 3-day (Figure 5.4c) and 4-day (Figure 5.4d) were established and assessed.

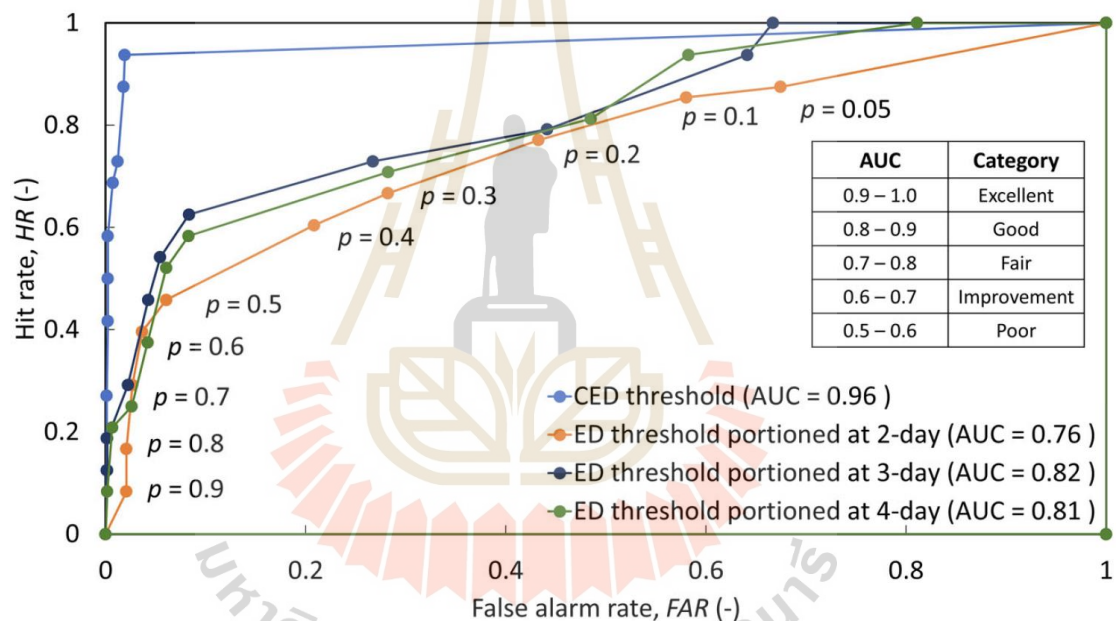


Figure 5.5 Receiver operating characteristic (*ROC*) curve and the corresponding area under the *ROC* curve (*AUC*) generated from the *ED* thresholds and the *CED* threshold.

Figure 5.5 presents the *ROC* curve and the corresponding *AUC* of three *ED* thresholds split at 2-day, 3-day, and 4-day. The performance was fair (*AUC* less than 0.76) for the *ED* threshold with the split point at 2-day. For the split point at 3-day and 4-day, the *ED* thresholds yielded good predictability of their *AUC* magnitudes greater than 0.80. Among three *ED* thresholds, the *ED* threshold that used 3-day as a

split point between short- and long-duration rainfalls exhibited the highest *AUC*. Hence, the split point at 3-day was chosen as a separator for establishing the *ED* threshold for short duration rainfall events (ED_S threshold) and the *ED* threshold for long duration rainfall events (ED_L threshold). Threshold parameters *a* and *b* for exceedance probabilities from 5 to 90% are reported in Table 5.4.

Table 5.4 Threshold parameters *a* and *b* (see Eq. 5.1) for exceedance probabilities from 5 to 90%. The threshold was portioned to two parts; ED_S (for short duration rainfall events) and ED_L (for long duration rainfall events) thresholds. The threshold was portioned using a split point at 3 days.

ED_S Threshold Prob. Level	Parameters		ED_L Threshold Prob. Level	Parameters	
	<i>a</i>	<i>b</i>		<i>a</i>	<i>b</i>
5	0.954	0.177	5	1.147	0.672
10	0.954	0.402	10	1.264	0.652
20	1.058	0.860	20	1.844	0.096
30	1.058	1.465	30	1.771	0.292
40	1.522	0.558	40	1.558	0.676
50	1.522	0.673	50	1.895	0.373
60	1.522	0.887	60	2.050	0.234
70	1.526	1.205	70	1.962	0.421
80	1.844	0.538	80	2.483	-0.002
90	1.960	0.542	90	2.509	-0.015

Table 5.5 Summarizes the four contingencies (TP , FP , FN , TN) and the six skill scores (HR , FAR , FA , CSI , HK , δ) obtained from the ED threshold for ten probabilistic levels.

Probabilistic level	Contingencies and skill scores									
	TP	FN	TN	FP	HR	FAR	FA	CSI	HK	δ
5	48	0	611	1223	1.00	0.67	0.96	0.04	0.33	0.67
10	45	3	658	1176	0.94	0.64	0.96	0.04	0.3	0.64
20	38	10	1025	809	0.79	0.44	0.96	0.04	0.35	0.49
30	35	13	1344	490	0.73	0.27	0.93	0.07	0.46	0.38
40	30	18	1681	153	0.63	0.08	0.84	0.15	0.54	0.38
50	26	22	1734	100	0.54	0.05	0.79	0.18	0.49	0.46
60	22	26	1756	78	0.46	0.04	0.78	0.17	0.42	0.54
70	14	34	1793	41	0.29	0.02	0.75	0.16	0.27	0.71
80	9	39	1831	3	0.19	0.00	0.25	0.18	0.19	0.81
90	6	42	1831	3	0.13	0.00	0.33	0.12	0.12	0.88

Table 5.5 summarizes the four contingency scores and the six skill scores at ten probabilistic levels from 5 to 90% produced by results obtained from the ED threshold portioned to short- and long-duration rainfall thresholds by 3-day duration. At low probabilistic levels, the threshold yielded very high FA value (i.e. $FA = 0.96$ at probabilistic level of 5%). Threshold with high FA results in the operators losing trust in its reliability. Furthermore, the CSI value generated by the threshold was much lower than 0.50 at every probabilistic level suggesting that the forecast had little or no skill. Hence, we concluded that the ED threshold is not practically useful in the study area.

5.6 The cumulative rainfall with rainfall event – duration threshold

For ease to account for antecedent rainfalls, cumulative rainfall over certain period prior to the failure day was integrated to the established threshold. Figure 5.6a presents the rainfall on a failure day (DR_f) against cumulative rainfall over 3-, 5-, 10-, 15-, 20-, 25-day periods prior to the failure day. The plots were divided into two

portions with a 1:1 line to clarify bias in the scattering, whether towards the rainfall on a failure day or cumulative rainfall prior to the failure day. From 48 triggered rainfall events, 34 events were biased toward cumulative rainfall of 3-day period prior to the failure day. The number of biasness toward cumulative rainfall increased to 35, 40, 42, 42, and 46 events when period of cumulative rainfall increased to 5-, 10- 15-, 20-, 25-day period, respectively. Therefore, cumulative rainfall over 25-day period prior to the failure day (CR_{25}) was considered as a suitable threshold variable for landslides in the studied area. Figure 5.5.6b presents a scatter plot of data points representing DR_f and CR_{25} for 48 triggered rainfall events. The scatter plot revealed that the highest value of CR_{25} that returned few numbers of triggered rainfall events was CR_{25} of 149 mm. Hence, the CR_{25} value of 140mm was an indicator that could potentially be used as a landslide-triggering threshold in the studied area.

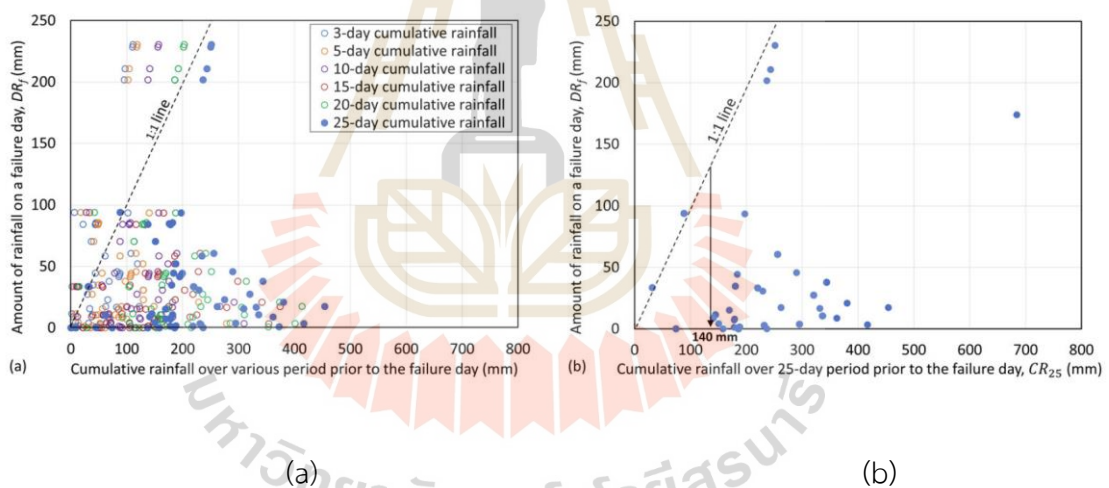


Figure 5.6 Rainfall on a failure day in mm was plotted with respect to cumulative rainfall over 3-, 10-, 15-, 20-, and 25- day period prior to the failure day (a). Rainfall on a failure day in mm was plotted with respect to cumulative rainfall over 25- day period before the failure day (b).

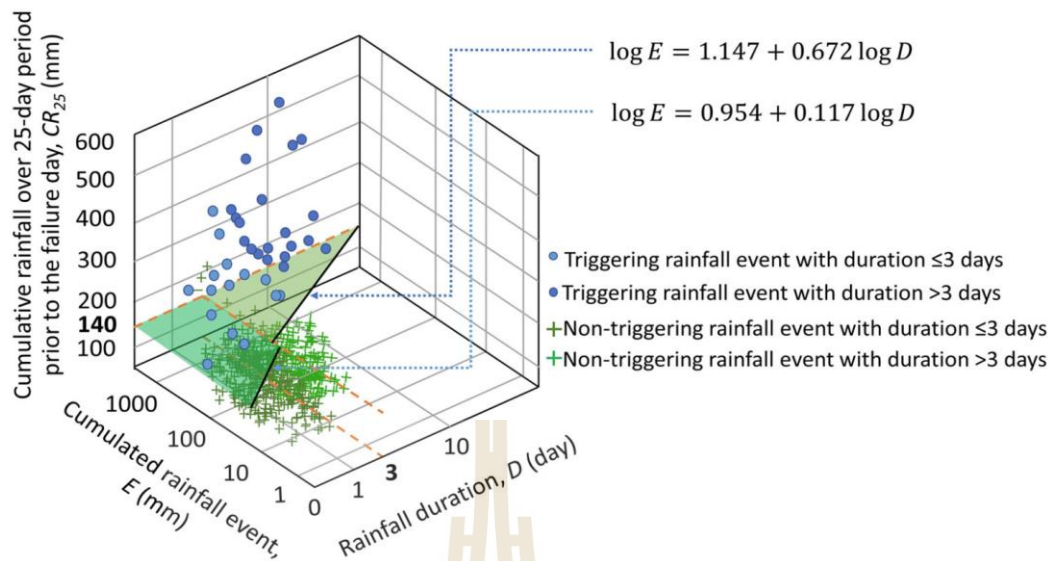


Figure 5.7 The *CED* threshold plotted in three -dimensional space. The threshold was portioned at 3-day becoming the *CED* threshold for rainfall events of their duration no longer than 3 days and the *CED* threshold for rainfall events of their duration longer than 3 days.

Table 5.6 Summarizes the four contingencies (*TP*, *FP*, *FN*, *TN*) and the six skill scores (*HR*, *FAR*, *FA*, *CSI*, *HK*, δ) obtained from the *CED* threshold for ten probabilistic levels.

Probabilistic level	Contingencies and skill scores									
	<i>TP</i>	<i>FN</i>	<i>TN</i>	<i>FP</i>	<i>HR</i>	<i>FAR</i>	<i>FA</i>	<i>CSI</i>	<i>HK</i>	δ
5	45	3	1799	35	0.94	0.02	0.44	0.54	0.92	0.07
10	42	6	1801	33	0.88	0.02	0.44	0.52	0.86	0.13
20	35	13	1812	22	0.73	0.01	0.39	0.50	0.72	0.27
30	33	15	1821	13	0.69	0.01	0.28	0.54	0.68	0.31
40	28	20	1830	4	0.58	0.00	0.13	0.54	0.58	0.42
50	24	24	1830	4	0.50	0.00	0.14	0.46	0.5	0.5
60	20	28	1830	4	0.42	0.00	0.17	0.38	0.41	0.58
70	13	35	1832	2	0.27	0.00	0.13	0.26	0.27	0.73
80	9	39	1832	2	0.19	0.00	0.18	0.18	0.19	0.81
90	6	42	1832	2	0.13	0.00	0.12	0.12	0.12	0.88

The CR_{25} of 140mm was introduced into the ED threshold presented in Figure 5.4c to establish a CED threshold portioned by rainfall duration (Figure 5.7). This threshold was portioned into a threshold for rainfall events of their duration no longer than 3 days, and a threshold for rainfall events of their duration longer than 3 days. Table 5.6 presents the four contingencies and the six skill scores for ten probabilistic levels from 5 to 90% calculated for the CED threshold. Introducing the CR_{25} of 140mm into the threshold resulted in notably fewer FP cases, and hence the FAR for the CED threshold was considerably lower than the FAR for the ED threshold. The reduction of FAR significantly improved the overall reliability of the threshold, indicated by the ROC curve and the corresponding AUC of the CED threshold (Figure 5.5). The reliability of prediction with the CED threshold was very good ($AUC = 0.96$). The FA of the CED threshold ($FA = 0.44$) yielded positive results since it was significantly lower than the FA yielded by the ED threshold ($FA = 0.96$). The best compromise between the minimum number of incorrect landslide predictions (FP , FN) and the maximum number of correct predictions (TP , TN), was indicated by combination of the largest values for the HK and the smallest value of the d . It was found that the best compromising predictions was obtained at probabilistic levels of 5% for the CED threshold ($HK = 0.92$ and $\delta = 0.07$). The CED thresholds proposed in this study can be employed as shown in Figure 5.8.

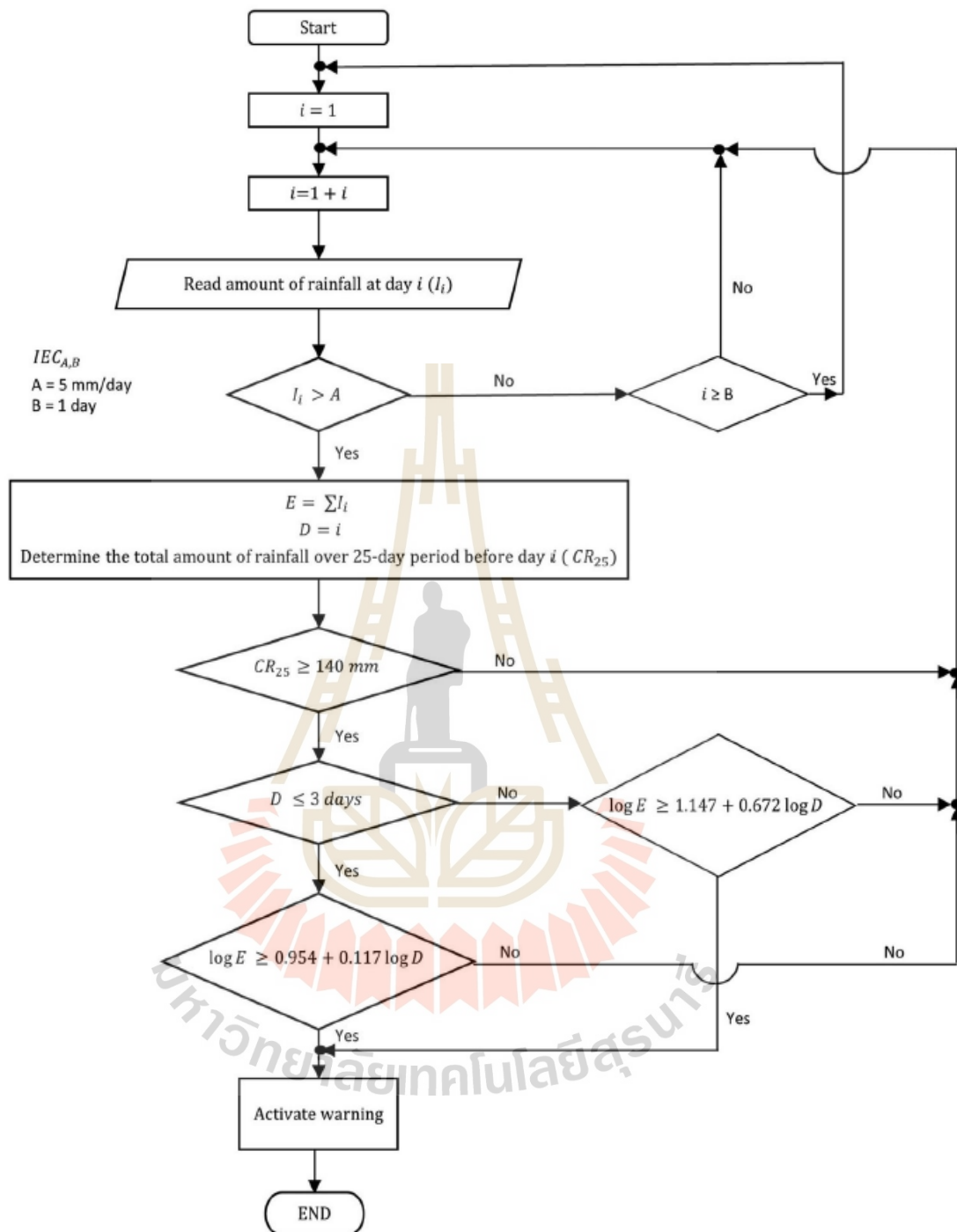


Figure 5.8 Flowchart of landslide rainfall assessment using the introduced threshold.

5.7 Conclusion

Rainfall data corresponding to 59 landslides recorded in Northern Thailand during the years 2002 to 2018 was used to establish landslide rainfall threshold in the study area. Based on the variation coefficient (*CV*) of inter-event times, a suitable inter-event criterion (*IEC*) to separate two consecutive rainfalls was $IEC_{5,1}$ standing for the condition that rainfall intensity was no greater than 5mm/day for at least 1 days. The threshold introduced in this study was a threshold that explicitly included rainfall event and antecedent rainfall parameters in the threshold, namely cumulative rainfall with rainfall event-duration (*CED*) threshold. 140mm of the cumulative rainfall over 25-day period prior to a failure day (CR_{25}) was found to be a suitable indicator to deal with antecedent rainfall events. Based on the threshold predictability and distribution of rainfall duration, a period of 3 days was chosen as an indicator to distinguish the rainfall event to short- and long-duration rainfall events. And the introduced threshold included the *CED* threshold for rainfall event of their duration no longer than 3 days and the *CED* threshold for rainfall events of their duration longer than 3 days. Introducing the CR_{25} of 140mm into the threshold resulted in notably fewer false positive (*FP*) cases, and hence the false alarm rate (*FAR*) for the *CED* threshold was considerably lower than the *FAR* for the rainfall event-duration (*ED*) threshold. The reduction of *FAR* significantly improved the overall reliability of the threshold, indicated by the magnitude of the area under the receiver operating characteristic. Furthermore, the false alarm ratio (*FA*) of the *CED* threshold yielded positive results since it was significantly lower than the *FA* yielded by the *ED* threshold. Since the *CED* threshold at probabilistic levels of 5% returned the largest Hanssen and Kuipers (*HK*) score and the smallest value of *d*, this threshold at probabilistic level of 5% can be recommended as the landslide rainfall threshold in Northern Thailand.

5.8 References

Ahmad R. 2003. **Developing early warning systems in Jamaica: rainfall thresholds for hydrological hazards**. In: National Disaster Management Conference, Ocho Rios, St Ann, Jamaica, Sept 9–10.

- Aleotti P. 2004. **A warning system for rainfall-induced shallow failures.** Eng Geol. 73(3–4): 247–265. <https://doi.org/10.1016/j.enggeo.2004.01.007>.
- Bonta JV, Rao AR. 1988. **Factors affecting the identification of independent storm events.** J Hydrol. 98(3–4):275–293. [https://doi.org/10.1016/0022-1694\(88\)90018-2](https://doi.org/10.1016/0022-1694(88)90018-2).
- Caine N. 1980. **The rainfall intensity - duration control of shallow landslides and debris flows.** Geogr Ann Ser A Phys Geogr. 62(1–2):23–27. <https://doi.org/10.1080/04353676.1980.11879996>.
- Chen HW, Chen CY. 2022. **Warning models for landslide and channelized debris flow under climate change conditions in Taiwan.** Water. 14(5) :695. <https://doi.org/10.3390/w14050695>.
- Chen D, Ou T, Gong L, Xu CY, Li W, Ho CH, Qian W. 2010. **Spatial interpolation of daily precipitation in China: 1951–2005.** Adv Atmos Sci. 27(6):1221–1232. <https://doi.org/10.1007/s00376-010-9151-y>.
- Chinkulkijniwat A, Horpibulsuk S, Bui Van D, Udomchai A, Goodary R, Arulrajah A. 2016. **Influential factors affecting drainage design considerations for mechanical stabilised earth walls using geocomposites.** Geosynthetics International. :1–18. doi:10.1680/jgein.16.00027.
- Chinkulkijniwat A, Tirametatarat T, Supotayan C, Yubonchit S, Horpibulsuk S, Salee R, Voottipruex P. 2019. **Stability characteristics of shallow landslide triggered by rainfall.** J Mt Sci. 16(9):2171–2183. <https://doi.org/10.1007/s11629-019-5523-7>.
- Chinkulkijniwat A, Yubonchit S, Horpibulsuk S, Jothityangkoon C, Jeeptaku C, Arulrajah A. 2016. **Hydrological responses and stability analysis of shallow slopes with cohesionless soil subjected to continuous rainfall.** Can Geotech J. 53(12):2001–2013. <https://doi.org/10.1139/cgj-2016-0143>.
- Crosta GB, Frattini P. 2001. **Rainfall thresholds for triggering soil slips and debris flow.** In: Proceedings of the 2nd EGS Plinius Conference on Mediterranean Storms: Publication CNR GNDCl. Vol. 2547, Oct; p. 463–487.

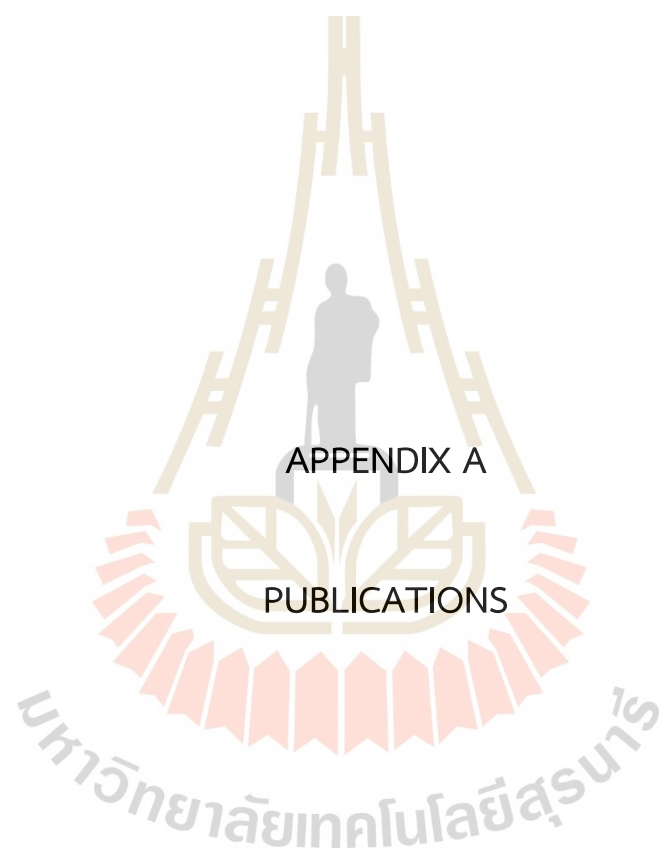
- Ditthakit P, Nakrod S, Viriyanantavong N, Tolche AD, Pham QB. 2021. **Estimating baseflow and baseflow index in ungauged basins using spatial interpolation techniques: a case study of the Southern River Basin of Thailand.** *Water*. 13(21):3113. <https://doi.org/10.3390/w13213113>.
- Environmental Geology Division. 2003. **A manual of landslide geo-hazard prevention and list of landslide risk villages of the north region of Thailand.** Bangkok, Thailand: Department of Mineral Resources, 113 pp. (in Thai)
- Fan L, McArdell B, Or D. 2016. **Linking rainfall-induced landslides with debris flows runoff patterns towards catchment scale hazard assessment.** *Geomorphology*. 280:1–15. <http://doi.org/10.1016/j.geomorph.2016.10.007>.
- Gariano SL, Brunetti MT, Iovine G, Melillo M, Peruccacci S, Terranova O, Vennari C, Guzzetti F. 2015. **Calibration and validation of rainfall thresholds for shallow landslide forecasting in Sicily, southern Italy.** *Geomorphology*. 228:653–665. <https://doi.org/10.1016/j.geomorph.2014.10.019>.
- Gariano SL, Melillo M, Peruccacci S, Brunetti MT. 2020. **How much does the rainfall temporal resolution affect rainfall thresholds for landslide triggering?** *Nat Hazards*. 100(2):655–670. <https://doi.org/10.1007/s11069-019-03830-x>.
- Gariano SL, Sarkar R, Dikshit A, Dorji K, Brunetti MT, Peruccacci S, Melillo M. 2019. **Automatic calculation of rainfall thresholds for landslide occurrence in Chukha Dzongkhag, Bhutan.** *Bull Eng Geol Environ*. 78(6): 4325–4332. <https://doi.org/10.1007/s10064-018-1415-2>.
- Gentile M, Courbin F, Meylan G. 2013. **Interpolating point spread function anisotropy.** *Astron Astrophys*. 549: A1. <https://doi.org/10.1051/0004-6361/201219739>.
- Germain D, Roy S, Guerra A. 2021. **Empirical rainfall thresholds for landslide occurrence in Serra do Mar, Angra dos Reis, Brazil.** In: Zhang Y, Cheng Q, editors. *Landslides*. IntechOpen. <https://doi.org/10.5772/intechopen.100244>.

- Giannecchini R, Galanti Y, D'Amato Avanzi G. 2012. **Critical rainfall thresholds for triggering shallow landslides in the Serchio River Valley (Tuscany, Italy)**. *Nat. Hazard Earth Sys.* 12. 829–842. <https://doi.org/10.5194/nhess-12-829-2012>.
- Giannecchini R, Galanti Y, D'Amato Avanzi G, Barsanti M. 2015. **Probabilistic rainfall thresholds for triggering debris flows in a human-modified landscape**. *Geomorphology*. 257:94–107. <https://doi.org/10.1016/j.geomorph.2015.12.012>.
- Grozavu A, Patriche CV. 2021. **Mapping landslide susceptibility at national scale by spatial multi-criteria evaluation**. *Geomatics Nat Hazards Risk*. 12(1):1127–1152. <https://doi.org/10.1080/19475705.2021.1914752>.
- Guzzetti F, Cardinali M, Reichenbach P. 1994. **The AVI project: a bibliographical and archive inventory of landslides and floods in Italy**. *Environ Manage.* 18(4):623–633. <https://doi.org/10.1007/bf02400865>.
- Guzzetti F, Peruccacci S, Rossi M, Stark CP. 2008. **The rainfall intensity-duration control of shallow landslides and debris flows: an update**. *Landslides*. 5(1):3–17. <https://doi.org/10.1007/s10346-007-0112-1>.
- He S, Wang J, Liu S. 2020. **Rainfall event-duration thresholds for landslide occurrences in China**. *Water*. 12(2):494. <https://doi.org/10.3390/w12020494>.
- lida T. 2004. **Theoretical research on the relationship between return period of rainfall and shallow landslides**. *Hydrol Process*. 18(4):739–756. <https://doi.org/10.1002/hyp.1264>.
- Indraratna B, Fatahi B, Khabbaz H. 2006. **Numerical analysis of matric suction effects of tree roots**. *Proc Inst Civ Eng - Geotech Eng*. 159(2):77–90. <https://doi.org/10.1680/geng.2006.159.2.77>.
- Kanjanakul C, Chub-uppakarn T, Chalermyanont T. 2016. **Rainfall thresholds for landslide early warning system in Nakhon Si Thammarat**. *Arab J Geosci*. 9:584–595. <https://doi.org/10.1007/s12517-016-2614-4>.
- Koenker R, Bassett G. 1978. **Regression quantiles**. *Econometrica*. 46(1):33. <https://doi.org/10.2307/1913643>.

- Komolvilas V, Tanapalungkorn W, Latcharote P, Likitlersuang S. 2021. **Failure analysis on a heavy rainfall-induced landslide in Huay Khab Mountain in Northern Thailand.** *J Mt Sci.* 18(10):2580–2596. <https://doi.org/10.1007/s11629-021-6720-8>.
- Kong YF, Tong WW. 2008. **Spatial exploration and interpolation of the surface precipitation data.** *Geogr. Res.* 27(5):1097–1108.
- Kurtzman D, Navon S, Morin E. 2009. **Improving interpolation of daily precipitation for hydrologic modelling: Spatial patterns of preferred interpolators.** *Hydrol Process.* 23(23):3281–3291. <https://doi.org/10.1002/hyp.7442>.
- Lee WY, Park SK, Sung HH. 2021. **The optimal rainfall thresholds and probabilistic rainfall conditions for a landslide early warning system for Chuncheon, Republic of Korea.** *Landslides.* 18(5):1721–1739. <https://doi.org/10.1007/s10346-020-01603-3>.
- Maturidi A, Kasim N, Taib AK, Azahar W, Tajuddin HA. 2020. **Empirically based rainfall threshold for landslides occurrence in Cameron Highlands, Malaysia.** *Civil Eng Architect.* 8(6):1481–1490. <https://doi.org/10.13189/cea.2020.080629>.
- Peruccacci S, Brunetti M, Gariano SL, Melillo M, Rossi M, Guzzetti F. 2017. **Rainfall thresholds for possible landslide occurrence in Italy.** *Geomorphology.* 290:39–57. <https://doi.org/10.1016/j.geomorph.2017.03.031>.
- Rosi A, Segoni S, Canavesi V, Monni A, Gallucci A, Casagli N. 2021. **Definition of 3D rainfall thresholds to increase operative landslide early warning system performances.** *Landslides.* 18(3):1045–1057. <https://doi.org/10.1007/s10346-020-01523-2>.
- Salee R, Chinkulkijniwat A, Yubonchit S, Horpibulsuk S, Wangfaoklang C, Soisompong S. 2022. **New threshold for landslide warning in the southern part of Thailand integrates cumulative rainfall with event rainfall depth-duration.** *Nat Hazards.* 113(1):125–141. <https://doi.org/10.1007/s11069-022-05292-0>.

- Schmidt-Thom_e P, Tatong T, Kunthasap P, Wathanaprida S. 2018. **Community based landslide risk mitigation in Thailand**. *Episodes*. 41(4) :225–233. <https://doi.org/10.18814/epiiugs/2018/018017>.
- Segoni S, Piciullo L, Gariano SL. 2018. **A review of the recent literature on rainfall thresholds for landslide occurrence**. *Landslides*.15(8):1483–1501. <https://doi.org/10.1007/s10346-018-0966-4>.
- Teerarungsigul S, Torizin J, Fuchs M, Kuhn F, Chonglakmani C. 2016. **An integrative approach for regional landslide susceptibility assessment using weight of evidence method: a case study of Yom River Basin, Phrae province, Northern Thailand**. *Landslides*. 13(5):1151–1165. <https://doi.org/10.1007/s10346-015-0659-1>.
- Thai Meteorological Department. 2022. **Monthly rainfall**. [accessed 2022 Aug 4]. <http://www.arcims.tmd.go.th/dailydata/MonthRain.php>.
- Vennari C, Gariano SL, Antronico L, Brunetti MT, Iovine G, Peruccacci S, Terranova O, Guzzetti F. 2014. **Rainfall thresholds for shallow landslide occurrence in Calabria, southern Italy**. *Nat Hazards Earth Syst Sci*. 14(2) : 317–330. <https://doi.org/10.5194/nhess-14-317-2014>.
- Vessia G, Parise M, Brunetti MT, Peruccacci S, Rossi M, Vennari C, Guzzetti F. 2014. **Automated reconstruction of rainfall events responsible for shallow landslides**. *Nat Hazards Earth Syst Sci*. 14(9):2399–2408. <https://doi.org/10.5194/nhess-14-2399-2014>.
- Wicki A, Lehmann P, Hauck C, Seneviratne SI, Waldner P, St€ahli M. 2020. **Assessing the potential of soil moisture measurements for regional landslide early warning**. *Landslides*.17(8):1881–1896. <https://doi.org/10.1007/s10346-020-01400-y>.
- Wieczorek G, Glade T. 2005. **Climatic factors influencing occurrence of debris flows**. In: Jakob M, Hungr O, editors. *Debris-flow hazards and related phenomena*. Berlin: Springer; p.325–362. https://doi.org/10.1007/3-540-27129-5_14

- Ya'acob N, Tajudin N, Azize A. 2019. **Rainfall-landslide early warning system (RLEWS) using TRMM precipitation estimates**. Indonesian J Electr Eng Comput Sci. 13(3):1259–1266. <https://doi.org/10.11591/ijeecs.v13.i3.pp.1259-1266>.
- Yang KH, Nguyen TS, Rahardjo H, Lin DG. 2021. **Deformation characteristics of unstable shallow slopes triggered by rainfall infiltration**. Bull Eng Geol Environ. 80(1):317–344. 2021 <https://doi.org/10.1007/s10064-020-01942-4>.
- Yang H, Wei F, Ma Z, Guo H, Su P, Zhang S. 2020. **Rainfall threshold for landslide activity in Dazhou, southwest China**. Landslides. 17(1):61–77. <https://doi.org/10.1007/s10346-019-01270-z>.
- Yang X, Xie X, Liu DL, Ji F, Wang L. 2015. **Spatial interpolation of daily rainfall data for local climate impact assessment over greater Sydney region**. Adv Meteorol. 2015:1–12. <https://doi.org/10.1155/2015/563629>.
- Yubonchit S, Chinkulkijniwat A, Horpibulsuk S, Jothityangkoon C, Arulrajah A, Suddeepong A p 2017. **Influence factors involving rainfall-induced shallow slope failure: numerical study**. Int J Geomech. 17(7):04016158.
- Yumuang S. 2006. **2001 debris flow and debris flood in Nam Ko area, Phetchabun province, central Thailand**. Environ Geol. 51(4):545–564. <https://doi.org/10.1007/s00254-006-0351-9>.
- Zhang K, Wang S, Bao HJ, Zhao XM. 2019. **Characteristics and influencing factors of rainfall-induced landslide and debris flow hazards in Shaanxi Province, China**. Nat. Hazard Earth Sys. 19:93–105. <https://doi.org/10.5194/nhess-19-93-2019>.



List of Publications

INTERNATIONAL JOURNAL PAPERS

- Salee, R., Chinkulkijniwat, A., Yubonchit, S., and Bui Van, D. (2022). **Rainfall Threshold for Landslide Warning in the Southern Thailand - An Integrated Landslide Susceptibility Map with Rainfall Event - Duration Threshold.** *Journal of Ecological Engineering*, 23(12), pp.124-133. <https://doi.org/10.12911/22998993/155023>.
- Salee, R., Chinkulkijniwat, A., Yubonchit, S. et al. **New threshold for landslide warning in the southern part of Thailand integrates cumulative rainfall with event rainfall depth-duration.** *Nat Hazards* 113, 125–141 (2022). <https://doi.org/10.1007/s11069-022-05292-0>
- Chinkulkijniwat, A., Salee, R., Horpibulsuk, S., Arulrajah, A., Hoy, M. (2022) **Landslide rainfall threshold for landslide warning in Northern Thailand,** *Geomatics, Natural Hazards and Risk*, 13:1, 2425-2441, DOI: 10.1080/19475705.2022.2120833.

Rainfall Threshold for Landslide Warning in Southern Thailand – An Integrated Landslide Susceptibility Map with Rainfall Event – Duration Threshold

Rattana Salee¹, Avirut Chinkulkijniwat^{1*}, Somjai Yubonchit², Duc Bui Van³

¹ Center of Excellence in Civil Engineering, School of Civil Engineering, Institute of Engineering, Suranaree University of Technology 111 University Avenue, Muang, Nakhon Ratchasima 30000, Thailand

² School of Civil Engineering, Rajamangala University of Technology Isan 744 Sura Narai Road, Muang District, Nakhon Ratchasima 30000, Thailand

³ Faculty of Civil Engineering, Hanoi University of Mining and Geology, North Tu Liem District, Hanoi City, Vietnam

* Corresponding author's e-mail: avirut@sut.ac.th

ABSTRACT

Southern Thailand is one of hotspots for landslides. So far, the rainfall triggered landslides in this region caused many sufferers and fatalities. On the basis of the rainfall data that triggered ninety-two landslide events during 1988–2018 and the landslide susceptibility maps published by the Department of Mineral Resources (DMR), this study introduced rainfall event-duration (*ED*) thresholds, namely *ED^m* and *ED^h* thresholds, for the places classified as the modest and the huge susceptibility levels, respectively. The modest susceptibility is a combination of very low, low, and moderate landslide susceptibility levels indicated in DMR maps. The huge susceptibility is a combination of high and very high landslide susceptibility levels indicated in DMR maps. Indicated by an area under the receiver operating characteristic curve (*AUC*), the *ED^m* and *ED^h* thresholds yielded the significantly better predictability than the original threshold did. Furthermore, the *ED^m* threshold yielded the perfect prediction with *AUC* of 1.00.

Keywords: rainfall threshold; landslide susceptibility level; contingency matrix; skill scores.

INTRODUCTION

Since the year 2000, the number of landslides per year has been increasing in Thailand (Schmidt-Thomé et al., 2017). Southern Thailand lies on the narrow part of the Malay Peninsula the landforms comprise two parallel mountain chains running north–south: the Phuket and Nakhon Srithammarat ranges; situated to the west and east, respectively. According to the report from the Department of Mineral Resources in 2019, this region is one of Thailand's hotspots for landslides. The landslides in 1988, which was known among of the worst natural disasters in the Thailand's history, also occurred in the Southern Thailand. Works on landslide risk assessment constitute one of vital contributions in

landslide mitigation measures. Since rainfall is commonly recognized as main temporal factor causing landslides, landslide rainfall threshold is commonly used as one of the vital components of landslide early warning system (Aleotti, 2004; Salee et al., 2022; Chinkulkijniwat et al., 2022). The most common parameters used to define the rainfall threshold are those based on characteristic of triggering landslide rainfall event (Caine, 1980; Aleotti, 2004; Guzzetti et al., 2008; Vennari et al., 2014; Vessia et al., 2014; He et al., 2020; Gariano et al., 2019; Peruccacci et al., 2017). Other than rainfall characteristics, a landslide can be influenced by many spatial factors, such as slope aspect, gradient, relative relief, lithology, degree of weathering, depth, permeability, porosity, etc. Incorporating these spatial factors to the

rainfall threshold might enhance the efficiency of the landslide prediction. A landslide susceptibility map carries the relevant information; relating to geomorphology, geological, meteorological soil, land use, land cover and hydrologic conditions, of the terrain and classifies the terrain into zones with differing likelihoods that landslides may occur. Integration of the landslide rainfall threshold and the landslide susceptibility map would benefit the landslide prediction. In fact, number of recent works reported the succession of the joint use of the landslide rainfall thresholds and the landslide susceptibility maps (Segoni et al., 2015; Jemec Aulfic et al., 2016; Segoni et al., 2018). Recently, the Department of Mineral Resources updated Thailand landslide susceptibility maps for the provincial level (<https://gis.dmr.go.th/DMR-GIS/gis>). These maps present five landslide susceptibility levels; including very high, high, moderate, low, and very low landslide susceptibility levels. This study used these susceptibility maps as a proxy to include the spatial factors carried by the landslide susceptibility map to the landslide rainfall threshold in the Southern Thailand. A contingency table and a set of skill scores were used to assess the performance of the threshold.

Data collection and rainfall characteristics in the study area

The authors gathered ninety-two landslide events that took place during 1988 to 2018 in the south of Thailand reported by the Department of Mineral Resources, Ministry of Natural Resources and Environment. Among ninety-two landslides, some landslides took place at the same time and their locations are close to each other. Under this condition, the largest landslide was chosen to represent the others. After this process, ninety-two landslides were reduced to eighty landslides. The Relevant rainfall data from the years when these eighty landslide events occurred were gathered from Thai Meteorological Department (TMD) rain gauge stations located in the catchment area (Figure 1) where the considered landslide is located. Inverse distance weighting (*IDW*) was employed to map the amount of rainfalls at the landslide locations.

To identify a rainfall event, a criterion that separates two consecutive rainfalls must be defined. The criterion is defined by a combination of the rainfall intensity threshold *A* and rainfall duration *B* and termed as inter-event criterion ($IEC_{A,B}$).

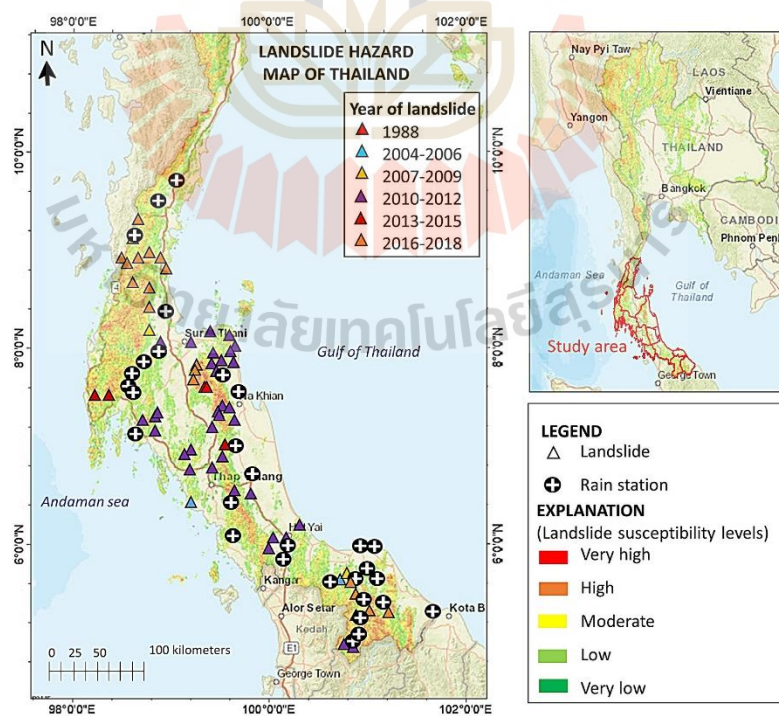


Figure 1. Locations of landslides and TMD rain gauge stations in the study area

The condition that distinguished two consecutive rainfall events had to satisfy the combined criterion. On the basis of an assumption that inter-event times have an exponential distribution for which the mean equals the standard deviation (Bonta and Rao 1988), the suitable IEC was identified on the basis of a variation coefficient (CV) of inter-event times equal to 1.0. Salee et al. (2022) reported that the inter-event criterion of $IEC_{2,1}$ can be used to distinguish two consecutive rainfalls in Southern Thailand. Accordingly, a criterion $IEC_{2,1}$ was used as the inter-event criterion to distinguish two consecutive rainfalls collected in this study. Distinction of two consecutive rainfall events is a condition that satisfied the combined criterion. As depicted

in Figure 2, if rainfall intensity is no greater than 2 mm/day for at least 1 day, two consecutive rainfall events are considered to have occurred.

Regarding to the landslide susceptibility maps published by the Department of Mineral Resources, there are five susceptibility levels of landslide; very low susceptibility (green color), low susceptibility (light green color), moderate susceptibility (yellow color), high susceptibility (orange color), and very high susceptibility (red color). Eighty landslide locations were mapped to the corresponding susceptible maps for the provincial level to identify the landslide susceptibility level at those locations. Figure 3 presents three landslides took place in Krung Ching subdistrict,

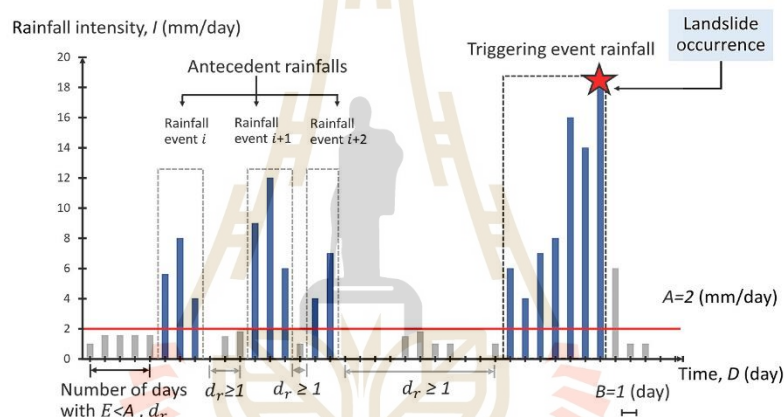


Figure 2. Definition of inter-event criteria used to separate two consecutive rainfalls in this study

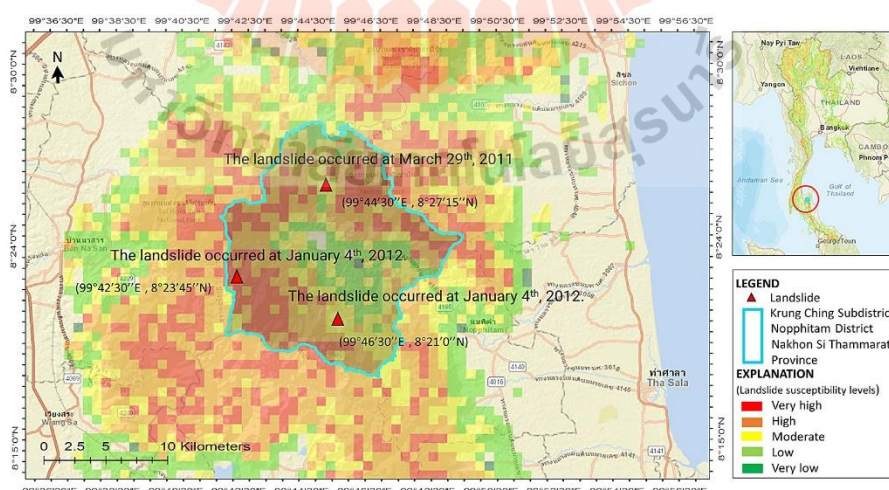


Figure 3. Landslide susceptibility map for Krung Ching subdistrict, Noppitam district, Nakhon Si Thammarat and locations of landslide took place in this area (<https://gis.dmr.go.th/DMR-GIS/gis>)

Table 1. Duration of rainfalls that caused eighty landslides during 1988–2018 categorized by landslide susceptibility level

Duration (day)	Landslide susceptibility levels				
	Very high	High	Moderate	Low	Very low
1	7	1	0	0	0
2	1	2	0	0	0
3	2	10	0	0	0
4	0	5	7	0	0
5	1	5	0	0	0
6	0	3	0	0	0
7	0	5	6	0	0
8	0	2	0	0	0
9	0	3	0	0	0
10	0	0	1	3	0
11	0	0	4	7	0
12	0	0	1	1	0
13	0	0	0	3	0
Total	11	36	19	14	0

Nopphitam district, Nakhon Si Thammarat (the other landslides had been mapped to the corresponding susceptibility maps in a similar manner). Table 1 summaries, from eighty landslides, the number of landslide events took place for each landslide susceptibility level in the Southern Thailand. A greater number of landslides was found for the higher landslide susceptibility level. However, the number of landslides for very high susceptibility was small. It was because the places classified as very high susceptibility level were generally far from communities; hence, many landslides were neglected and not reported. Table 1 also presents, from the triggering rainfall events, distribution of duration for the rainfalls that triggered the landslides at the places of different susceptibility levels. There is no doubt that many of the landslides at the very high susceptibility places were caused by rainfall events that lasts for only one-day. In turn, no landslide at very low to moderate susceptibility places occurred with rainfall duration less than 4 days.

Landslide triggering rainfall thresholds and the assessment

Figure 4 presents the rainfall event (E) and rainfall duration (D) data points of non-triggering-rainfalls (open circles) and triggering-rainfalls (gray circles) plotted on a double logarithmic scale. On the basis of Eq. 1, the landslide rainfall

threshold was analyzed from rainfall event (E) and duration (D) of triggering-rainfalls,

$$\log_{10}E = a + b\log_{10}D \quad (1)$$

where: a and b are regression coefficients.

With the above-mentioned relationship, the threshold gave a straight line in double logarithmic scale. Quantile regression (Koenker and Bassett, 1978; Koenker and Hallock, 2001; Koenker, 2009) was employed to fit the specified

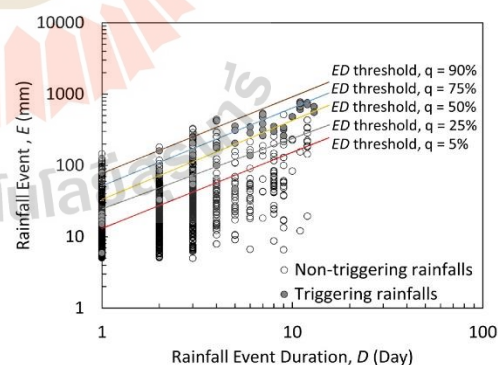


Figure 4. Relationship between rainfall event (E) and its duration (D) form triggering rainfalls and non-triggering rainfalls in the Southern Thailand. Gray circles represent the triggering rainfalls that caused landslides and open circles represent the non-triggering rainfall events. The ED threshold drawn from quantile regression at various probability levels of triggering rainfall events

Table 2. Threshold parameters a and b for the ED , ED^m , and ED^h thresholds at exceedance probabilities from 5 to 90%

Probabilistic level (%)	ED parameters		ED^m parameters		ED^h parameters	
	a	b	a	b	a	b
5	3.322	1.130	1.283	1.188	1.065	1.508
10	1.992	1.689	1.223	1.342	1.081	1.523
25	0.773	1.932	1.650	0.922	1.226	1.455
50	1.322	1.444	1.565	1.206	1.555	1.204
75	1.833	1.008	1.626	1.197	1.943	0.870
80	1.893	0.941	1.827	1.019	2.004	0.805
85	1.965	0.888	1.827	1.020	1.962	0.892
90	2.045	0.810	2.260	0.604	1.962	0.908

percentiles of the triggering events. The ED threshold given at various probability levels from 5–90% was presented in Figure 4. The corresponding magnitudes of parameters a and b for the ED threshold are given in Table 2.

For ease of incorporating the landslide susceptibility level to the rainfall threshold, the susceptibility level was re-categorized from five levels to two levels; termed as the modest susceptibility level and the huge susceptibility level. The modest level is the combination of the very low, low, and moderate susceptibility levels indicated in the landslide susceptibility maps. The huge level is the combination of the high, and very high susceptibility levels indicated in the landslide susceptibility maps. Among eighty events, thirty-three and forty-seven events occurred at the locations classified as the modest level and the huge level, respectively. Figure 5a presents rainfall event (E) and rainfall

duration (D) data points of non-triggering-rainfalls (open circle) and triggering-rainfalls (colored circle) plotted on a double logarithmic scale. Indeed, this plot is Figure 4 modified by grouping the data with susceptibility levels (the modest level and the huge level). The green color plots are for the rainfalls that took place at the modest susceptibility places and the red color plots are for the rainfalls that took place at the huge susceptibility places. The ED threshold for the modest level places (ED^m threshold) and that for the huge level places (ED^h threshold) at various probability levels together with scatter plots, in double logarithmic rainfall event–duration plane, of non-triggering and triggering-rainfalls are given in Figure 5b. The threshold parameters a and b for exceedance probabilities from 5 to 90% of the ED^m and ED^h thresholds are given in Table 2.

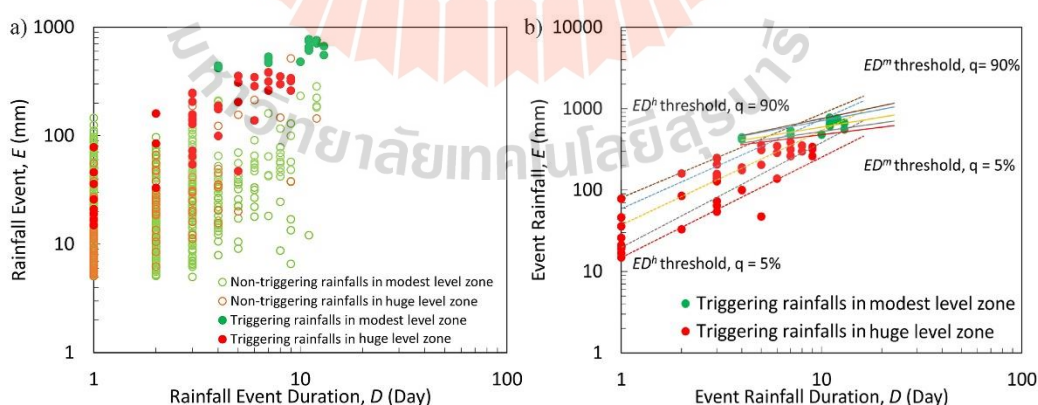


Figure 5. a) Relationship between rainfall event (E) and its duration (D) from triggering rainfalls and non-triggering rainfalls in the Southern Thailand. Red circles represent the triggering rainfalls that caused landslides at the huge susceptibility places and green circles represent that at the modest susceptibility places. In turn, open green circles and open red circles are for the non-triggering rainfalls in the modest and huge susceptibility places, respectively. b) The ED^m and ED^h thresholds drawn from quantile regression at various probability levels of triggering rainfalls at the modest and the huge susceptibility places, respectively

Assessment of the thresholds

The aforementioned thresholds were assessed through a contingency table and a receiver operating characteristic (ROC) curve. There are four scenarios in contingency table; including (1) true positives (TP), (2) true negative (TN), (3) false positive (FP), and (4) false negative (FN). Figure 6 presents TP, FN, FP, and TN defined from threshold value and distribution curve of triggering rainfall events and those of non-triggering rainfall events. TP indicated the cases in which landslides were correctly predicted, FN indicated the cases in which landslides took place without prediction, FP indicated the cases in which landslides were forecasted but did not take place, and TN stood for the correct prediction of a rainfall event without a landslide. These contingencies were employed to calculate the following skill scores; i) a hit rate (HR) which is defined as number of correct prediction per total number of event rainfall: $HR = TP / (TP + FN)$, ii) a false alarm rate (FAR) which is defined as number of false alarm per the total number of non-event rainfall: $FAR = FP / (FP + TN)$, and iii) Hanssen and Kuipers skill score (HK): $HK = HR - FAR$. HK is proportional to the frequency of events being forecast by equal emphasis on ability to forecast both events and nonevents. The receiver operating characteristic curves (ROC curve), HR against FAR, was plotted at various probabilistic levels of landslide threshold and the areas under the ROC curves (AUC) were determined. At each threshold probabilistic level, the Euclidean distance δ was calculated from the distance between the point corresponding to the threshold on the ROC curve and the perfect point of coordinate (0,1).

Assessment of the thresholds was conducted by considering triggering and non-triggering rainfall events that took place at the places corresponding to the established thresholds. For the ED threshold, the rainfall events that took place in the whole study area were employed for the assessment. In turn, for the assessment of the ED^m and ED^h thresholds, only the rainfall events at the places classified to the corresponding susceptibility levels were employed. Furthermore, the considered data indicated that the rainfall events that caused landslides at the modest level places had duration no shorter than 4 days; the authors of this paper implied that the rainfall events of their duration shorter than 4 days did not cause landslides at the modest level places. Hence, for the rainfalls at the modest level places, only the rainfall events having their duration no shorter than 4 days were used for the assessment of ED^m threshold.

RESULTS AND DISCUSSIONS

Table 3 summarizes the four contingencies (TP, FP, FN, TN) and the four skill scores (HR, FAR, HK, δ) for ten probabilistic levels (from 5 to 90%) from the ED, the ED^m and the ED^h thresholds. The best compromise between the minimum number of incorrect landslide predictions (FP, FN) and the maximum number of correct predictions (TP, TN), indicated by combination of the largest values for the HK and the smallest value of the δ , were obtained at 15%, 5%, and 10% for the ED, the ED^m , and the ED^h thresholds, respectively. Since the assessment of ED^m threshold was conducted by considering

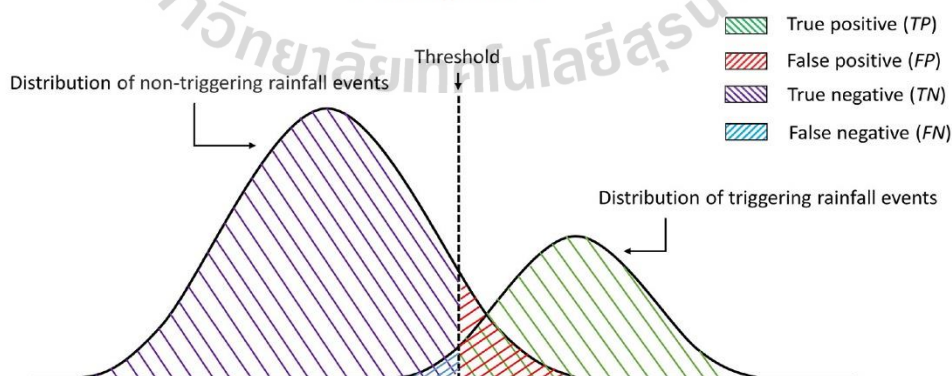


Figure 6. Distribution of triggering and non-triggering rainfalls and the threshold to define the meaning of true positive (TP), true negative (TN), false positive (FP), and false negative (FN)

only the rainfall events having a duration no shorter than 4 days, the number of rainfall in contingency table for the ED^m threshold was not as high as that reported in the contingency table for the ED^b threshold.

Figure 7 presents the *ROC* curves obtained from the ED , ED^m , and ED^b thresholds. The areas under the *ROC* curves (*AUC*), indicating prediction capability, are also reported in Figure 7. Incorporating landslide susceptibility into the threshold resulted in an improvement of the threshold performance. Even at very high and high landslide susceptibility places, the threshold established particularly these zones (ED^b threshold) which exhibited significantly better performance ($AUC = 0.89$) than the ED threshold ($AUC = 0.71$). Since there was no non-triggering rainfall event laid above the ED^m threshold, this threshold yielded *FAR* of 0.0 at every

probabilistic level. This character was expressed through the *ROC* curve of the ED^m threshold that indicated perfect performance with *AUC* of 1.00. The years in which landslides occurred at very low to moderate landslide susceptibility places are presented in Table 4. Twenty landslides from thirty-three landslides took place in two periods (gray shaded rows in Table 4); 1) the period from the late 2010 to the early 2011, and 2) the year 2017. During the period from late 2010 to the early 2011, there were fourteen landslides were reported in this study. For late 2010, a tropical depression in November over Southern Thailand caused very heavy rain occupied widely over southern east-coast. Lastly, the daily maximum rainfall recorded 396 mm/day at Don Sak, Surat Thani. Thereafter in March 2011, an active low pressure cell caused intense rainfall over the Southern Region of Thailand,

Table 3. Summary of the four contingencies (*TP*, *FP*, *FN*, *TN*) and the four skill scores (*HR*, *FAR*, *HK*, δ) obtained from the ED , ED^m , and ED^b thresholds for nine probabilistic levels

Threshold	Probabilistic level (%)	Contingencies and skill scores							
		<i>TP</i>	<i>FN</i>	<i>TN</i>	<i>FP</i>	<i>HR</i>	<i>FAR</i>	<i>HK</i>	δ
ED	5	77	3	848	1312	0.96	0.61	0.36	0.61
	10	72	8	884	1276	0.9	0.59	0.31	0.6
	15	62	18	1299	861	0.78	0.4	0.38	0.46
	25	40	40	1358	802	0.5	0.37	0.13	0.62
	50	21	59	2026	134	0.26	0.06	0.2	0.74
	75	15	65	2046	114	0.19	0.05	0.13	0.81
	80	12	68	2091	69	0.15	0.03	0.12	0.85
	85	8	72	2123	37	0.1	0.02	0.08	0.9
90	4	76	2149	11	0.05	0.01	0.04	0.95	
ED^m	5	28	3	151	0	0.9	0	0.9	0.1
	10	26	5	151	0	0.84	0	0.84	0.16
	15	26	5	151	0	0.84	0	0.84	0.16
	25	23	8	151	0	0.74	0	0.74	0.26
	50	17	14	151	0	0.55	0	0.55	0.45
	75	8	23	151	0	0.26	0	0.26	0.74
	80	5	26	151	0	0.16	0	0.16	0.84
	85	6	25	151	0	0.19	0	0.19	0.81
90	4	27	151	0	0.13	0	0.13	0.87	
ED^b	5	46	1	800	301	0.98	0.27	0.71	0.27
	10	43	4	846	255	0.91	0.23	0.68	0.25
	15	41	6	859	242	0.87	0.22	0.65	0.25
	25	35	12	900	201	0.74	0.18	0.56	0.31
	50	24	23	1052	49	0.51	0.04	0.47	0.49
	75	11	36	1069	32	0.23	0.03	0.2	0.77
	80	11	36	1078	23	0.23	0.02	0.21	0.77
	85	6	41	1081	20	0.13	0.02	0.11	0.87
90	3	44	1086	15	0.06	0.01	0.05	0.94	

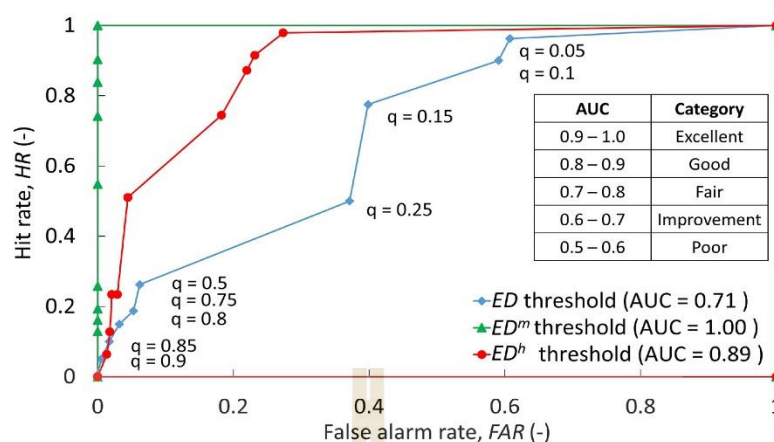


Figure 7. Receiver operating characteristic (ROC) and corresponding area under the ROC curve (AUC) of the ED, ED^m and ED^h thresholds

resulting in unprecedented flash floods and landslides in many provinces in Southern of Thailand. It was noted that in 2011, Thailand experienced the worst flood in over fifty years, as volume of flood water occupied more than half the country. For the 2017, there were six landslides reported in our study. In this year, a significantly strong southwest monsoon extended over Southern Thailand in January resulting in series of torrential rainfalls. The total amount of rainfall from December 30th to January 31st exceeded 1,000 mm in many provinces. According to Jin and Fu (2019), the maximum 24-h

accumulated precipitation of up to 330 mm appeared around Nakhon Si Thammarat province on January 5th and the maximum 24-h accumulated precipitation of up to 420 mm appeared around the Pattani province on January 7th. In short, the locations classified to the zone of very low to moderate landslide susceptibility could suffer from landslide only if they experience unusual torrential rainfalls. The ED^m threshold established in this study laid above rainfall event of 400 mm which could represent unusual torrential rainfalls, and hence 100% of usual rainfalls were not predicted.

Table 4. Number of landslides with respect to time that landslide occurred at the very low to moderate susceptibility places

Month	Year	Number of landslide in modest susceptibility places		
		Moderate	Low	Very low
	1988–2009	4	2	-
Nov.	2010	3	3	-
Mar.	2011	3	5	-
Jan.	2012	2	1	-
Jul.	2013	1	-	-
Nov.	2013	-	-	-
Oct.	2014	-	1	-
Jan.	2017	4	2	-
Jul.	2017	-	-	-
Sep.	2017	-	1	-
Nov.	2017	1	-	-
Dec.	2017	-	-	-
Mar.	2018	-	-	-
Jul.	2018	-	-	-
Aug.	2018	1	-	-

CONCLUSIONS

Landslide rainfall threshold based on rainfall event and rainfall duration (ED threshold) was proposed for landslide prediction in the Southern Thailand. Other than rainfall characteristic, a landslide can be influenced by various spatial factors, such as slope conditions, lithology, soil type, and hydrologic conditions. Incorporation of such factors to the rainfall threshold might enhance the predictability of the rainfall threshold. For this purpose, the landslide susceptibility maps at provincial level published by the Department of Mineral Resources (<https://gis.dmr.go.th/DMR-GIS/gis>) were used as a proxy to allow the connection between the ED threshold and the spatial factors. To facilitate the process, five susceptibility levels, ranging from very low to very high, indicated in the landslide susceptibility maps, were regrouped to two susceptibility levels (the modest and the huge susceptibility levels). The modest susceptibility level was a combination of very low, low, and moderate susceptibility levels indicated in the maps. The huge susceptibility level was a combination of high and very high susceptibility levels indicated in the map. Two ED thresholds, namely ED^m and ED^h thresholds, were introduced, each for different susceptibility level. The ED^m threshold was established for landslide warning at the places classified as very low to moderate susceptibility levels, while the ED^h threshold was established for the places classified as high and very high susceptibility levels. The following conclusions were drawn from this study:

- 1) On the basis of the rainfall event that triggered 99 landslides in Southern Thailand in 1988–2018, a rainfall event-duration (ED) threshold was introduced for landslide warning in the whole Southern Thailand. However, the predictability of the ED threshold was fair with an area under a receiver operating characteristic curve (AUC) of 0.71.
- 2) Integration of the landslide rainfall threshold and the landslide susceptibility map gave a new set of ED thresholds (ED^m and ED^h thresholds). These thresholds provided much better predictions than the original ED threshold. The AUC for the ED^h threshold was 0.89 comparing with AUC of 0.71 for the ED threshold. In turn, the ED^m threshold provided perfect prediction with AUC of 1.00.
- 3) For the landslides reported in this study, it was found that the landslides in very low to

moderate landslide susceptibility level zones were triggered only by the rainfall events having duration no shorter than 4 days. Under these conditions, many rainfall events with their duration shorter than 4 days were filtered out before the assessment of the ED^m threshold. Furthermore, the cumulated rainfall of triggered events was found greater than 400 mm, indicating that landslides in such places would be triggered by unusual torrential rainfall.

REFERENCES

1. Aleotti P. 2004. A warning system for rainfall-induced shallow failures. *Eng Geol.*, 73, 247–265. <https://doi.org/10.1016/j.enggeo.2004.01.007>
2. Bonta J.V., Rao A.R. 1988. Factors affecting the identification of independent storm events. *Journal of Hydrology*, 98(3–4), 275–293. [https://doi.org/10.1016/0022-1694\(88\)90018-2](https://doi.org/10.1016/0022-1694(88)90018-2)
3. Caine, N. 1980. The Rainfall Intensity: Duration Control of Shallow Landslides and Debris Flows. *Geografiska Annaler. Series A, Physical Geography*, 62(1/2), 23–27. <https://doi.org/10.2307/520449>
4. Chinkulkijniwat A., Salee R., Horpibulsuk S., Arulrajah A., Hoy M. 2022. Landslide rainfall threshold for landslide warning in Northern Thailand. *Geomatics, Natural Hazards and Risk*, 13(1), 2425–2241. <https://doi.org/10.1080/19475705.2022.2120833>
5. Department of Mineral Resources 2019. Department of Mineral Resources, 75/10 Rama 6 Road, Thung Phayathai Sub-district, Ratchathewi District, Bangkok 10400, Thailand. webmaster@dmr.mail.go.th
6. Department of Mineral Resources 2022. Landslide susceptibility map (last assess September 15th, 2022). <https://gis.dmr.go.th/DMR-GIS/gis>
7. Gariano S.L., Melillo M., Peruccacci S., Brunetti M.T. 2019. How much does the rainfall temporal resolution affect rainfall thresholds for landslide triggering? *Natural Hazards*, 100, 655–670. <https://doi.org/10.1007/s11069-019-03830-x>
8. Guzzetti F., Peruccacci S., Rossi M., Stark C.P. 2008. The rainfall intensity-duration control of shallow landslides and debris flows: an update. *Landslides*, 5, 3–17. <https://doi.org/10.1007/s10346-007-0112-1>
9. He S., Wang J., Liu S. 2020. Rainfall Event–Duration Thresholds for Landslide Occurrences in China. *Water* 12(2), 494. <https://doi.org/10.3390/w12020494>
10. Jemec Auflič M., Šinigoj J., Krivic M., Podboj M., Peternel T., Komac M. 2016. Landslide prediction

- system for rainfall induced landslides in Slovenia (Maspren). *Geologija*, 59, 259–271. <https://doi.org/10.5474/geologija.2016.016>
11. Jin S., Fu S. 2020. Mechanisms accounting for the repeated occurrence of torrential rainfall over South Thailand in early January 2017, *Atmospheric and Oceanic Science Letters*, 13(2), 155–162. <https://doi.org/10.1080/16742834.2019.1706427>
 12. Koenker R., Bassett G. 1978. Regression Quantiles. *Econometrica* 46(1), 33. <https://doi.org/10.2307/1913643>
 13. Koenker R. 2009. Quantile Regression in R: A Vignette. Available at <http://www.econ.uiuc.edu/~roger/research/rq/vig.pdf>.
 14. Koenker R., Hallock K.F. 2001. Quantile regression. *Journal of Economic Perspectives*, 15(4), 143–156. <https://doi.org/10.1257/jep.15.4.143>
 15. Salee R., Chinkulkijniwat A., Yubonchit S., Horpibulsuk S., Wangfaoklang C., Soisompong S. 2022. New threshold for landslide warning in the southern part of Thailand integrates cumulative rainfall with event rainfall depth-duration. *Natural Hazards*, 113(1), 125–141. <https://doi.org/10.1007/s11069-022-05292-0>
 16. Schmidt-Thomé P., Tatong T., Kunthasap P., Wathanaprida S. 2018. Community based landslide risk mitigation in Thailand. *Episodes*, 41(4), 225–233. <https://doi.org/10.18814/epiugs/2018/018017>
 17. Segoni S., Lagomarsino D., Fanti R., Moretti S., Casagli N. 2015. Integration of rainfall thresholds and susceptibility maps in the Emilia Romagna (Italy) regional-scale landslide warning system. *Landslides*, 12, 773–785. <https://doi.org/10.1007/s10346-014-0502-0>
 18. Segoni S., Tofani V., Rosi A., Catani F., Casagli N. 2018. Combination of Rainfall Thresholds and Susceptibility Maps for Dynamic Landslide Hazard Assessment at Regional Scale. *Front. Earth Sci.*, 6, 85. <https://doi.org/10.3389/feart.2018.00085>
 19. Vennari C., Gariano S.L., Antronico L., Brunetti M.T., Iovine G., Peruccacci S., Guzzetti F. 2014. Rainfall thresholds for shallow landslide occurrence in Calabria, southern Italy. *Natural Hazards and Earth System Sciences*, 14(2), 317–330. <https://doi.org/10.5194/nhess-14-317-2014>
 20. Vessia G., Parise M., Brunetti M.T., Peruccacci S., Rossi M., Vennari C., Guzzetti F. 2014. Automated reconstruction of rainfall events responsible for shallow landslides. *Natural Hazards and Earth System Sciences*, 14(9), 2399–2408. <https://doi.org/10.5194/nhess-14-2399-2014>.



New threshold for landslide warning in the southern part of Thailand integrates cumulative rainfall with event rainfall depth-duration

Rattana Salee¹ · Avirut Chinkulkijniwat¹ · Somjai Yubonchit³ · Suksun Horpibulsuk² · Chadanit Wangfaoklang⁴ · Sirirat Soisompong⁵

Received: 5 June 2021 / Accepted: 18 February 2022
 © The Author(s), under exclusive licence to Springer Nature B.V. 2022

Abstract

A landslide-triggering rainfall threshold for the southern part of Thailand was introduced. The new threshold explicitly integrates the variables of event rainfall and cumulative rainfall from precipitation data corresponding to 92 landslide events in the study area. To determine event rainfall, a suitable inter-event criterion (*IEC*) had to be defined that separated two consecutive rainfalls. A rainfall intensity no greater than 2 mm/day lasting at least 1 day ($IEC_{2,1}$) was the criterion established to separate two consecutive rainfalls in the study area. Using quantile regression, an event rainfall depth-duration (*ED*) threshold was drawn at a probability level of 5%. A 20-day cumulative event rainfall depth (CR_{20}) was the most suitable duration of cumulative rainfall depth. A CR_{20} of 100 mm was the third rainfall variable to give a threshold that integrated cumulative rainfall with event rainfall depth-duration (*CED*). This threshold is proposed for the study area depicted in three-dimensional space. The *CED* threshold is implemented by an assessment of CR_{20} followed by an assessment of *ED*. The hit rate (*HR*) of the *CED* threshold is a little lower than the *HR* of the *ED* threshold, but the *CED* threshold is far better than the *ED* threshold in terms of false alarm rate (*FAR*) since the CR_{20} of 100 mm filters out many non-triggering rainfalls prior to the assessment of the event rainfall.

Keywords Landslide · Rain fall threshold · Quantile regression · Inter-event criteria · Three dimensional rainfall threshold · South of Thailand

1 Introduction

Landslides are considered as one of major natural hazards that result in economic and human losses every year. Risk analysis and assessment is an important tool for landslides management. In fact, risk assessment has been broadly applied in various geotechnical works (Lyu et al 2020; Lin et al. 2021a, b, c; Kardani et al. 2021; Zheng et al. 2021). As for risk assessment in landslides, reliable landslides early warning system (LEWS) is one of

✉ Avirut Chinkulkijniwat
 avirut@sut.ac.th

Extended author information available on the last page of the article

the vital components. Because of ease in measurement of their monitoring variables, landslide rainfall thresholds are extensively used as part of developing an efficient LEWS. Since Thailand is not among the world's landslide hotspots, limited attempts have been devoted to establish landslide rainfall threshold in Thailand. According to Segoni et al. (2018), there is only one landslide rainfall threshold in Thailand (Kanjanakul et al. 2016) published in journals indexed in Scopus or ISI Web of Knowledge database during 2008–2016. It is a threshold, which was defined using monthly rainfall measures, established for a very specific place, i.e., at Sichon District in Nakhon Si Thammarat Province, Southern Thailand. However, landslide events in Thailand have caused significant damage to residents and infrastructure, and loss of human life as reported in Phien-Wej et al. (1993), Yumuang (2006). Accordingly, this study aims to determine the appropriate landslide-triggering rainfall threshold for the south of Thailand. The south of Thailand sits on a narrow peninsula between the Gulf of Thailand to the east and the Andaman Sea to the west. As reported by Arai et al. (2019), the mean annual rainfall in the south during 1981–2017 was more than 2000 mm, versus about 1500 mm from the center to the northern and northeastern regions in this country. According to Department of Mineral Resources (2019), this region experiences rainfall-triggered landslides most frequently comparing to other regions of Thailand.

There are ways the threshold can be determined: using a physical approach or an empirical approach. Since the physical approach requires high-resolution images and relevant data such as groundwater conditions, shear strength of sloping soils, and geological soil profiles, it is more suitable for the assessment of conditions over small areas (Guzzetti et al. 2007a, b). The empirical approach, which is more widely employed, uses the statistical analysis of rainfall datasets collected in the area that experienced the rainfall-triggered landslide. The thresholds established by the empirical approach can be grouped into three categories: (1) thresholds obtained from precipitation measurements for specific landslide events, (2) thresholds based on cumulative or antecedent rainfall conditions, and (3) other thresholds, incorporating hydrological thresholds (Guzzetti et al. 2007a, b). Thresholds in the first category are the most widely used since they are easy to establish and require few input data (Rosi et al. 2020). The most commonly used type of rainfall threshold is the intensity–duration (*ID*) threshold. Since the introduction of the first global *ID* threshold by Caine (1980), reports have been published about the threshold by Peruccacci et al. (2012); Segoni et al. (2014); Gariano et al. (2015); Peruccacci et al. (2017); and Guzzetti et al. (2005a) and (2005b). The literature also contains reports about the rainfall event-duration (*ED*) threshold (Vennari et al. 2014; Vessia et al. 2014; He et al. 2020; Gariano et al. 2020; Peruccacci et al. 2017). Gariano et al. (2020) pointed out that the two rainfall variables in the *ED* threshold are not dependent on each other, whereas in the case of the *ID* threshold, the average rainfall intensity depends on the rainfall duration. For this reason, the *ED* threshold was preferred in this study since two rainfall parameters must be considered independently.

One key important of determining a threshold based on a precipitation event is the identification of the starting point of the rainfall event (Guzzetti et al. 2008). To resolve this problem, studies by Kim et al. (1991); Dahal and Hasegawa (2008); Glade (2000); Hasnawir and Kubota (2008); Giannecchini et al. (2012); and Khan et al. (2012), focused either on the relationship between daily rainfall and cumulative rainfall or used *ID* thresholds established from continuous rainfall events. This approach avoids the need to identify the start point of a rainfall event. Furthermore, the rainfall event and the cumulative rainfall are implicitly incorporated. Although this approach underpins reports that both event and antecedent rainfalls influence slope stability (Rahardjo et al. 2011; Rahimi et al. 2011; Wicki et al. 2020; Rosi et al. 2020; Kim et al. 2020; Yang et al. 2020), it might lead to

misinformation in some magnitudes of event rainfall. Based on the aforementioned concerns, this paper aims to: (1) establish an *ED* threshold for the south of Thailand through a suitable criterion that identifies the starting point of event rainfall and (2) explicitly incorporate a cumulative rainfall variable to the event rainfall threshold.

1.1 Data collection

Ninety-two landslide events that took place in the south of Thailand from 1988 to 2020 were considered. Data were collected mainly from scientific papers published by the Department of Mineral Resources, Ministry of Natural Resources and Environment and partly from local newspapers. Landslide information had to convey at least the following details: (1) the date of the occurrence of the landslide, (2) the location of the landslide event, and (3) consequential damages. Among 92 events, 50 events took place on the east side of the study area and the 42 events took place on the west side. The rainfall data associated with each landslide were gathered from Thai Meteorological Department (TMD) rain gage stations located in the catchment area where the considered landslide is located. The locations of landslide events and TMD rain gage stations in the study area are indicated in Fig. 1. Inverse distance weighting (*IDW*), which assigned a larger weight, based on inverse functions of distance, to a station closer to a landslide location than a station further away, is most commonly used method and usually used as standard method for comparison (Li et al. 2011). Although it is deterministic or non-geostatistic modeling, number of literatures reports that *IDW* is one of reliable methods for spatial interpolation in various applications, i.e., point spread function (Gentile et al. 2012), baseflow and baseflow index (Ditthakit et al. 2021). As for interpolation of rainfall data, Kong and Tong (2008), Kurtzman et al. (2009), Chen et al. (2010), Yang et al. (2015), among others, reported successful application of *IDW* in various locations. Accordingly, *IDW* was employed in this study to approximate rainfall data at the landslide locations. Figure 2 presents the distribution of landslide events on the west side (Fig. 2a) and the east side (Fig. 2b) with respect to the different monsoon periods: southwest, northeast, and pre-monsoons. The southwest monsoon blows from the Indian Ocean during June to September. It brings more rain to the west side than the east. During November to January, northeasterly winds bring heavy rainfall to the east side. As expected, on the east side, more landslides (46%) occurred during the northeast monsoon than at any other time, while more landslides (43%) on the west side occurred during the southwest monsoon. On the west side, 36% of landslides took place during the pre-monsoon period compared to 16% on the east side.

1.2 Geological setting of the study area

Southern Thailand lies on the narrow part of the Malay Peninsula whose landforms comprise two parallel mountain chains running north–south: the Phuket and Nakhon Srithammarat ranges; situated to the west and east, respectively. Alluvial fans, foothills, alluvial plains, and coastal plains can be found alongside the ranges. Geologically, the southern part of Thailand consists of a succession of Paleozoic and Mesozoic sedimentary and metamorphic rocks, intruded by Late Paleozoic to Mesozoic igneous rocks, and covered by Cenozoic sedimentary rock or sediments. According to Ridd et al. (2011), the upper part of the study area is dominated by upper Paleozoic sedimentary rock, which is intruded by chains of granitic bodies rising up to 1000 m in height through forested mountains. The lower part of the study area comprises a main chain of granitic mountains which continues

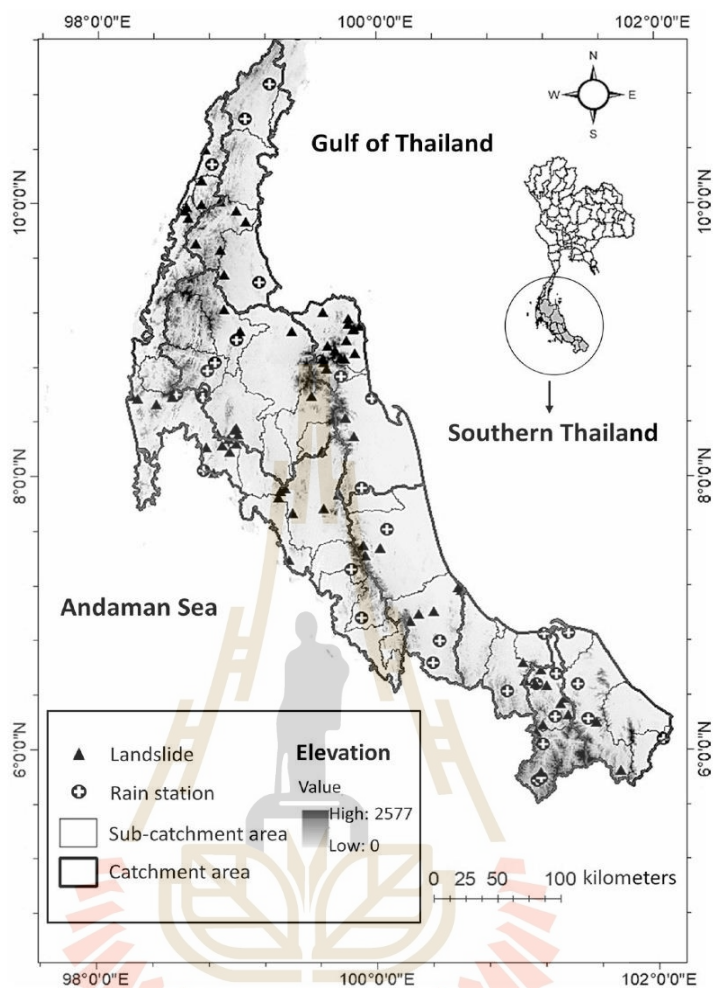


Fig. 1 Location of the landslide as depicted by the black triangle, and location of the Rain station shown by the black circle. The area in thick black line represents catchment area locations. The thin black line area is a representation of sub catchment area locations. The gradient black and white area will show the elevation value of the area. (Figure created using ESRI ArcGIS 10.5 software, <https://www.esri.com/en-us/arcgis/about-arcgis/overview>)

north into the Gulf of Thailand, forming islands such as Koh Samui, Koh Phangang, and Koh Tao. Khao Luang, where the worst landslide disaster in Thailand took place in 1988, belongs to this chain of granite bodies. Since many landslides have occurred on Khao Luang, reports of landslide investigations in this area have indicated that most landslides developed within a thin layer of residual soil even though the weathering of granite was more than 10 m deep.

Due to the tropical temperatures and high annual precipitation, weathering of granitic rocks in the study area is generally deep. The residual soils consist of a thin capping veneer of sandy to silty clay which changes transitionally to a clayey to silty, coarse sand layer that preserves some relics of the rock structure. This layer, which is very hard but friable when dry, becomes weak when wet. Its medium permeability permits easy water filtration and a

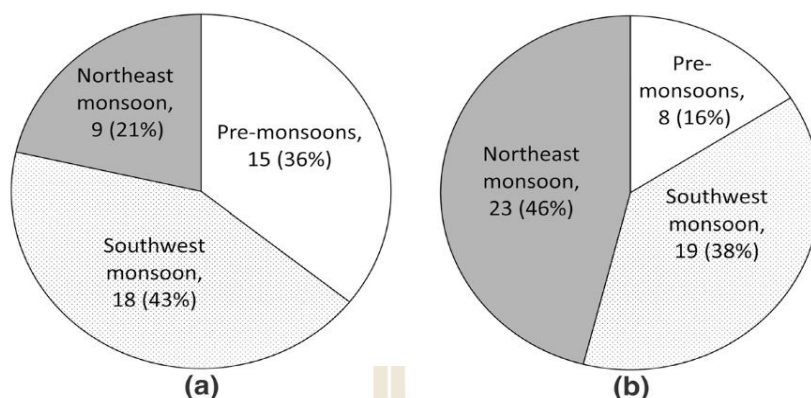


Fig. 2 Number of landslide events (the proportion is presented in parenthesis) associated with different monsoon periods; including southwest, northeast, and pre-monsoons, on the west side (Fig. 2a) and on the east side (Fig. 2b) of the study area

build-up of high water pressure underneath the capping layer. These physical characteristics of the weathered materials make them susceptible to slide or flow on steep slopes.

1.3 Rainfall characterization

In order to characterize a rainfall event in the study area, criteria must be identified that enable distinction between two consecutive rainfalls. The inter-event criterion (*IEC*) used in this study to separate two consecutive rainfalls is shown in Fig. 3. The inter-event criterion $IEC_{A,B}$ is a combination of the rainfall intensity threshold *A* and rainfall duration *B*. In Fig. 3, if rainfall intensity is no greater than *A* mm/day for at least *B* consecutive days, two consecutive rainfall events were considered to have occurred, defined by two different results. Conversely, if the rainfall intensity and duration between two rainfalls do not meet the *IEC*, these two rainfalls are not separate and are considered as one continuous rainfall. Determination of a suitable *IEC* is crucial for establishing the landslide-triggering rainfall threshold. An *IEC* which is easy to meet might result in the rejection of some continuous rainfall, and an *IEC* which is hard to meet might produce too long a rainfall duration that

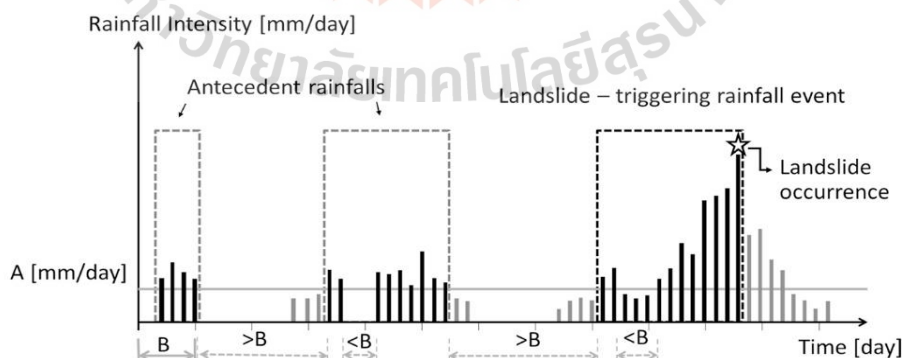


Fig. 3 Definition of inter-event criteria used to separate two consecutive rainfalls in this study

Table 1 A set of inter-event criteria used to characterize rainfall data in the study area

	Number of days, B (day)		
	1	2	3
Rainfall intensity, A (mm/day)			
0	$IEC_{0,1}$	$IEC_{0,2}$	$IEC_{0,3}$
1	$IEC_{1,1}$	$IEC_{1,2}$	$IEC_{1,3}$
2	$IEC_{2,1}$	$IEC_{2,2}$	$IEC_{2,3}$
5	$IEC_{5,1}$	$IEC_{5,2}$	$IEC_{5,3}$

Table 2 Basics statistics of rainfall depth corresponding to various inter-event criteria

	Rainfall depth (mm)			Rainfall intensity (mm/day)			Rainfall duration (day)		
	Max	Mean	SD	Max	Mean	SD	Max	Mean	SD
$IEC_{0,1}$	1916.9	58.3	133.1	115.9	7.9	11.1	67	6.3	7.6
$IEC_{0,2}$	4007.8	124.5	256.2	101.4	7.7	10.7	190	14.1	18.8
$IEC_{0,3}$	4019.7	197.7	349.8	63.4	7.4	9.1	196	21.9	28.3
$IEC_{1,1}$	1351.1	44.7	101.8	142.6	9.5	12.0	53	4.0	4.0
$IEC_{1,2}$	1916.6	85.6	167.7	142.6	9.2	12.0	65	8.4	9.1
$IEC_{1,3}$	2739.0	146.3	257.6	142.6	9.2	12.0	195	15.2	18.0
$IEC_{2,1}$	1351.1	41.2	97.5	153.9	11.0	13.1	26	3.1	3.0
$IEC_{2,2}$	1881.1	66.9	145.4	142.6	10.2	12.4	61	5.8	6.3
$IEC_{2,3}$	2125.8	116.6	213.1	142.6	10.4	13.1	92	11.1	12.4
$IEC_{5,1}$	1311.6	43.6	102.0	145.8	15.3	16.1	24	2.6	2.6
$IEC_{5,2}$	1323.9	54.1	128.1	145.8	13.3	13.1	32	3.5	3.5
$IEC_{5,3}$	1397.1	72.1	165.7	125.0	12.9	12.8	57	5.1	6.4

includes independent rainfall events. Saito et al. (2010) used a 24-h duration to define a rainfall event in Japan; Brunetti et al. (2010) proposed different periods without rainfall for late spring and summer (2 days) and for the other seasons (4 days). In South Korea, Hong et al. (2017) analyzed ID thresholds through skill scores; including receiver operating characteristic (ROC) plots and threat scores (TS), and concluded that 12 h was a suitable inter-event time for separating two different rainfall events for landslide prediction. In this study, the suitable IEC was identified using rainfall data from the years in which landslide events occurred in the study areas.

A set of twelve variables examined to identify the suitable $IEC_{A,B}$ is given in Table 1. Statistics of rainfall characteristics including rainfall depth, rainfall intensity, and rainfall duration, calculated from the different IEC are given in Table 2. The max, mean and standard deviation for rainfall depth more than doubled, as rainfall duration increased from 1 to 3 days, except when the rainfall intensity threshold was equal to 5 mm/day. We inferred that setting rainfall intensity threshold A at 5 mm/day reduced the sensitivity of the rainfall depth to the B variable. From the data for years corresponding to studied landslide events, the average rainfall intensity ranged from 7.4 mm/day at $IEC_{0,3}$ to 15.3 mm/day at $IEC_{5,1}$. The average rainfall intensity was more sensitive to variation of A than variation of B . A greater value of A resulted in a higher average rainfall intensity. As for the rainfall duration, the average rainfall duration varied widely from 2.6 days at $IEC_{5,3}$ to 21.9 days

at $IEC_{0,3}$. The max, mean and standard deviation of rainfall duration became lower with the increasing magnitude of A. Furthermore, at low magnitudes of A, the max, mean and standard deviation for rainfall duration were more sensitive to variation in B than the max, mean and standard deviation for rainfall duration at high magnitudes of A.

In order to determine a suitable IEC , two consecutive rainfalls were identified for each IEC . All inter-event times between the two consecutive rainfalls were read and then employed to calculate the variation coefficient (CV) of inter-event times, where the CV was the ratio of the standard deviation to the mean. Based on an assumption that inter-event times have an exponential distribution for which the mean equals the standard deviation (Bonta and Rao. 1988), the suitable IEC was identified on the basis of a variation coefficient (CV) of inter-event times equal to 1.0. Since the suitable IEC can vary depending on seasonal and climatic conditions, and there is a clear distinction between two consecutive rainfalls in the pre-monsoon period, the determination of the suitable IEC was based on a dataset that excluded rainfall events in the pre-monsoon period. The $IECs$ that returned a CV near 1.0 were selected as candidate suitable criteria. Based on Table 3, which presents statistics of rainfall inter-event time, there were two inter-event criteria that gave a CV close to 1.0: $IEC_{2,1}$ and $IEC_{5,1}$.

1.4 Event rainfall depth-duration (ED) threshold

The event rainfalls that corresponded to the 92 landslides studied were established based on the inter-event criteria $IEC_{2,1}$ and $IEC_{5,1}$. They are presented in double logarithmic rainfall event depth–duration planes in Fig. 4a, b, respectively. Rainfall events that took place on the west side are represented by an open triangle and those on the east side are represented by a cross. To determine whether there were any differences between the distributions of the two plots, we conducted a 2-dimensional Kolmogorov Smirnov test, which extends an earlier idea due to Peacock (1983) and an implementation proposed by Fasano and Franceschini (1987). Table 4 presents the Kolmogorov–Smirnov statistic D with significance level for the event rainfall depth versus duration established using $IEC_{2,1}$ and $IEC_{5,1}$. The significance levels for both inter-event criteria were greater than 0.90. These results indicated that there was no significant difference between the event rainfall depth and duration that satisfied the criteria $IEC_{2,1}$ and $IEC_{5,1}$ for landslides studied on the east side and those studied

Table 3 Basic statistics of inter-event duration corresponding to various inter-event criteria

Inter-event criteria	Max. (mm)	Mean (mm)	SD (mm)	CV
$IEC_{0,1}$	30	4.1	5.1	1.23
$IEC_{0,2}$	26	5.0	4.5	0.90
$IEC_{0,3}$	25	6.7	4.2	0.64
$IEC_{1,1}$	29	3.5	3.9	1.13
$IEC_{1,2}$	30	5.1	4.8	0.93
$IEC_{1,3}$	28	6.8	4.8	0.71
$IEC_{2,1}$	28	4.3	4.4	1.03
$IEC_{2,2}$	30	6.1	5.6	0.92
$IEC_{2,3}$	30	8.0	6.3	0.79
$IEC_{5,1}$	30	5.7	6.0	1.05
$IEC_{5,2}$	29	7.1	5.6	0.79
$IEC_{5,3}$	30	7.4	5.5	0.73

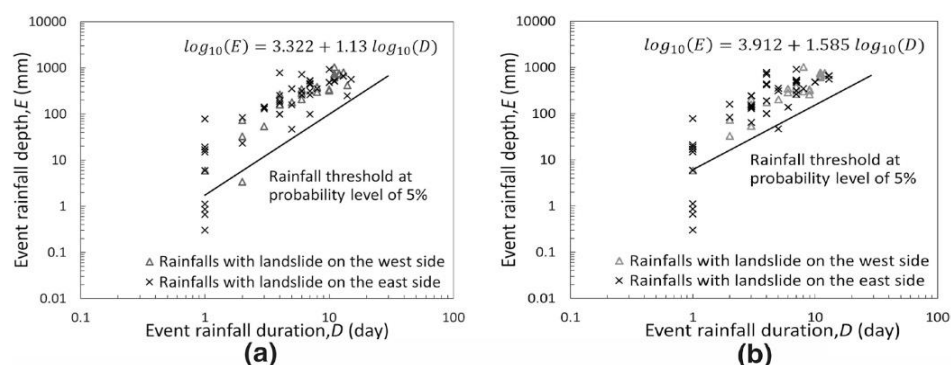


Fig. 4 Scatter plot, in double logarithmic rainfall event depth–duration plane, of 92 triggering events established using (a) $IEC_{2,1}$ and (b) $IEC_{5,1}$. Rainfall thresholds at probability level of 5% based on triggering events defined by inter-event criteria (a) $IEC_{2,1}$ and (b) $IEC_{5,1}$

Table 4 Two-dimensional Kolmogorov–Smirnov test results determined the variation in the distributions of the scatter plots (in double logarithmic rainfall event depth–duration plane) for event rainfalls corresponding to landslides on the west and east sides of the study area

	Kolmogorov–Smirnov statistic D	Corresponding probability (Significant level)
$IEC_{2,1}$	0.383	0.936
$IEC_{5,1}$	0.445	0.976

The test was conducted for event rainfalls that triggered landslides

on the west side. Therefore, the ED threshold could be established by combining rainfall data corresponding to landslides on both sides of the study area. The landslide-triggering rainfall threshold was analyzed using rainfall event depth and duration based on Eq. 1.

$$\log_{10} E = a + b \log_{10} D \quad (1)$$

where a and b are regression coefficients. With the above relationship, the threshold gave a straight line in double logarithmic scale. ED thresholds are given at a probability level of 5% corresponding to landslide-triggering rainfalls defined by inter-event criteria $IEC_{2,1}$ (Fig. 4a) and $IEC_{5,1}$ (Fig. 4b). Quantile regression, which was introduced by Koenker and Bassett (1978), to fit specified percentiles of a response, was performed in the R program using the package “quantreg” (Koenker et al. 2001; Koenker 2009).

The performances of these thresholds were assessed through analysis of the contingency matrix, skill scores, and the receiver operating characteristic (ROC). The contingency matrix comprised four scenarios; including true positive (TP), true negative (TN), false positive (FP), and false negative (FN). These scenarios were based on two conditions (1) whether rainfall triggers a landslide or not, and (2) whether the threshold gives a warning or not. As depicted in Fig. 5a, true positive (TP) stood for the outcome that the landslide was correctly predicted, false negative (FN) indicated a missed alarm in which case a landslide took place without prediction, false positive (FP) indicated a false alarm in which case a landslide was forecasted but did not take place, and true negative (TN) stood for the

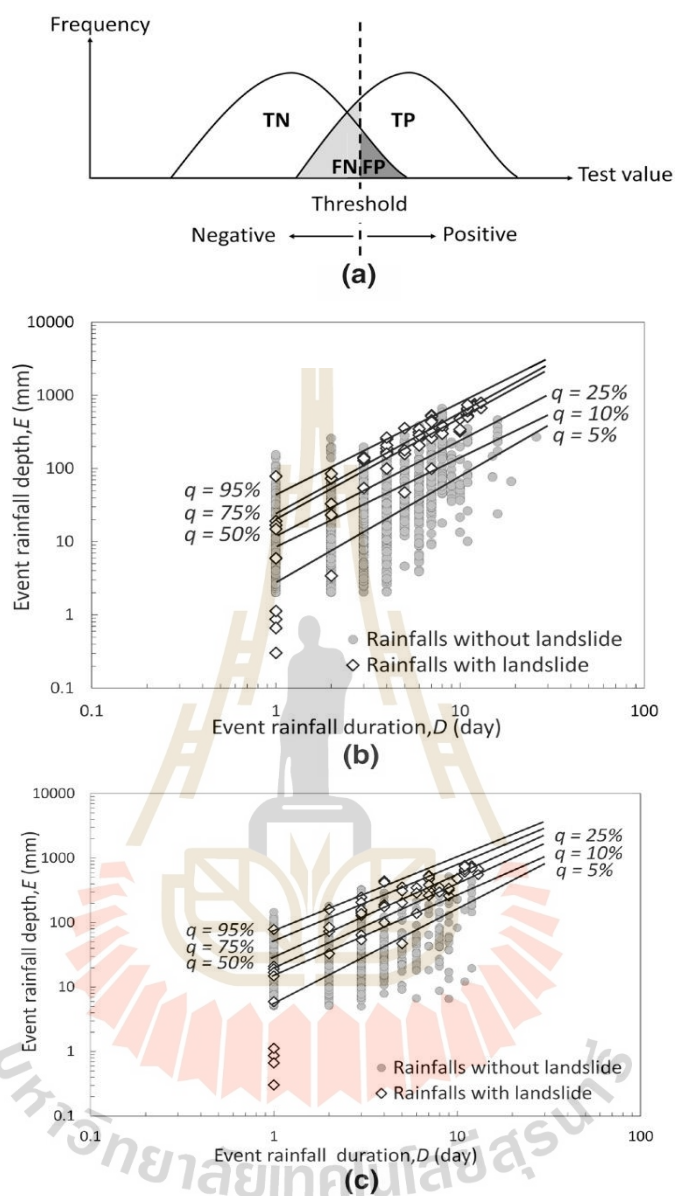


Fig. 5 a Definition of true positive (TP), true negative (TN), false positive (FP), and false negative (FN) in the contingency matrix. Results from quantile regression at various probability levels and scatter plot, in double logarithmic rainfall event depth–duration plane, of triggering events and non-triggering events in established using **b** $IEC_{2,1}$ and **c** $IEC_{5,1}$

correct prediction of a rainfall event without a landslide. Skill scores, including hit rate (HR) and false alarm rate (FAR), were calculated according to Eqs. 2, and 3, respectively. The optimal prediction was one that yielded an HR of 1 and an FAR of 0. The distance between the optimal prediction and the prediction result could indicate the performance

of the prediction: the closer the prediction result to the perfect point, the better the prediction performance. The receiver operating characteristic (ROC) curve, HR against FAR , was plotted at various probabilistic levels of landslide threshold and the areas under the ROC curves (AUC) were determined. The larger the AUC , the better the predictive capability.

$$HR = \frac{TP}{TP + FN} \quad (2)$$

$$FAR = \frac{FP}{FP + TN} \quad (3)$$

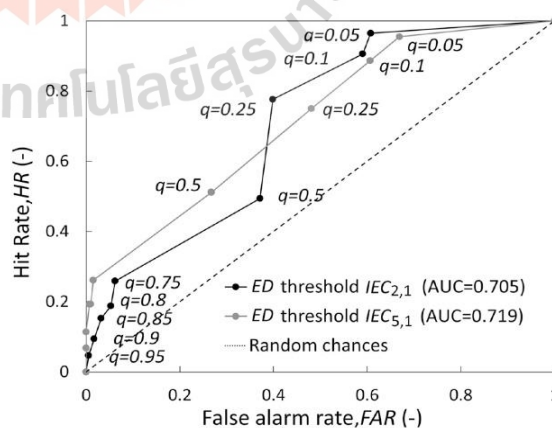
Figure 5b, c depicts scatter plots, in double logarithmic rainfall event depth–duration plane, of triggering and non-triggering rainfall events together with thresholds at various probabilistic levels from 5 to 95% for the inter-event criteria $IEC_{2,1}$ and $IEC_{5,1}$, respectively. The ROC curves are given in Fig. 6. Each curve was drawn for rainfall data created using each IEC and the dots on each curve represent the variation of the threshold setting. The area under ROC curve (AUC) for the inter-event criteria $IEC_{5,1}$ was slightly greater than the AUC for the inter-event criteria $IEC_{2,1}$. However, at high HR , the ROC curve for $IEC_{2,1}$ possesses the notable lower FAR than the ROC curve for $IEC_{5,1}$ does. The ED threshold based on $IEC_{2,1}$ is preferable to the ED threshold based on $IEC_{5,1}$. Hence the ED threshold based on $IEC_{2,1}$ will be further elaborated and proposed as the threshold for the study area. This ED threshold could be written as:

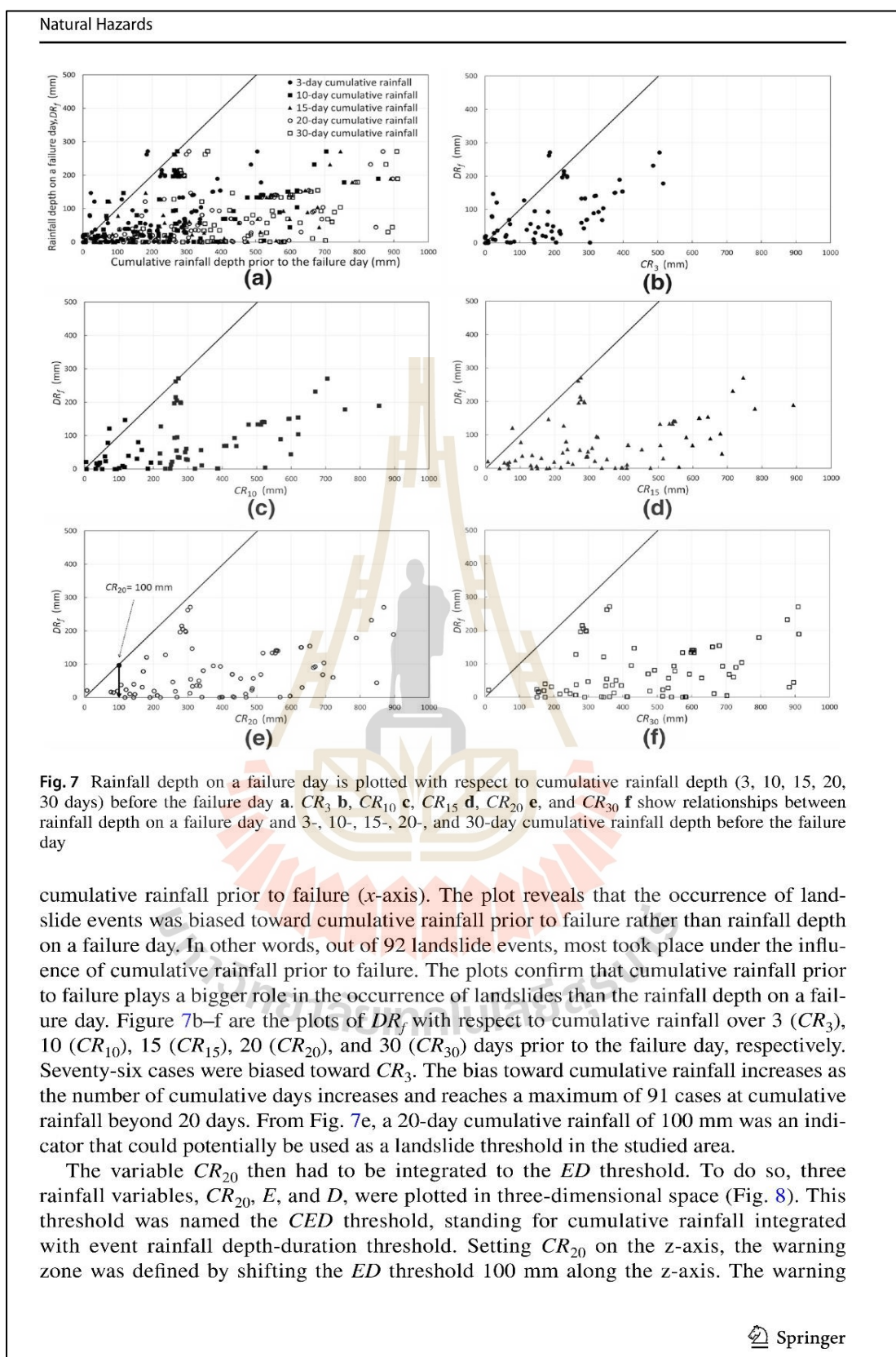
$$\log_{10}(E) + 3.322 + 1.13 \log_{10}(D) \quad (4)$$

1.5 CED Threshold: an integrated cumulative rainfall with event rainfall depth-duration threshold

Figure 7a presents rainfall depth on a failure day (DR_f) with respect to cumulative rainfall over various periods prior to the failure day. A 1:1 line divides the plots into two zones to clarify bias in the scattering toward either rainfall depth on a failure day (y-axis) or

Fig. 6 Receiver operating characteristic (ROC) curves for ED thresholds established based on inter-event criteria $IEC_{2,1}$ and $IEC_{5,1}$





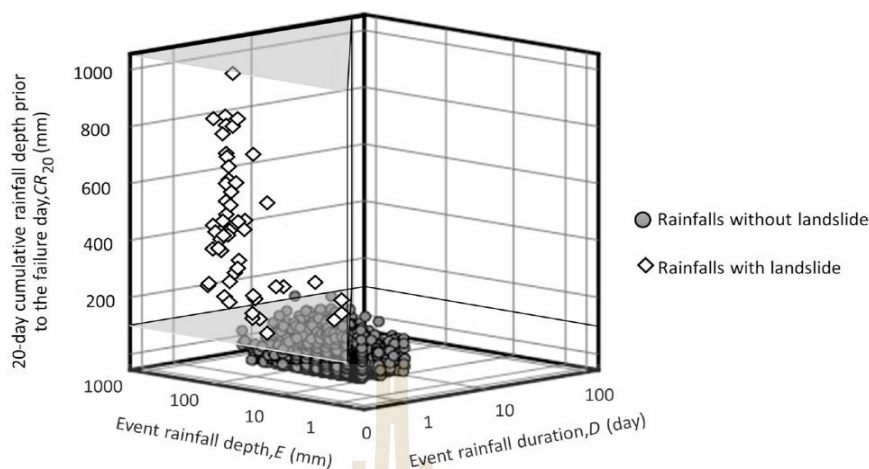
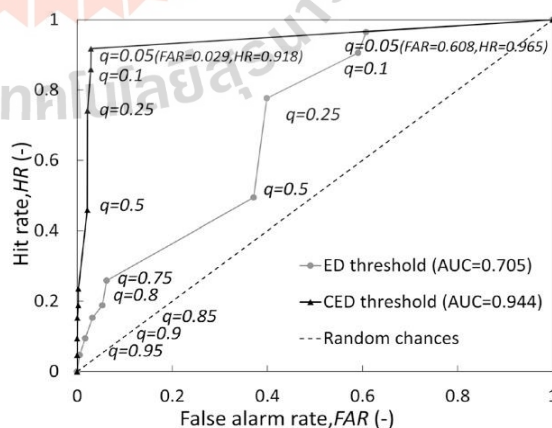


Fig. 8 CED threshold plotted in three -dimensional space

zone in Fig. 8 is the zone above the gray-shaded area. The performance of the 3D threshold was compared with that of the ED threshold through ROC curves and skill scores. The ROC curves are given in Fig. 9. For the ED threshold and the CED threshold, the areas under the ROC curves (AUC) were 0.705 and 0.944, respectively, indicating that the predictive capability of the CED threshold was much better than the predictive capability of the ED threshold. Since many rainfall events having CR_{20} lower than 100 mm were excluded from the FP score, the false alarm rate produced by the CED threshold is much lower than the false alarm rate produced by the ED threshold. Since 4 out of 92 landslide events had CR_{20} lower than 100 mm (Fig. 7e), at low probabilistic levels, four fewer true positive (TP) events were indicated by the CED threshold than by the ED threshold. Accordingly, at low probabilistic levels, the HR of the CED threshold was a bit lower than the HR of the ED threshold. At a 5% probabilistic level, the HR of the CED threshold was 0.918 compared with an HR of 0.965 for the ED threshold.

Fig. 9 Receiver operating characteristic (ROC) curves for ED and CED thresholds



2 Conclusions

Rainfall events corresponding to 92 landslides in the south of Thailand were used to establish a landslide-triggering rainfall threshold. Event rainfall and cumulative rainfall were found to play important roles in landslide initiation in the study area. Event rainfall depth (E), duration of event rainfall (D), and cumulative rainfall depth of 20 days prior to the failure day (CR_{20}), were explicitly included in the threshold in a 3-dimensional plot. The following conclusions were drawn from this study.

- The suitable inter-event criterion to separate two consecutive rainfalls (IEC) was identified using three parameters: (1) an inter-event criterion (IEC) that returned the variation coefficient (CV) of inter-event times closest to 1.0, (2) an IEC that returned the highest value of the AUC of receiver operating characteristic curves, and (3) an IEC that, at high HR , possess the lower FAR .
- Based on the procedure stated above, the suitable inter-event criterion was $IEC_{2,1}$. This variable describes a rainfall condition having an intensity no greater than 2 mm/day for at least 1 consecutive day. Event rainfalls based on $IEC_{2,1}$ were used to draw an ED threshold. The proposed ED threshold was based on quantile regression at a probability level of 5% and it is written as: $\log_{10}(E) + 3.322 + 1.13 \log_{10}(D)$.
- Cumulative rainfall of 100 mm for 20 days prior to a failure day (CR_{20}) was chosen as an extra rainfall variable added to the proposed ED threshold. The new threshold, namely the CED threshold, was plotted in 3-dimensional space integrating two rainfall variables from event rainfall and one variable from cumulative rainfall.
- The new CED threshold is implemented by assessing of the CR_{20} first followed by assessment of the event rainfall using the ED threshold. The implementation is conducted in the following manner:
 - The CR_{20} assessment determines whether cumulative rainfall exceeds 100 mm.
 - If the CR_{20} is not over 100 mm, it is presumed that land sliding will not happen.
 - If CR_{20} is equal to or more than 100 mm, the event rainfall will be assessed through the ED threshold. If the event rainfall returns a rainfall depth and duration above the ED threshold, the landslide warning will be activated.
- Although the CED threshold provides a little lower hit rate (HR) than the ED threshold does, the CED threshold performs much better in terms of false alarm rate (FAR) than the ED threshold does since many rainfalls are filtered by the 20-day cumulative rainfall (CR_{20}) lower limit of 100 mm prior to the assessment of the event rainfall.
- The area under the receiver operating characteristics curve (AUC) was significantly bigger for the CED threshold than for the ED threshold. This result indicates the superiority of the CED threshold, particularly in the view of the respective false alarm rates.

Funding This research was funded by Suranaree University of Technology (IRD7-712-63-12-06).

Availability of data and material The datasets generated during and/or analyzed during the current study are available from the corresponding author on reasonable request.

Declarations

Conflict of interest The authors declare that they have no known competing financial interests or personal relationships that could have appeared to influence the work reported in this paper.

References

- Arai S, Urayama K, Tebakari T, Archvarahuprok B (2019) Characteristics of gridded rainfall data for Thailand from 1981–2017. *Eng J* 23(6):461–468. <https://doi.org/10.4186/ej.2019.23.6.461>
- Bonta JV, Rao AR (1988) Factors affecting the identification of independent storm events. *J Hydrol* 98(3–4):275–293. [https://doi.org/10.1016/0022-1694\(88\)90018-2](https://doi.org/10.1016/0022-1694(88)90018-2)
- Brunetti MT, Peruccacci S, Rossi M, Luciani S, Valigi D, Guzzetti F (2010) Rainfall thresholds for the possible occurrence of landslides in Italy. *Nat Hazards Earth Syst Sci* 10(3):447–458. <https://doi.org/10.5194/nhess-10-447-2010>
- Caine N (1980) The Rainfall intensity: duration control of shallow landslides and debris flows. *Geogr Ann Series A Phys Geogr* 62(1/2):23. <https://doi.org/10.2307/520449>
- Chen D, Ou T, Gong L, Xu CY, Li W, Ho CH, Qian W (2010) Spatial interpolation of daily precipitation in China: 1951–2005. *Adv Atmos Sci* 27:1221–1232. <https://doi.org/10.1007/s00376-010-9151-y>
- Dahal RK, Hasegawa S (2008) Representative rainfall thresholds for landslides in the Nepal Himalaya. *Geomorphology* 100(3–4):429–443. <https://doi.org/10.1016/j.geomorph.2008.05.013>
- Department of Mineral Resources (2019) The Best practices for landslide risk management in Thailand. Department of Mineral Resources, 75/10 Rama 6 Road, Thung Phayathai Sub-district, Ratchathewi District, Bangkok 10400, Thailand. webmaster@dmr.mail.go.th
- Ditthakit P, Nakrod S, Viriyantavong N, Tolche AD, Pham QB (2021) Estimating baseflow and baseflow index in ungauged basins using spatial interpolation techniques: a case study of the southern river basin of Thailand. *Water* 13:3113. <https://doi.org/10.3390/w13213113>
- Fasano G, Franceschini A (1987) A multidimensional version of the Kolmogorov–Smirnov test. *Mon Not R Astron Soc* 225(1):155–170. <https://doi.org/10.1093/mnras/225.1.155>
- Gariano SL, Brunetti MT, Iovine G, Melillo M, Peruccacci S, Terranova O, Guzzetti F (2015) Calibration and validation of rainfall thresholds for shallow landslide forecasting in sicily, southern Italy. *Geomorphology* 228:653–665. <https://doi.org/10.1016/j.geomorph.2014.10.019>
- Gariano SL, Melillo M, Peruccacci S, Brunetti MT (2020) How much does the rainfall temporal resolution affect rainfall thresholds for landslide triggering? *Nat Hazards*. <https://doi.org/10.1007/s11069-019-03830-x>
- Gentile M, Courbin F, Meylan G (2012) Interpolating point spread function anisotropy. *Astron Astrophys*. <https://doi.org/10.1051/0004-6361/201219739>
- Giannecchini R, Galanti Y, D’Amato Avanzi G (2012) Critical rainfall thresholds for triggering shallow landslides in the Serchio river valley (Tuscany, Italy). *Nat Hazard* 12(3):829–842. <https://doi.org/10.5194/nhess-12-829-2012>
- Glade T (2000) Applying probability determination to refine landslide-triggering rainfall thresholds using an empirical “antecedent daily rainfall model.” *Pure Appl Geophys* 157(6–8):1059–1079. <https://doi.org/10.1007/s000240050017>
- Guzzetti F, Salvati P, Stark CP (2005a) Evaluation of risk to the population posed by natural hazards in Italy. In: Hungr O, Fell R, Couture R, Eberhardt E (eds) *Landslide risk management*. Taylor, Francis Group, London, pp 381–389
- Guzzetti F, Stark CP, Salvati P (2005b) Evaluation of flood and landslide risk to the population of Italy. *Environ Manag* 36(1):15–36. <https://doi.org/10.1007/s00267-003-0257-1>
- Guzzetti F, Peruccacci S, Rossi M, Stark CP (2007a) The rainfall intensity–duration control of shallow landslides and debris flows: an update. *Landslides* 5(1):3–17. <https://doi.org/10.1007/s10346-007-0112-1>
- Guzzetti F, Peruccacci S, Rossi M, Stark C (2007b) Rainfall thresholds for the initiation of landslides in central and southern Europe. *Meteorol Atmos Phys* 98:239–267. <https://doi.org/10.1007/s00703-007-0262-7>
- Guzzetti F, Peruccacci S, Rossi M, Stark CP (2008) The rainfall intensity–duration control of shallow landslides and debris flows: an update. *Landslides* 5:3–17. <https://doi.org/10.1007/s10346-007-0112-1>
- Hasnawir KT (2008) Analysis of critical value of rain-fall to induce landslide and debris–flow in Mt. Bawakaraeng Caldera, South Sulawesi, Indonesia. *J Fac Agric Kyushu Univ* 53(2):523–527. <https://doi.org/10.5109/12868>

Natural Hazards

- He S, Wang J, Liu S (2020) Rainfall event-duration thresholds for landslide occurrences in China. *Water* 12(2):494. <https://doi.org/10.3390/w12020494>
- Hong H, Liu J, Zhu AX, Shahabi H, Pham BT, Chen W, Bui DT (2017) A novel hybrid integration model using support vector machines and random subspace for weather-triggered landslide susceptibility assessment in the Wuning area (China). *Environ Earth Sci*. <https://doi.org/10.1007/s12665-017-6981-2>
- Kanjanakul C, Chub-uppakarn T, Chalermyanont T (2016) Rainfall thresholds for landslide early warning system in Nakhon Si Thammarat. *Arabian J Geosci*. <https://doi.org/10.1007/s12517-016-2614-4>
- Kardani N, Zhou AN, Nazem M, Shen SS (2021) Improved prediction of slope stability using a hybrid stacking ensemble method based on finite element analysis and field data. *J Rock Mech Geotech Eng*. <https://doi.org/10.1016/j.jrmge.2020.05.011>
- Khan YA, Lateh H, Baten MA, Kamil AA (2012) Critical antecedent rainfall conditions for shallow landslides in Chittagong city of Bangladesh. *Environ Earth Sci* 67:97–106. <https://doi.org/10.1007/s12665-011-1483-0>
- Kim SK, Hong WP, Kim YM (1991) Prediction of rainfall-triggered landslides in Korea. In: Bell DH (ed) *Landslides*, 2nd edn. A.A Balkema Rotterdam, pp 989–994
- Kim SW, Chun KW, Kim M, Catani F, Choi B, Seo JI (2020) Effect of antecedent rainfall conditions and their variations on shallow landslide-triggering rainfall thresholds in South Korea. *Landslides*. <https://doi.org/10.1007/s10346-020-01505-4>
- Koenker R, Bassett G (1978) Regression quantiles. *Econometrica* 46(1):33. <https://doi.org/10.2307/1913643>
- Koenker R, Hallock KF (2001) Quantile regression. *J Econ Perspect* 15(4):143–156. <https://doi.org/10.1257/jep.15.4.143>
- Koenker R (2009) Quantile regression in R: A Vignette. Available at <http://www.econ.uiuc.edu/~roger/research/rq/vig.pdf>
- Kong YF, Tong WW (2008) Spatial exploration and interpolation of the surface precipitation data. *Geogr Res* 27(5):1097–1108
- Kurtzman D, Navon S, Morin E (2009) Improving interpolation of daily precipitation for hydrologic modeling: spatial patterns of preferred interpolators. *Hydrol Process* 23:3281–3329
- Li J, Heap AD, Potter A, Daniell JJ (2011) Application of machine learning methods to spatial interpolation of environmental variables. *Environ Model Softw* 26(12):1647–1659
- Lin SS, Shen SL, Zhou AN, Xu YS (2021a) Risk assessment and management of excavation system based on fuzzy set theory and machine learning methods. *Autom Constr* 122:103490. <https://doi.org/10.1016/j.autcon.2020.103490>
- Lin SS, Shen SL, Zhou AN, Xu YS (2021b) Novel model for risk identification during karst excavation. *Reliab Eng Syst Saf* 209:107435. <https://doi.org/10.1016/j.res.2021.107435>
- Lin SS, Shen SL, Zhang N, Zhou AN (2021c) Comprehensive environmental impact evaluation for concrete mixing station (CMS) based on improved TOPSIS method. *Sustain Cities Soc* 69:102838. <https://doi.org/10.1016/j.scs.2021.102838>
- Lyu HM, Zhou WH, Shen SL, Zhou AN (2020) Inundation risk assessment of metro system using AHP and TFN-AHP in Shenzhen. *Sustain Cities Soc* 56:102103. <https://doi.org/10.1016/j.scs.2020.102103>
- Peacock JA (1983) Two-dimensional goodness-of-fit testing in astronomy. *Mon Not R Astron Soc* 202(3):615–627. <https://doi.org/10.1093/mnras/202.3.615>
- Peruccacci S, Brunetti MT, Luciani S, Vennari C, Guzzetti F (2012) Lithological and seasonal control on rainfall thresholds for the possible initiation of landslides in central Italy. *Geomorphology* 139–140:79–90. <https://doi.org/10.1016/j.geomorph.2011.10.005>
- Peruccacci S, Brunetti MT, Gariano SL, Melillo M, Rossi M, Guzzetti F (2017) Rainfall thresholds for possible landslide occurrence in Italy. *Geomorphology* 290:39–57. <https://doi.org/10.1016/j.geomorph.2017.03.031>
- Phien-Wej N, Nutalaya P, Aung Z, Zhibin T (1993) Catastrophic landslides and debris flows in Thailand. *Bull Int Assoc Eng Geol* 48:93–100. <https://doi.org/10.1007/BF02594981>
- Rahardjo H, Melinda F, Leong EC, Rezaur RB (2011) Stiffness of a compacted residual soil. *Eng Geol* 120(1–4):60–67. <https://doi.org/10.1016/j.enggeo.2011.04.006>
- Rahimi A, Rahardjo H, Leong EC (2011) Effect of Antecedent Rainfall Patterns on Rainfall-Induced Slope Failure. *J Geotech Geoenviron Eng* 137(5):483–491. [https://doi.org/10.1061/\(asce\)gt.1943-5606.0000451](https://doi.org/10.1061/(asce)gt.1943-5606.0000451)
- Ridd MF, Barber AJ, Crow MJ (2011) The Geology of Thailand. *Geol Soc Lond*. <https://doi.org/10.1144/GOTH>
- Rosi A, Segoni S, Canavesi V, Monni A, Gallucci A, Casagli N (2020) Definition of 3D rainfall thresholds to increase operative landslide early warning system performances. *Landslides*. <https://doi.org/10.1007/s10346-020-01523-2>

- Saito H, Nakayama D, Matsuyama H (2010) Relationship between the initiation of a shallow landslide and rainfall intensity-duration threshold in Japan. *Geomorphology* 118:167–175. <https://doi.org/10.1016/j.geomorph.2009.12.016>
- Segoni S, Lagomarsino D, Fanti R, Moretti S, Casagli N (2014) Integration of rainfall thresholds and susceptibility maps in the Emilia Romagna (Italy) regional-scale landslide warning system. *Landslides* 12:773–785. <https://doi.org/10.1007/s10346-014-0502-0>
- Segoni S, Piciullo L, Gariano SL (2018) A review of the recent literature on rainfall thresholds for landslide occurrence. *Landslides* 15:1483–1501. <https://doi.org/10.1007/s10346-018-0966-4>
- Vennari C, Gariano SL, Antronico L, Brunetti MT, Iovine G, Peruccacci S, Guzzetti F (2014) Rainfall thresholds for shallow landslide occurrence in Calabria, southern Italy. *Nat Hazard* 14(2):317–330. <https://doi.org/10.5194/nhess-14-317-2014>
- Vessia G, Parise M, Brunetti MT, Peruccacci S, Rossi M, Vennari C, Guzzetti F (2014) Automated reconstruction of rainfall events responsible for shallow landslides. *Nat Hazard* 14(9):2399–2408. <https://doi.org/10.5194/nhess-14-2399-2014>
- Wicki A, Lehmann P, Hauck C, Seneviratne SI, Waldner P, Stähli M (2020) Assessing the potential of soil moisture measurements for regional landslide early warning. *Landslides*. <https://doi.org/10.1007/s10346-020-01400-y>
- Yang X, Xie X, Liu DL, Ji F, Wang L (2015) Spatial interpolation of daily rainfall data for local climate impact assessment over greater Sydney region. *Adv Meteorol*. <https://doi.org/10.1155/2015/563629>
- Yang W, Liu L, Shi P (2020) Detecting precursors of an imminent landslide along the Jinsha River. *Nat Hazards Earth Syst Sci* 20:3215–3224. <https://doi.org/10.5194/nhess-20-3215-2020>
- Yumuang S (2006) 2001 debris flow and debris flood in Nam Ko area, Phetchabun province, Central Thailand. *Environ Geol* 51:545–564
- Zheng Q, Lyu HM, Zhou AN, Shen SL (2021) Risk assessment of geohazards along Cheng-Kun railway using fuzzy AHP incorporated into GIS. *Geomat Nat Haz Risk* 12:1508–1531. <https://doi.org/10.1080/19475705.2021.1933614>

Publisher's Note Springer Nature remains neutral with regard to jurisdictional claims in published maps and institutional affiliations.

Authors and Affiliations

Rattana Salee¹ · Avirut Chinkulkijniwat¹  · Somjai Yubonchit³ ·
Suksun Horpibulsuk² · Chadanit Wangfaoklang⁴ · Sirirat Soisompong⁵

Rattana Salee
saleerattana6155@gmail.com

Somjai Yubonchit
Somjai.yu@rmuti.ac.th

Suksun Horpibulsuk
suksun@g.sut.ac.th

Chadanit Wangfaoklang
Chadanit55@gmail.com

Sirirat Soisompong
pam-4501@hotmail.com

¹ School of Civil Engineering, Institute of Engineering, Suranaree University of Technology, 111 University Avenue, Muang District, Nakhon Ratchasima 30000, Thailand

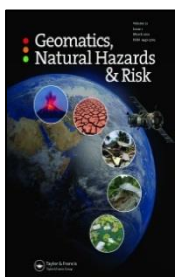
² Center of Excellence in Civil Engineering, School of Civil Engineering, Suranaree University of Technology, 111 University Avenue, Muang District, Nakhon Ratchasima 30000, Thailand

³ School of Civil Engineering, Rajamangala University of Technology Isan, 744 Sura Narai Road, Muang District, Nakhon Ratchasima 30000, Thailand

Natural Hazards

- ⁴ Syntec Construction Public Co., Ltd, 555/7-11 Sukhumvit 63, Sukhumvit Rd., Klongton Nua, Wattana, Bangkok 10110, Thailand
- ⁵ Christiani&Nielsen (Thai) Public Co., Ltd., 727 La Salle Road, Bangna Tai, Bangna District, Bangkok 10260, Thailand





Landslide rainfall threshold for landslide warning in Northern Thailand

Avirut Chinkulkijniwat, Rattana Salee, Suksun Horpibulsuk, Arul Arulrajah & Menglim Hoy

To cite this article: Avirut Chinkulkijniwat, Rattana Salee, Suksun Horpibulsuk, Arul Arulrajah & Menglim Hoy (2022) Landslide rainfall threshold for landslide warning in Northern Thailand, Geomatics, Natural Hazards and Risk, 13:1, 2425-2441, DOI: 10.1080/19475705.2022.2120833

To link to this article: <https://doi.org/10.1080/19475705.2022.2120833>

© 2022 The Author(s). Published by Informa UK Limited, trading as Taylor & Francis Group.

Published online: 09 Sep 2022.

Submit your article to this journal

Article views: 576

View related articles

View Crossmark data

Landslide rainfall threshold for landslide warning in Northern Thailand

Avirut Chinkulkijniwat^a , Rattana Salee^b, Suksun Horpibulsuk^c , Arul Arulrajah^d , and Menglim Hoy^c

^aCenter of Excellent in Civil Engineering, School of Civil Engineering, Institute of Engineering, Suranaree University of Technology, Nakhon Ratchasima, Thailand; ^bSchool of Civil Engineering, Institute of Engineering, Suranaree University of Technology, Nakhon Ratchasima, Thailand; ^cCenter of Excellence in Innovation for Sustainable Infrastructure Development, Institute of Engineering, Suranaree University of Technology, Nakhon Ratchasima, Thailand. ^dDepartment of Civil and Construction Engineering, Swinburne University of Technology, Melbourne, Australia

ABSTRACT

Northern Thailand is a hotspot for landslides. Rainfall-triggered landslides in this region have caused much suffering and many fatalities. In this work, a landslide-triggering rainfall threshold for Northern Thailand is proposed based on rainfall data relating to 48 triggering rainfall events that caused 59 landslides in the study area. To account for different mechanism of landslide formation, the threshold was portioned into two parts for different duration of rainfall events. A split point of 3 days was chosen as a separator for portioning the threshold to be 1) a threshold for rainfall events of duration no longer than 3 days and 2) a threshold for rainfall events of duration longer than 3 days. The threshold also required a suitable variable for antecedent rainfalls which was found to be cumulative rainfall over 25-day period (CR_{25}) of 140 mm. Therefore, the thresholds combining cumulative rainfall with rainfall event - duration (CED) were established by incorporating the CR_{25} of 140 mm into the traditional ED threshold. This is the first attempt to incorporate the difference mechanism of landslide formation by dividing the CED threshold to two portions for difference rainfall duration. The introduced threshold shows positive sign of the prediction, particularly in term of false alarm rate, false alarm ratio, and critical success index. The introduced threshold will be useful for landslide warning system in the study area.

ARTICLE HISTORY

Received 15 June 2022
Accepted 30 August 2022

KEYWORDS

Landslide rainfall threshold;
Rainfall duration;
Contingency tables;
Northern Thailand

Introduction

Every year, landslides result in economic and human losses. Understanding, managing, monitoring, and preventing these major natural hazards can mitigate the human and economic impacts. Studies of the many different aspects of landslide hazards

CONTACT Avirut Chinkulkijniwat  avirut@sut.ac.th

This article has been republished with minor changes. These changes do not impact the academic content of the article.

© 2022 The Author(s). Published by Informa UK Limited, trading as Taylor & Francis Group.

This is an Open Access article distributed under the terms of the Creative Commons Attribution License (<http://creativecommons.org/licenses/by/4.0/>), which permits unrestricted use, distribution, and reproduction in any medium, provided the original work is properly cited.

have investigated triggering factors and hydrological responses (Chinkulkijniwat, Yubonchit et al. 2016; Chinkulkijniwat, Horpibulsuk et al., 2016; 2019; Yang et al. 2021), biological stability (Indraratna et al. 2006), and landslide hazard assessment (Grozavu and Patriche 2021). Work carried out on landslide risk assessment has made some of the most vital contributions to landslide mitigation measures. Since rainfall is known to be an important factor in landslide events (Iida 2004; Fan et al. 2016), landslide rainfall thresholds are commonly utilized as an important component of landslide early warning systems (Guzzetti et al. 1994; Aleotti 2004; Wieczorek and Glade 2005; Ya'acob et al. 2019; Maturidi et al. 2020; Yang et al. 2020; Rosi et al. 2021). The most common parameters used to define landslide-triggering rainfall thresholds are based on event rainfall parameters, particularly the parameter that combines rainfall intensity and rainfall event duration, known as the *ID* threshold (Caine 1980; Crosta and Frattini 2001; Ahmad 2003; Aleotti 2004; Guzzetti et al. 2008; Yubonchit et al. 2017). Since the rainfall variables used to predict the *ID* threshold are not independent (Gariano et al. 2020), certain studies (Vennari et al. 2014; Vessia et al. 2014; Gariano et al. 2015; Peruccacci et al. 2017; Gariano et al. 2019; He et al. 2020; Germain et al. 2021; Lee et al. 2021) have preferred to use a threshold that takes into account event rainfall and rainfall duration, known as the *ED* threshold.

Thailand's Northern Region regularly experiences rainfall-triggered landslides that cause tragedy, injuries and loss of life (Yumuang 2006; Teerarungsigul et al. 2016; Komolvilas et al. 2021). In 2001, 176 people lost their lives in rainfall-triggered landslide events in the area. In 2006, 87 fatalities were recorded, and in 2018, eight people died but 260 casualties were reported. In 2003, Thailand's Environmental Geology Division reported that 6563 villages, in 1084 rural subdistricts, in 54 provinces, mostly in Northern Thailand, were located in landslide hazard zones. According to Segoni et al. (2018), who conducted a review of the recent literatures on rainfall thresholds for landslide occurrence published in journals indexed in Scopus or ISI Web of Knowledge database during 2008–2016, there was only one report for landslide rainfall threshold in Thailand (Kanjanaikul et al. 2016) during the period of 2008–2016. The present work determines a landslide rainfall threshold at regional scale for Northern Thailand. The introduced threshold was modified from a landslide rainfall threshold for the Southern Thailand region that combined cumulative rainfall with rainfall event - duration, known as the *CED* threshold (Salee et al. 2022). The modification was achieved by portioning the *CED* threshold to two portions; one for short duration rainfall events and the other for long duration rainfall events. In general, the short duration, high intensity rainfall events involved shallow landslides, while the long duration, low to medium intensity rainfall events caused deep seat landslides (Caine 1980; Giannecchini et al. 2012, 2015; Zhang et al. 2019). Taking rainfall duration into account in an established landslide rainfall threshold, the difference mechanism of landslide formation might be incorporated to the threshold. Contingency tables and sets of skill scores were used to assess the performances of the thresholds. The threshold introduced in this study will be useful for rainfall-triggered landslide warning in Northern Thailand. Furthermore, this study shows the first attempt to

incorporate the difference mechanism of landslide formation by dividing the *CED* threshold to two portions for difference durations of rainfall event.

Background of the study area

The Northern Thailand region (Figure 1) consists of nine administrative provinces, namely Chiang Rai, Mae Hong Son, Chiang Mai, Lamphun, Lampang, Phayao, Nan, Phrae, and Uttaradit. The region covers approximately 93,691 km². The landscape of Northern Thailand is dominated by mountain ranges in the western and northeastern parts of the region. These ranges are part of the wider system that covers neighboring Burma and Laos. Broadly defined based on geological composition, there are two mountainous subsystems in the study area. In the western part of the region, mountains run southwards from the Daen Lao Range with the two parallel chains of the Thanon Thong Chai Range, which includes the highest mountain in Thailand, Doi Inthanon (2,565 m above mean sea level). In the northeastern part of the region, parallel ranges extending into northern Laos include the Khun Tan Range, the Phi Pan Nam Range, the Phlueng Range, and the western part of the Luang Prabang Range. There also exists a set of strike-slip faults in this region. However, landslides triggered by seismic events are rare in Thailand, and the most recent earthquakes in 2006 and 2014 did not lead to significant landslides (Schmidt-Thomé et al. 2018). The annual average minimum and maximum temperatures are 4 and 40 °C, respectively. The average annual rainfall of 943.2 mm is spread over 122 days on average. Rainfall in this area is under the influence of the southwest monsoon, which starts in May and ends in October. Streams of warm moist air from the Indian Ocean bring abundant rain to the region, especially to the windward side of mountain ranges. However, the southwest monsoon is not the only source of precipitation during this period. The influence of the Inter Tropical Convergence Zone and tropical cyclones can also deposit large amounts of rain. Based on the available records, all major landslides in this area have been triggered by heavy rainfall caused by tropical cyclones. Landslides in Phrae and Phetchabun provinces in 2001 were triggered by continuous heavy rain that fell during Typhoon Usagi. Several landslides in Uttaradit, Sukhothai, Phrae, Lampang and Nan provinces in 2006 were caused by continuous heavy rainfall in the wake of Typhoon Xangsane. More recently, in 2018, landslides at Huay Khab village in Nan province followed ten days of continuous rainfall caused by Typhoon Son-Tinh.

Data collection and rainfall characterization

This study considered 59 landslide events recorded in Northern Thailand during the years 2002 to 2018. Data were collected mainly from scientific papers published by the Department of Mineral Resources, Ministry of Natural Resources and Environment and partly from local newspapers. For an event to be taken into consideration, the available information had to convey at least the following details: (1) the date of the occurrence of the landslide, (2) the location of the landslide event, and (3) consequential damages. Triggered and non-triggered rainfall data from the years

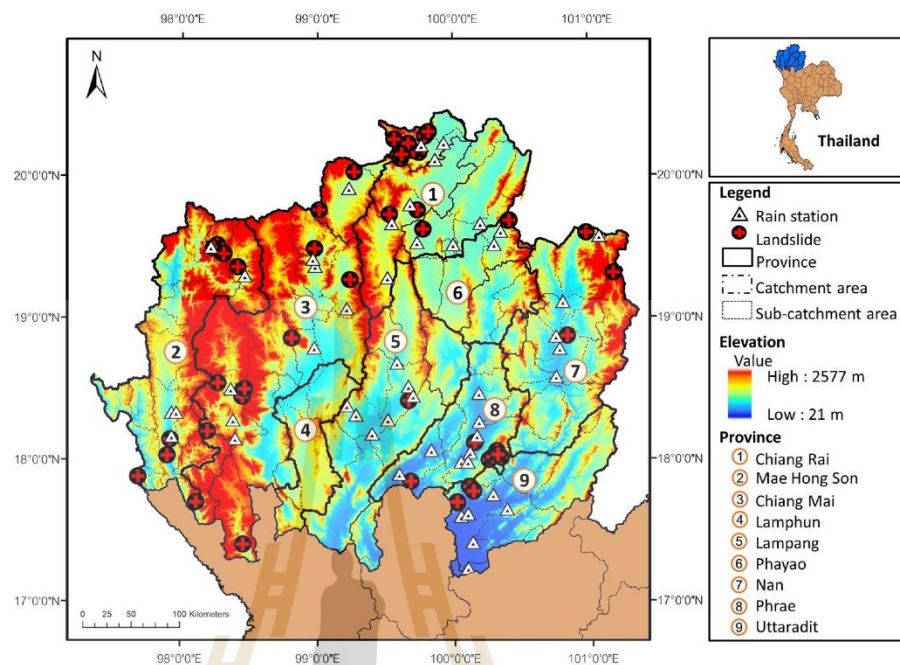


Figure 1. Location of the landslide as depicted by the red cross on black circle, and location of the Rain station shown by the white triangle. The area in dot-dash line represents boundary of catchment area. The thin dot line represents boundary of sub catchment area. The gradient color shows the elevation value of the area.

when these landslide events occurred were gathered from Thai Meteorological Department (TMD) rain gauge stations. These rain gauge stations located in the catchment area where the considered landslides were located. The locations of landslide events and TMD rain gauge stations in the study area are indicated in Figure 1. To estimate rainfall at landslide locations, rainfall data from TMD rain gauge stations was processed by use of inverse distance weighting (IDW). Based on inverse functions of distance, IDW assigned a larger weight to a station closer to a landslide location than it assigned to a station further away. Although, IDW is a deterministic model, it has been considered a reliable method of spatial interpolation in applications such as point spread function (Gentile et al. 2013), and baseflow measurement and baseflow index calculation (Ditthakit et al. 2021). IDW has also been successfully applied to the interpolation of rainfall data in various locations by Kong and Tong (2008), Kurtzman et al. (2009), Chen et al. (2010), and Yang et al. (2015) among others.

In order to characterize rainfall in this region, criteria must be identified that enable distinction between two consecutive rainfalls. The inter - event criterion (IEC) used in this study to separate two consecutive rainfalls is shown in Figure 2. In Figure 2, the inter-event criterion $IEC_{A,B}$ is a combination of the rainfall intensity threshold A and duration B. The condition that distinguished two consecutive rainfall events had to satisfy the combined criterion. If rainfall intensity was no greater than A mm/day for at least B consecutive days, two consecutive rainfall events were

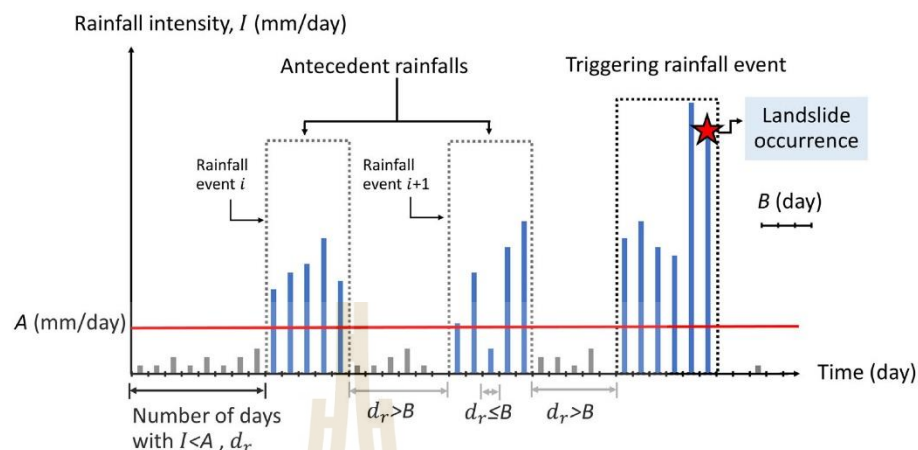


Figure 2. The chart shows how consecutive rainfall events were determined to have satisfied both conditions of the inter-event criterion used to define a single rainfall event in this study.

considered to have occurred. Conversely, if the rainfall intensity and duration of two rainfalls did not meet the $IEC_{A,B}$, these two rainfalls were considered as one continuous rainfall. The determination of a suitable IEC was crucial to establishing a suitable landslide-triggering rainfall threshold. An IEC which is easy to meet might result in the rejection of a continuous rainfall, and an IEC which is hard to meet might produce too long a rainfall duration that includes independent rainfall events.

In this study, the suitable IEC was identified using all rainfall data (both triggered and non-triggered rainfall events) from the years in which landslide events occurred in the study areas. Since the suitable IEC can vary depending on seasonal and climatic conditions, and there is a clear distinction between two consecutive rainfalls in the pre-monsoon period, the determination of the suitable IEC in this study was based on a dataset that excluded inter-event rainfall in the pre-monsoon period. Twelve sets of variables A and B were examined to identify the suitable $IEC_{A,B}$. For each $IEC_{A,B}$, all inter-event times between every consecutive rainfalls were read and then employed to calculate the mean and the standard deviation of the inter-event times. Based on an assumption that inter-event times have an exponential distribution for which the mean equals the standard deviation (Bonta and Rao 1988), the suitable IEC was identified on the basis of a variation coefficient (CV) of inter-event times equal to 1.0. The variation coefficient (CV), defined as the ratio of the standard deviation to the mean, was calculated and presented in Table 1. As expressed in Table 1, the IEC that returned the CV closest to 1.0 was the $IEC_{5,1}$, which stands for the condition that rainfall intensity was no greater than 5 mm/day for at least 1 days.

Based on rainfall events defined by $IEC_{5,1}$, frequency distributions tables were produced of rainfall duration in days (Table 2) and rainfall event in mm (Table 3) for rainfall events from the years in which landslide events occurred in the study areas. Eighty-four percent of the collected rainfalls lasted no longer than 3 days. With regard to a depth of rainfall, it was found that eighty-three percent of the collected rainfalls fell to a depth no greater than 50 mm. Figure 3 presents average monthly rainfall in

Table 1. Basic statistics of inter-event duration corresponding to various inter-event criteria.

Inter-event criteria	Mean [day]	SD [day]	CV [-]
$IEC_{0,1}$	3.00	3.49	1.16
$IEC_{0,2}$	5.32	4.02	0.75
$IEC_{0,3}$	6.81	4.03	0.59
$IEC_{1,1}$	3.19	3.64	1.14
$IEC_{1,2}$	5.79	4.60	0.79
$IEC_{1,3}$	7.25	4.62	0.64
$IEC_{2,1}$	3.30	3.64	1.10
$IEC_{2,2}$	5.06	4.07	0.80
$IEC_{2,3}$	6.67	4.21	0.63
$IEC_{5,1}$	3.64	3.79	1.04
$IEC_{5,2}$	5.10	4.04	0.79
$IEC_{5,3}$	6.52	4.18	0.64

Table 2. Frequency distribution of rainfall duration.

Duration [day]	Number of rainfall events [-]	Number of rainfall events [%]
1	881	46.8
2	410	21.8
3	298	15.8
4	121	6.4
5	56	3.0
6	48	2.6
7	37	2.0
8	14	0.7
9	9	0.5
11	2	0.1
12	2	0.1
13	1	0.1
15	2	0.1
17	1	0.1

Remark: The rainfall events were defined by $IEC_{5,1}$.

Table 3. Frequency distribution of rainfall event in mm.

Rainfall event [mm]	Number of rainfall event [-]	Number of rainfall event [%]	Cumulated number of rainfall event [%]
0 - 10	658	35.0	35.0
11 - 20	356	18.9	53.9
21 - 30	250	13.3	67.2
31 - 40	179	9.5	76.7
41 - 50	114	6.1	82.7
51 - 60	46	2.4	85.2
61 - 70	62	3.3	88.5
71 - 80	33	1.8	90.2
81 - 90	44	2.3	92.6
91 - 100	24	1.3	93.8
101 - 110	36	1.9	95.7
111 - 120	12	0.6	96.4
121 - 130	14	0.7	97.1
131 - 140	10	0.5	97.7
141 - 150	2	0.1	97.8
151 - 200	24	1.3	99.0
>200	18	1.0	100.0

Remark: The rainfall events were defined by $IEC_{5,1}$.

mm (blue line) calculated from rainfall data in this study compared with 30-year average monthly rainfall from years 1981–2010 (gray column) and monthly rainfall of the recent year 2021 (green column) sourced from Thai Meteorological Department

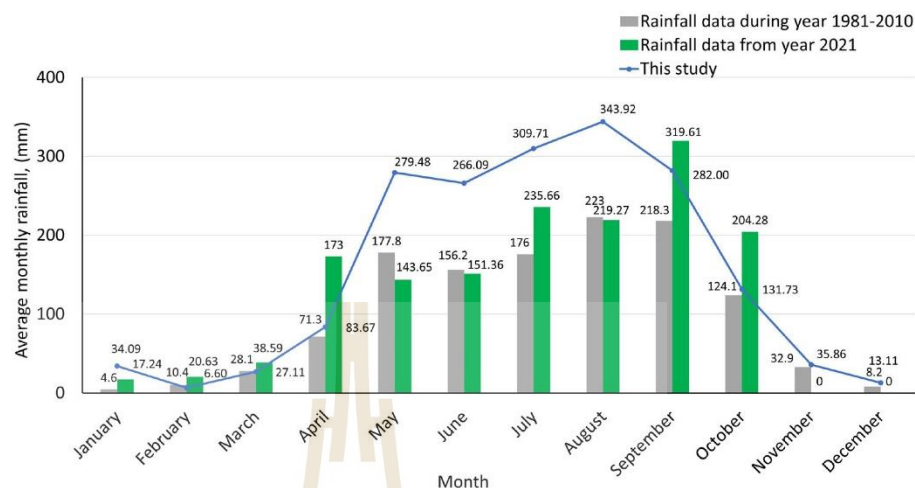


Figure 3. Average monthly rainfall in mm derived from gauge data for 30-year period from 1981 to 2010 (gray column) and for the recent year 2021 (green column). The blue line represents average monthly rainfall from data extracted in years when landslides occurred and from rain gauges located in the catchment areas where landslides had occurred.

(2022). The rainfall data gathered in this study produced a similar distribution to the results from gauge readings throughout the Northern Thailand. Since the rainfall data in this study were collected from the years when the landslide events occurred and from selected rain gauge stations located in the same catchments with the considered landslides, the average monthly rainfall from rainfall data in this study was surely higher than the 30-year average and the recent year.

Measures of evaluation

In the evaluation of the performance of the thresholds to be established in this study, we considered various measures that are applied in the contingency table, comprising numbers of true positives (*TP*), true negatives (*TN*), false positives (*FP*), and false negatives (*FN*), and were employed in diagnosing landslide rainfall threshold in the study area. A hit rate (*HR*) in Eq. 1 indicates the proportion of the correctly predicted landslide triggered rainfall events among all triggered rainfall events. The *HR* ranges from zero (0) at the poor end to one (1) at the good end. A false alarm rate (*FAR*) in Eq. 2 measures the number of false alarms per total number of non-triggering rainfalls. A false alarm ratio (*FA*) in Eq. 3 measures the fraction of forecasted events that did not occur. The *FAR* and *FA* range from zero (0) at the good end to one (1) at the poor end. A Hanssen-Kuiper skill score (*KH*) in Eq. 4 represents the hit rate with respect to the false alarm rate and remain positive while the hit rate is higher than the false alarm rate. The best possible *KH* score is 1, which is returned when the *HR* is 1 and the *FAR* is 0. The worst possible *KH* is 0, which is returned when $HR = FAR$. A critical success index (*CSI*) in Eq. 5 combines *HR* and *FA* into one score for low frequency events. This score measures the fraction of observed and/or forecast events that were correctly predicted. It ranges from zero (0) at the poor

end to one (1) at the good end.

$$HR = \frac{TP}{TP + FN} \quad (1)$$

$$FAR = \frac{FP}{FP + TN} \quad (2)$$

$$FA = \frac{FP}{TP + FP} \quad (3)$$

$$HK = HR - FAR \quad (4)$$

$$CSI = \frac{TP}{TP + FP + FN} \quad (5)$$

Other than the aforementioned scores, the receiver operating characteristic (ROC) curves of HR against FAR were plotted at various probabilistic levels of landslide threshold and the corresponding areas under the ROC curves (AUC) were calculated to determine predictability. Furthermore, for each probabilistic level, the Euclidean distance, δ , was calculated between the point corresponding to the threshold on the ROC curve and the ideal coordinate (0,1).

The event rainfall – duration thresholds

Based on rainfall events defined by $IEC_{5,1}$, rainfall event (E) and rainfall duration (D) data points of non-triggering- and triggering-rainfalls plotted on a double logarithmic scale were plotted on a double logarithmic scale in Figure 4a. The threshold was being established from rainfall event (E) and rainfall duration (D) of landslide-triggering rainfall events in Northern Thailand. Quantile regression (Koenker and Bassett 1978) was employed to generate sets of rainfall thresholds at various probabilistic levels using Eq. 6.

$$\log_{10} E = a + b \log_{10} D \quad (6)$$

where a and b are regression coefficients. Using the above relationship, the ED threshold gave a straight line in double logarithmic scale.

To account for short- and long-duration rainfall events, the rainfall events were divided to two groups: short- and long- duration rainfall events. However, due to wide variety of hydrogeological conditions, a time at a split point between short- and long-duration rainfall thresholds lays over a range from many hours to few days. He et al. (2020) divided rainfalls to two groups; short- and long-duration rainfalls, using 48 hours as a split point to establish landslide rainfall threshold in China. Wicki et al. (2020) used rainfall duration of 6 hours to classified if the rainfall is short- or long-duration rainfalls. Chen and Chen (2022) characterized rainfalls that triggered landslide in Taiwan to three types; including high rainfall intensity over a short duration

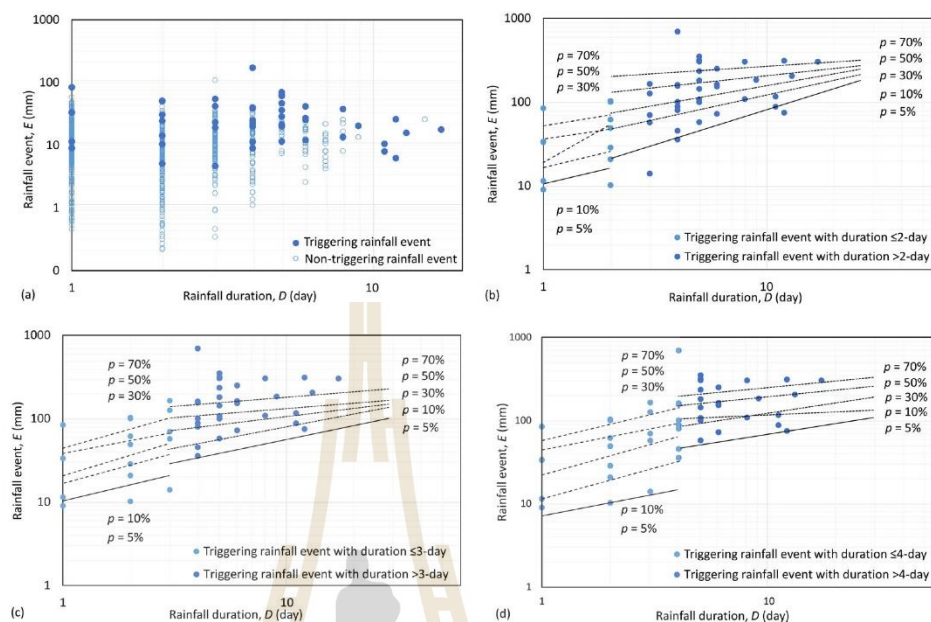


Figure 4. (a) From the data of non-triggering and triggering rainfalls, double logarithmic scatter plots were built from data points of rainfall event versus rainfall duration. The rainfall event - duration (ED) threshold was determined at various probability levels using quantile regression. (b) The ED threshold was divided to two categories; short duration rainfall threshold and log duration rainfall threshold, using a split point at 2 days, (c) The ED threshold using a split point at 3 days, (d) The ED threshold using a split point at 4 days.

(<12 h), high-intensity and prolonged rainfall, and high cumulative rainfall over a long duration (>36 h). Based on distribution of rainfall duration presented in Table 2, most of the rainfall events (almost 70%) last no longer than 2 days and there are few rainfall events (less than 10%) last longer than 4 days. Therefore, a time at a split point between short- and long-duration rainfall thresholds could be within 2–4 days. In order to define a suitable split point, three sets of the ED thresholds having their split point at 2-day (Figure 4b), 3-day (Figure 4c) and 4-day (Figure 4d) were established and assessed.

Figure 5 presents the ROC curve and the corresponding AUC of three ED thresholds split at 2-day, 3-day, and 4-day. The performance was fair (AUC less than 0.76) for the ED threshold with the split point at 2-day. For the split point at 3-day and 4-day, the ED thresholds yielded good predictability of their AUC magnitudes greater than 0.80. Among three ED thresholds, the ED threshold that used 3-day as a split point between short- and long-duration rainfalls exhibited the highest AUC. Hence, the split point at 3-day was chosen as a separator for establishing the ED threshold for short duration rainfall events (ED_s threshold) and the ED threshold for long duration rainfall events (ED_l threshold). Threshold parameters a and b for exceedance probabilities from 5 to 90% are reported in Table 4.

Table 5 summarizes the four contingency scores and the six skill scores at ten probabilistic levels from 5 to 90% produced by results obtained from the ED

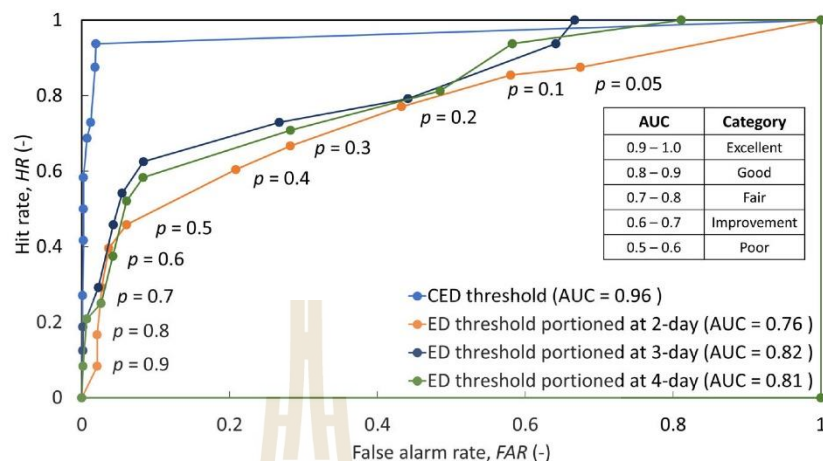


Figure 5. Receiver operating characteristic (ROC) curve and the corresponding area under the ROC curve (AUC) generated from the ED thresholds and the CED threshold.

Table 4. Threshold parameters *a* and *b* (see Eq. 1) for exceedance probabilities from 5 to 90%. The threshold was portioned to two parts; ED_S (for short duration rainfall events) and ED_L (for long duration rainfall events) thresholds. The threshold was portioned using a split point at 3 day.

ED_S Threshold Prob. level	Parameters		ED_L Threshold Prob. level	Parameters	
	<i>a</i>	<i>b</i>		<i>a</i>	<i>b</i>
5	0.954	0.177	5	1.147	0.672
10	0.954	0.402	10	1.264	0.652
20	1.058	0.86	20	1.844	0.096
30	1.058	1.465	30	1.771	0.292
40	1.522	0.558	40	1.558	0.676
50	1.522	0.673	50	1.895	0.373
60	1.522	0.887	60	2.050	0.234
70	1.526	1.205	70	1.962	0.421
80	1.844	0.538	80	2.483	-0.002
90	1.960	0.542	90	2.509	-0.015

Table 5. Summarizes the four contingencies (*TP*, *FP*, *FN*, *TN*) and the six skill scores (*HR*, *FAR*, *FA*, *CSI*, *HK*, δ) obtained from the ED threshold for ten probabilistic levels.

Probabilistic level	Contingencies and skill scores									
	<i>TP</i>	<i>FN</i>	<i>TN</i>	<i>FP</i>	<i>HR</i>	<i>FAR</i>	<i>FA</i>	<i>CSI</i>	<i>HK</i>	δ
5	48	0	611	1223	1.00	0.67	0.96	0.04	0.33	0.67
10	45	3	658	1176	0.94	0.64	0.96	0.04	0.30	0.64
20	38	10	1025	809	0.79	0.44	0.96	0.04	0.35	0.49
30	35	13	1344	490	0.73	0.27	0.93	0.07	0.46	0.38
40	30	18	1681	153	0.63	0.08	0.84	0.15	0.54	0.38
50	26	22	1734	100	0.54	0.05	0.79	0.18	0.49	0.46
60	22	26	1756	78	0.46	0.04	0.78	0.17	0.42	0.54
70	14	34	1793	41	0.29	0.02	0.75	0.16	0.27	0.71
80	9	39	1831	3	0.19	0.00	0.25	0.18	0.19	0.81
90	6	42	1831	3	0.13	0.00	0.33	0.12	0.12	0.88

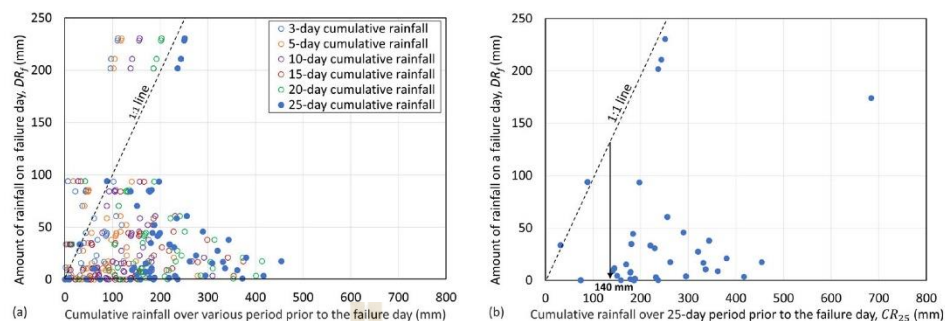


Figure 6. Rainfall on a failure day in mm was plotted with respect to cumulative rainfall over 3-, 10-, 15-, 20-, and 25-day period prior to the failure day (a). Rainfall on a failure day in mm was plotted with respect to cumulative rainfall over 25-day period before the failure day (b).

threshold portioned to short- and long-duration rainfall thresholds by 3-day duration. At low probabilistic levels, the threshold yielded very high FA value (i.e. $FA = 0.96$ at probabilistic level of 5%). Threshold with high FA results in the operators losing trust in its reliability. Furthermore, the CSI value generated by the threshold was much lower than 0.50 at every probabilistic levels suggesting that the forecast had little or no skill. Hence, we concluded that the ED threshold is not practically useful in the study area.

The cumulative rainfall with rainfall event – duration threshold

For ease to account for antecedent rainfalls, cumulative rainfall over certain period prior to the failure day was integrated to the established threshold. Figure 6a presents the rainfall on a failure day (DR_f) against cumulative rainfall over 3-, 5-, 10-, 15-, 20-, 25-day periods prior to the failure day. The plots were divided into two portions with a 1:1 line to clarify bias in the scattering, whether towards the rainfall on a failure day or cumulative rainfall prior to the failure day. From 48 triggered rainfall events, 34 events were biased toward cumulative rainfall of 3-day period prior to the failure day. The number of biasness toward cumulative rainfall increased to 35, 40, 42, 42, and 46 events when period of cumulative rainfall increased to 5-, 10- 15-, 20-, 25-day period, respectively. Therefore, cumulative rainfall over 25-day period prior to the failure day (CR_{25}) was considered as a suitable threshold variable for landslides in the studied area. Figure 6b presents a scatter plot of data points representing DR_f and CR_{25} for 48 triggered rainfall events. The scatter plot revealed that the highest value of CR_{25} that returned few number of triggered rainfall events was CR_{25} of 149 mm. Hence, the CR_{25} value of 140 mm was an indicator that could potentially be used as a landslide-triggering threshold in the studied area.

The CR_{25} of 140 mm was introduced into the ED threshold presented in Figure 4c to establish a CED threshold portioned by rainfall duration (Figure 7). This threshold was portioned into a threshold for rainfall events of their duration no longer than 3 days, and a threshold for rainfall events of their duration longer than 3 days. Table 6 presents the four contingencies and the six skill scores for ten probabilistic levels from 5 to 90% calculated for the CED threshold. Introducing the CR_{25} of 140 mm

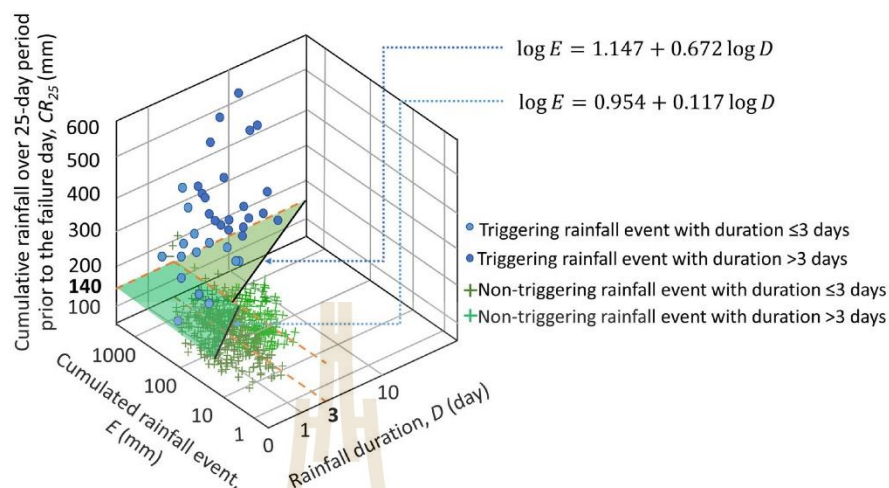


Figure 7. The *CED* threshold plotted in three-dimensional space. The threshold was portioned at 3-day becoming the *CED* threshold for rainfall events of their duration no longer than 3 days and the *CED* threshold for rainfall events of their duration longer than 3 days.

Table 6. Summarizes the four contingencies (*TP*, *FP*, *FN*, *TN*) and the six skill scores (*HR*, *FAR*, *FA*, *CSI*, *HK*, δ) obtained from the *CED* threshold for ten probabilistic levels.

Probabilistic level	Contingencies and skill scores									
	<i>TP</i>	<i>FN</i>	<i>TN</i>	<i>FP</i>	<i>HR</i>	<i>FAR</i>	<i>FA</i>	<i>CSI</i>	<i>HK</i>	δ
5	45	3	1799	35	0.94	0.02	0.44	0.54	0.92	0.07
10	42	6	1801	33	0.88	0.02	0.44	0.52	0.86	0.13
20	35	13	1812	22	0.73	0.01	0.39	0.50	0.72	0.27
30	33	15	1821	13	0.69	0.01	0.28	0.54	0.68	0.31
40	28	20	1830	4	0.58	0.00	0.13	0.54	0.58	0.42
50	24	24	1830	4	0.50	0.00	0.14	0.46	0.50	0.50
60	20	28	1830	4	0.42	0.00	0.17	0.38	0.41	0.58
70	13	35	1832	2	0.27	0.00	0.13	0.26	0.27	0.73
80	9	39	1832	2	0.19	0.00	0.18	0.18	0.19	0.81
90	6	42	1832	2	0.13	0.00	0.25	0.12	0.12	0.88

into the threshold resulted in notably fewer *FP* cases, and hence the *FAR* for the *CED* threshold was considerably lower than the *FAR* for the *ED* threshold. The reduction of *FAR* significantly improved the overall reliability of the threshold, indicated by the *ROC* curve and the corresponding *AUC* of the *CED* threshold (Figure 5). The reliability of prediction with the *CED* threshold was very good (*AUC* = 0.96). The *FA* of the *CED* threshold (*FA* = 0.44) yielded positive results since it was significantly lower than the *FA* yielded by the *ED* threshold (*FA* = 0.96). The best compromise between the minimum number of incorrect landslide predictions (*FP*, *FN*) and the maximum number of correct predictions (*TP*, *TN*), was indicated by combination of the largest values for the *HK* and the smallest value of the δ . It was found that the best compromising predictions was obtained at probabilistic levels of 5% for the *CED* threshold (*HK* = 0.92 and δ = 0.07). The *CED* thresholds proposed in this study can be employed as shown in Figure 8.

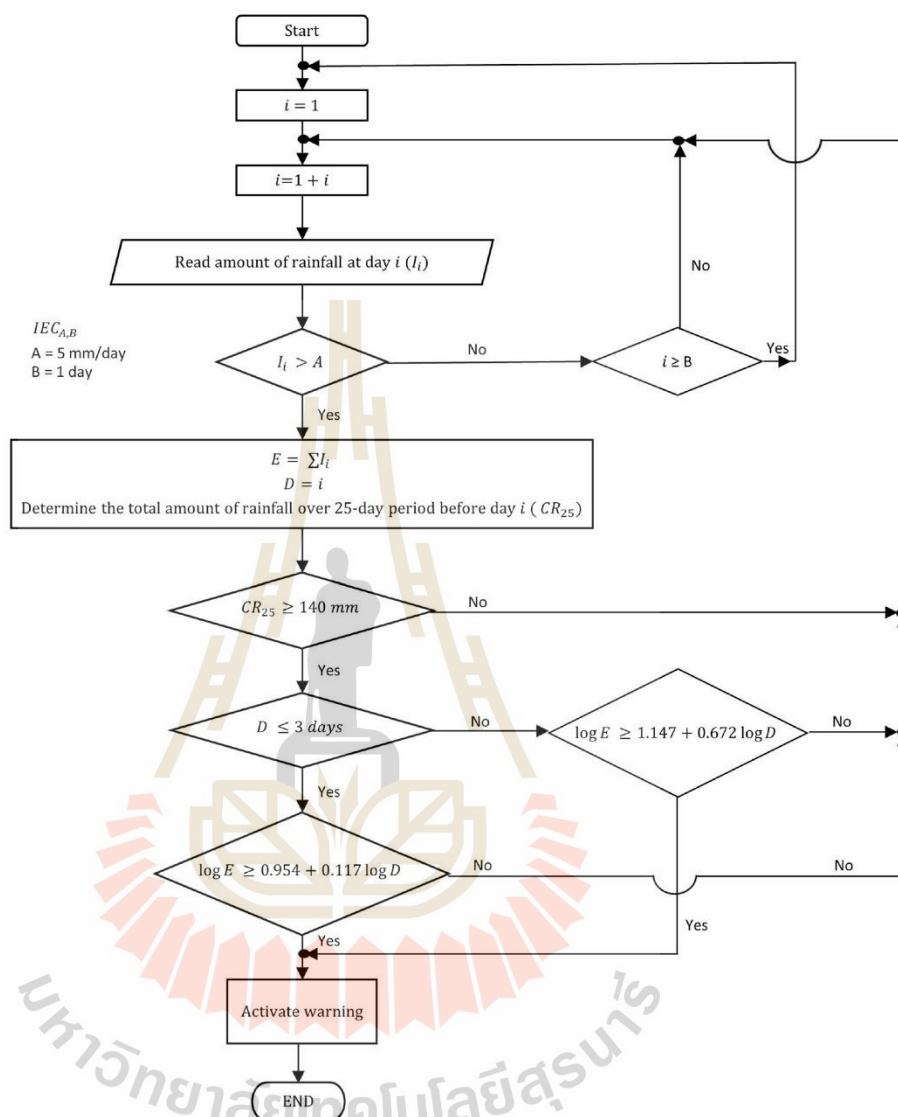


Figure 8. Flowchart of landslide rainfall assessment using the introduced threshold.

Conclusion

Rainfall data corresponding to 59 landslides recorded in Northern Thailand during the years 2002 to 2018 was used to establish landslide rainfall threshold in the study area. Based on the variation coefficient (CV) of inter-event times, a suitable inter-event criterion (IEC) to separate two consecutive rainfalls was $IEC_{5,1}$ standing for the condition that rainfall intensity was no greater than 5 mm/day for at least 1 days. The threshold introduced in this study was a threshold that explicitly included rainfall event and antecedent rainfall parameters in the threshold, namely cumulative rainfall with rainfall event-duration (CED) threshold. 140 mm of the cumulative rainfall over 25-day period prior to a failure day (CR_{25}) was found to be a

suitable indicator to deal with antecedent rainfall events. Based on the threshold predictability and distribution of rainfall duration, a period of 3 days was chosen as an indicator to distinguish the rainfall event to short- and long-duration rainfall events. And the introduced threshold included the *CED* threshold for rainfall event of their duration no longer than 3 days and the *CED* threshold for rainfall events of their duration longer than 3 days. Introducing the CR_{25} of 140 mm into the threshold resulted in notably fewer false positive (*FP*) cases, and hence the false alarm rate (*FAR*) for the *CED* threshold was considerably lower than the *FAR* for the rainfall event-duration (*ED*) threshold. The reduction of *FAR* significantly improved the overall reliability of the threshold, indicated by the magnitude of the area under the receiver operating characteristic. Furthermore, the false alarm ratio (*FA*) of the *CED* threshold yielded positive results since it was significantly lower than the *FA* yielded by the *ED* threshold. Since the *CED* threshold at probabilistic levels of 5% returned the largest Hanssen and Kuipers (*HK*) score and the smallest value of δ , this threshold at probabilistic level of 5% can be recommended as the landslide rainfall threshold in Northern Thailand.

List of abbreviations and symbols

<i>AUC</i>	area under receiver operating characteristic curve
<i>CED</i> threshold	cumulative rainfall with rainfall event – duration threshold.
CR_{25}	cumulative rainfall over 25-day period before a failure day.
<i>CSI</i>	critical success index
<i>CV</i>	coefficient of variation
<i>E</i>	rainfall event in mm
<i>ED</i> threshold	rainfall event – duration threshold
ED_L threshold	rainfall event – duration threshold for long duration rainfalls
ED_S threshold	rainfall event – duration threshold for short duration rainfalls
<i>D</i>	duration of rainfall event in day
DR_f	rainfall event in mm on a failure day
<i>FA</i>	false alarm ratio
<i>FAR</i>	false alarm rate
<i>FN</i>	false negative
<i>FP</i>	false positive
<i>HK</i>	Hanssen and Kuipers score
<i>HR</i>	hit rate
<i>IEC</i>	inter – event time criterion
<i>ROC</i>	receiver operating characteristic
<i>TP</i>	true positive
<i>TN</i>	true negative
δ	Euclidean distance from the ideal co-ordinate 0,1.

Availability of data and material

The datasets generated during and/or analysed during the current study are available from the corresponding author on reasonable request.

Conflict of interest

The authors declare that they have no known competing financial interests or personal relationships that could have appeared to influence the work reported in this paper.


Funding

This work was financially supported by Suranaree University of Technology (IRD7-712-65-12-19).

ORCID

Avirut Chinkulkijniwat  <http://orcid.org/0000-0003-4905-7991>

Suksun Horpibulsuk  <http://orcid.org/0000-0003-1965-8972>

Arul Arulrajah  <http://orcid.org/0000-0003-1512-9803>

References

- Ahmad R. 2003. Developing early warning systems in Jamaica: rainfall thresholds for hydrological hazards. In: National Disaster Management Conference, Ocho Rios, St Ann, Jamaica, Sept 9–10.
- Aleotti P. 2004. A warning system for rainfall-induced shallow failures. *Eng Geol.* 73(3–4): 247–265. <https://doi.org/10.1016/j.enggeo.2004.01.007>.
- Bonta JV, Rao AR. 1988. Factors affecting the identification of independent storm events. *J Hydrol.* 98(3–4):275–293. [https://doi.org/10.1016/0022-1694\(88\)90018-2](https://doi.org/10.1016/0022-1694(88)90018-2).
- Caine N. 1980. The rainfall intensity - duration control of shallow landslides and debris flows. *Geogr Ann Ser A Phys Geogr.* 62(1–2):23–27. <https://doi.org/10.1080/04353676.1980.11879996>.
- Chen HW, Chen CY. 2022. Warning models for landslide and channelized debris flow under climate change conditions in Taiwan. *Water.* 14(5):695. <https://doi.org/10.3390/w14050695>.
- Chen D, Ou T, Gong L, Xu CY, Li W, Ho CH, Qian W. 2010. Spatial interpolation of daily precipitation in China: 1951–2005. *Adv Atmos Sci.* 27(6):1221–1232. <https://doi.org/10.1007/s00376-010-9151-y>.
- Chinkulkijniwat A, Horpibulsuk S, Bui Van D, Udomchai A, Goodary R, Arulrajah A. 2016. Influential factors affecting drainage design considerations for mechanical stabilised earth walls using geocomposites. *Geosynthetics International.* :1–18. doi:10.1680/jgein.16.00027.
- Chinkulkijniwat A, Tirametatarat T, Supotayan C, Yubonchit S, Horpibulsuk S, Salee R, Voottipruex P. 2019. Stability characteristics of shallow landslide triggered by rainfall. *J Mt Sci.* 16(9):2171–2183. <https://doi.org/10.1007/s11629-019-5523-7>.
- Chinkulkijniwat A, Yubonchit S, Horpibulsuk S, Jothityangkoon C, Jeeptaku C, Arulrajah A. 2016. Hydrological responses and stability analysis of shallow slopes with cohesionless soil subjected to continuous rainfall. *Can Geotech J.* 53(12):2001–2013. <https://doi.org/10.1139/cgj-2016-0143>.
- Crosta GB, Frattini P. 2001. Rainfall thresholds for triggering soil slips and debris flow. In: *Proceedings of the 2nd EGS Plinius Conference on Mediterranean Storms: Publication CNR GNDCL.* Vol. 2547, Oct; p. 463–487.
- Ditthakit P, Nakrod S, Viriyantavong N, Tolche AD, Pham QB. 2021. Estimating baseflow and baseflow index in ungauged basins using spatial interpolation techniques: a case study of the Southern River Basin of Thailand. *Water.* 13(21):3113. <https://doi.org/10.3390/w13213113>.
- Environmental Geology Division. 2003. A manual of landslide geo-hazard prevention and list of landslide risk villages of the north region of Thailand. Bangkok, Thailand: Department of Mineral Resources, 113 p. (in Thai)
- Fan L, McArdell B, Or D. 2016. Linking rainfall-induced landslides with debris flows runoff patterns towards catchment scale hazard assessment. *Geomorphology.* 280:1–15. <http://doi.org/10.1016/j.geomorph.2016.10.007>.
- Gariano SL, Brunetti MT, Iovine G, Melillo M, Peruccacci S, Terranova O, Vennari C, Guzzetti F. 2015. Calibration and validation of rainfall thresholds for shallow landslide forecasting in Sicily, southern Italy. *Geomorphology.* 228:653–665. <https://doi.org/10.1016/j.geomorph.2014.10.019>.

- Gariano SL, Melillo M, Peruccacci S, Brunetti MT. 2020. How much does the rainfall temporal resolution affect rainfall thresholds for landslide triggering? *Nat Hazards*. 100(2):655–670. <https://doi.org/10.1007/s11069-019-03830-x>.
- Gariano SL, Sarkar R, Dikshit A, Dorji K, Brunetti MT, Peruccacci S, Melillo M. 2019. Automatic calculation of rainfall thresholds for landslide occurrence in Chukha Dzongkhag, Bhutan. *Bull Eng Geol Environ*. 78(6):4325–4332. <https://doi.org/10.1007/s10064-018-1415-2>.
- Gentile M, Courbin F, Meylan G. 2013. Interpolating point spread function anisotropy. *Astron Astrophys*. 549:A1. <https://doi.org/10.1051/0004-6361/201219739>.
- Germain D, Roy S, Guerra A. 2021. Empirical rainfall thresholds for landslide occurrence in Serra do Mar, Angra dos Reis, Brazil. In: Zhang Y, Cheng Q, editors. *Landslides*. IntechOpen. <https://doi.org/10.5772/intechopen.100244>.
- Giannecchini R, Galanti Y, D'Amato Avanzi G. 2012. Critical rainfall thresholds for triggering shallow landslides in the Serchio River Valley (Tuscany, Italy). *Nat. Hazard Earth Sys*. 12. 829–842. <https://doi.org/10.5194/nhess-12-829-2012>.
- Giannecchini R, Galanti Y, D'Amato Avanzi G, Barsanti M. 2015. Probabilistic rainfall thresholds for triggering debris flows in a human-modified landscape. *Geomorphology*. 257: 94–107. <https://doi.org/10.1016/j.geomorph.2015.12.012>.
- Grozavu A, Patriche CV. 2021. Mapping landslide susceptibility at national scale by spatial multi-criteria evaluation. *Geomatics Nat Hazards Risk*. 12(1):1127–1152. <https://doi.org/10.1080/19475705.2021.1914752>.
- Guzzetti F, Cardinali M, Reichenbach P. 1994. The AVI project: a bibliographical and archive inventory of landslides and floods in Italy. *Environ Manage*. 18(4):623–633. <https://doi.org/10.1007/bf02400865>.
- Guzzetti F, Peruccacci S, Rossi M, Stark CP. 2008. The rainfall intensity-duration control of shallow landslides and debris flows: an update. *Landslides*. 5(1):3–17. <https://doi.org/10.1007/s10346-007-0112-1>.
- He S, Wang J, Liu S. 2020. Rainfall event-duration thresholds for landslide occurrences in China. *Water*. 12(2):494. <https://doi.org/10.3390/w12020494>.
- Iida T. 2004. Theoretical research on the relationship between return period of rainfall and shallow landslides. *Hydrol Process*. 18(4):739–756. <https://doi.org/10.1002/hyp.1264>.
- Indraratna B, Fatahi B, Khabbaz H. 2006. Numerical analysis of matric suction effects of tree roots. *Proc Inst Civ Eng - Geotech Eng*. 159(2):77–90. <https://doi.org/10.1680/geng.2006.159.2.77>.
- Kanjanakul C, Chub-uppakarn T, Chalermyanont T. 2016. Rainfall thresholds for landslide early warning system in Nakhon Si Thammarat. *Arab J Geosci*. 9:584–595. <https://doi.org/10.1007/s12517-016-2614-4>.
- Koenker R, Bassett G. 1978. Regression quantiles. *Econometrica*. 46(1):33. <https://doi.org/10.2307/1913643>.
- Komolvilas Y, Tanapalungkorn W, Latcharote P, Likitlersuang S. 2021. Failure analysis on a heavy rainfall-induced landslide in Huay Khab Mountain in Northern Thailand. *J Mt Sci*. 18(10):2580–2596. <https://doi.org/10.1007/s11629-021-6720-8>.
- Kong YF, Tong WW. 2008. Spatial exploration and interpolation of the surface precipitation data. *Geogr. Res*. 27(5):1097–1108.
- Kurtzman D, Navon S, Morin E. 2009. Improving interpolation of daily precipitation for hydrologic modelling: Spatial patterns of preferred interpolators. *Hydrol Process*. 23(23): 3281–3291. <https://doi.org/10.1002/hyp.7442>.
- Lee WY, Park SK, Sung HH. 2021. The optimal rainfall thresholds and probabilistic rainfall conditions for a landslide early warning system for Chuncheon, Republic of Korea. *Landslides*. 18(5):1721–1739. <https://doi.org/10.1007/s10346-020-01603-3>.
- Maturidi A, Kasim N, Taib AK, Azahar W, Tajuddin HA. 2020. Empirically based rainfall threshold for landslides occurrence in Cameron Highlands, Malaysia. *Civil Eng Architect*. 8(6):1481–1490. <https://doi.org/10.13189/cea.2020.080629>.
- Peruccacci S, Brunetti M, Gariano SL, Melillo M, Rossi M, Guzzetti F. 2017. Rainfall thresholds for possible landslide occurrence in Italy. *Geomorphology*. 290:39–57. <https://doi.org/10.1016/j.geomorph.2017.03.031>.

- Rosi A, Segoni S, Canavesi V, Monni A, Gallucci A, Casagli N. 2021. Definition of 3D rainfall thresholds to increase operative landslide early warning system performances. *Landslides*. 18(3):1045–1057. <https://doi.org/10.1007/s10346-020-01523-2>.
- Salee R, Chinkulkijniwat A, Yubonchit S, Horpibulsuk S, Wangfaoklang C, Soisompong S. 2022. New threshold for landslide warning in the southern part of Thailand integrates cumulative rainfall with event rainfall depth-duration. *Nat Hazards*. 113(1):125–141. <https://doi.org/10.1007/s11069-022-05292-0>.
- Schmidt-Thomé P, Tatong T, Kunthasap P, Wathanaprida S. 2018. Community based landslide risk mitigation in Thailand. *Episodes*. 41(4):225–233. <https://doi.org/10.18814/epiiugs/2018/018017>.
- Segoni S, Piciullo L, Gariano SL. 2018. A review of the recent literature on rainfall thresholds for landslide occurrence. *Landslides*. 15(8):1483–1501. <https://doi.org/10.1007/s10346-018-0966-4>.
- Teerarungsikul S, Torizin J, Fuchs M, Kuhn F, Chonglakmani C. 2016. An integrative approach for regional landslide susceptibility assessment using weight of evidence method: a case study of Yom River Basin, Phrae province, Northern Thailand. *Landslides*. 13(5): 1151–1165. <https://doi.org/10.1007/s10346-015-0659-1>.
- Thai Meteorological Department. 2022. Monthly rainfall. [accessed 2022 Aug 4]. <http://www.arcims.tmd.go.th/dailydata/MonthRain.php>.
- Vennari C, Gariano SL, Antronico L, Brunetti MT, Iovine G, Peruccacci S, Terranova O, Guzzetti F. 2014. Rainfall thresholds for shallow landslide occurrence in Calabria, southern Italy. *Nat Hazards Earth Syst Sci*. 14(2):317–330. <https://doi.org/10.5194/nhess-14-317-2014>.
- Vessia G, Parise M, Brunetti MT, Peruccacci S, Rossi M, Vennari C, Guzzetti F. 2014. Automated reconstruction of rainfall events responsible for shallow landslides. *Nat Hazards Earth Syst Sci*. 14(9):2399–2408. <https://doi.org/10.5194/nhess-14-2399-2014>.
- Wicki A, Lehmann P, Hauck C, Seneviratne SI, Waldner P, Stähli M. 2020. Assessing the potential of soil moisture measurements for regional landslide early warning. *Landslides*. 17(8):1881–1896. <https://doi.org/10.1007/s10346-020-01400-y>.
- Wieczorek G, Glade T. 2005. Climatic factors influencing occurrence of debris flows. In: Jakob M, Hungr O, editors. *Debris-flow hazards and related phenomena*. Berlin: Springer; p. 325–362. https://doi.org/10.1007/3-540-27129-5_14
- Ya'acob N, Tajudin N, Azize A. 2019. Rainfall-landslide early warning system (RLEWS) using TRMM precipitation estimates. *Indonesian J Electr Eng Comput Sci*. 13(3):1259–1266. <https://doi.org/10.11591/ijeecs.v13.i3.pp1259-1266>.
- Yang KH, Nguyen TS, Rahardjo H, Lin DG. 2021. Deformation characteristics of unstable shallow slopes triggered by rainfall infiltration. *Bull Eng Geol Environ*. 80(1):317–344. 2021 <https://doi.org/10.1007/s10064-020-01942-4>.
- Yang H, Wei F, Ma Z, Guo H, Su P, Zhang S. 2020. Rainfall threshold for landslide activity in Dazhou, southwest China. *Landslides*. 17(1):61–77. <https://doi.org/10.1007/s10346-019-01270-z>.
- Yang X, Xie X, Liu DL, Ji F, Wang L. 2015. Spatial interpolation of daily rainfall data for local climate impact assessment over greater Sydney region. *Adv Meteorol*. 2015:1–12. <https://doi.org/10.1155/2015/563629>.
- Yubonchit S, Chinkulkijniwat A, Horpibulsuk S, Jothityangkoon C, Arulrajah A, Suddeepong A p 2017. Influence factors involving rainfall-induced shallow slope failure: numerical study. *Int J Geomech*. 17(7):04016158.
- Yumuang S. 2006. 2001 debris flow and debris flood in Nam Ko area, Phetchabun province, central Thailand. *Environ Geol*. 51(4):545–564. <https://doi.org/10.1007/s00254-006-0351-9>.
- Zhang K, Wang S, Bao HJ, Zhao XM. 2019. Characteristics and influencing factors of rainfall-induced landslide and debris flow hazards in Shaanxi Province, China. *Nat. Hazard Earth Sys*. 19:93–105. <https://doi.org/10.5194/nhess-19-93-2019>.

BIOGRAPHY

Miss. Rattana Salee was born in September 17, 1995 in Surin Province, Thailand. She obtained has Bachelor's degree in Civil Engineering from the School of Civil Engineering, Suranaree University of Technology in 2018, respectively. Then, she has been awarded an OROG Scholarship from the Thailand Research Fund (TRF) in 2018 under her Advisor's Prof. Dr. Avirut Chinkulkijniwat for Ph.D. study in the School of Civil Engineering, Suranaree University of Technology. During Ph.D. study (2018-2022), she has worked as a teaching assistant for Surveying Laboratory and Soil Mechanics Laboratory. she has published 3 international ISI journal papers during Ph.D. study.

